ULPGC
Universidad de
Las Palmas de
Gran Canaria

DOCTORADO EN INGENIERÍA QUÍMICA, MECÁNICA Y DE FABRICACIÓN

ANÁLISIS TERMOECONÓMICO DE UNA PLANTA DE PRODUCCIÓN DE CAFÉ SOLUBLE INTEGRADO A UNA UNIDAD DE PRODUCCIÓN DE BIOCOMBUSTIBLES

Autora:
Diana Lucía Tinoco Caicedo

Director:
Ana María Blanco Marigorta

Co-director:
Alexis Lozano Medina

Las Palmas de Gran Canaria
Enero 2022

D. Mario Domingo Monzón Verona, COORDINADOR DEL PROGRAMA DE DOCTORADO en Ingenierías Química, Mecánica y de Fabricación DE LA UNIVERSIDAD DE LAS PALMAS DE GRAN CANARIA

INFORMA,

De que la Comisión Académica del Programa de Doctorado, en su sesión de fecha ..... tomó el acuerdo de dar el consentimiento para su tramitación, a la tesis doctoral titulada " Análisis termoeconómico de una planta de producción de café soluble integrado a una unidad de producción de biocombustibles" presentada por la doctoranda Dª. Diana Lucía Tinoco Caicedo y dirigida por la Doctora Ana María Blanco Marigorta y codirigida por el Doctor Alexis Lozano Medina, solicitando la Mención Internacional por disponer de los requisitos para ello de acuerdo con el Arto 18 del Reglamento de Estudios de Doctorado.

Y para que así conste, y a efectos de lo previsto en el Artº 11 del Reglamento de Estudios de Doctorado (BOULPGC 04/03/2019) de la Universidad de Las Palmas de Gran Canaria, firmo la presente en Las Palmas de Gran Canaria, a _____ de _____ de dos mil veintidos.

UNIVERSIDAD DE LAS PALMAS DE GRAN CANARIA
ESCUELA DE DOCTORADO

Programa de doctorado en Ingenierías Química, Mecánica y de Fabricación.

Título de la Tesis:
Análisis termoeconómico de una planta de producción de café soluble integrado a una unidad de producción de biocombustibles

Tesis Doctoral presentada por Dª. Diana Lucía Tinoco Caicedo

Dirigida por el Dr. Dª. Ana María Blanco Marigorta

Codirigida por el Dr. D. Alexis Lozano Medina

Las Palmas de Gran Canaria, a 21 de Enero de 2022

La Directora, El Codirector, La Doctoranda,

AGRADECIMIENTOS

A Dios por su guía y sustento.

A mi directora, Dra. Ana María Blanco, y co-director Dr. Alexis Lozano Medina por su guía y consejos en el desarrollo del trabajo de tesis.

A los directivos y jefes de área de la planta de café soluble localizada en Guayaquil, Ecuador por su confianza depositada en mi para buscar mejoras a sus procesos.

A la Facultad de Ciencias Naturales y Matemáticas y el Decanato de Investigación de la Escuela Superior Politécnica del Litoral, por su apoyo en el desarrollo de este proyecto de investigación y en el proceso de publicación de los artículos científicos.

Al Centro de Energías Renovales y Alternativas (CERA) de la Escuela Superior Politécnica del Litoral, por su colaboración en el desarrollo del proyecto.

A los ayudantes de investigación y compañeros de trabajo que me prestaron su ayuda en el desarrollo del proyecto.

A mi familia por su apoyo incondicional.

RESUMEN

La creciente demanda de alimentos hace que las industrias de alimentos sean consideradas como no sostenibles a largo plazo, dado a su alto consumo de energía en procesos de calentamiento, enfriamiento y cocción. Además, generan grandes cantidades de desechos orgánicos que van a rellenos sanitarios y no se les da ningún valor agregado. Específicamente la industria de café soluble se considera una de las industrias de alimentos que mayor consumo de energía tiene. Además, se estima que el 40% de su materia prima es desechada como bagazo de café a vertederos [1].

Esto ha hecho que varios estudios se hayan centrado en la valorización del bagazo de café [2–5]. Dado su alto poder calorífico varias investigaciones se han centrado en estudiar experimentalmente su conversión a biocombustibles [1,6,7]. Esto ha permitido proponer alternativas para reducir el consumo de combustibles fósiles y de esta forma acercarse más a una economía circular. Sin embargo, uno de los principales obstáculos para que se pueda llevar a cabo el proceso productivo a gran escala de biocombustibles es su alto costo de producción y su alto impacto ambiental [8].

El análisis exergoeconómico ha sido aplicado a diferentes procesos productivos [9–12]. Se han determinado oportunidades para reducir el impacto ambiental y costos de producción mediante la cuantificación de la tasa de exergía destruída, costos operativos y de inversión.

El objetivo general de esta tesis doctoral es incrementar la eficiencia exergética y reducir los costos operativos de un proceso productivo de café soluble. Para ello, se propone la producción de biocombustibles a partir de bagazo de café. Los objetivos específicos que permitirán el cumplimiento de este objetivo general son:

- Realizar un análisis exergoeconómico de las principales líneas de producción de café soluble usando datos reales de una planta ubicada en Guayaquil, Ecuador.
- Proponer un proceso productivo para el aprovechamiento del bagazo de café y su conversión a biocombustibles mediante la simulación del proceso.
- Integrar al proceso una fuente de energía renovable mediante la simulación de un sistema de trigeneración.

- Realizar un análisis exergoeconómico a la propuesta de rediseño del proceso y compararlo con el caso base.

El tema de tesis desarrollado está relacionado con la línea de investigación de energías renovables del programa de doctorado en Ingenierías Química, Mecánica y de Fabricación. Las publicaciones científicas realizadas dentro del tema de esta tesis doctoral evalúan la situación actual del proceso industrial en cuanto a su eficiencia exergética y su impacto en los costos. Además, estas publicaciones proponen alternativas para el uso de su desecho agroindustrial para la producción de biocombustibles que sean utilizados dentro del proceso productivo. De esta forma se piensa incrementar la sustentabilidad del proceso junto con su economía circular. Se ha realizado la publicación de tres artículos y existen otros dos que actualmente están en fase de revisión. Estos artículos en su conjunto abarcan el tema central de la tesis doctoral dentro de la línea de investigación indicada.

Se llevó a cabo un análisis exergoeconómico de todo el proceso productivo para el diagnóstico de la planta. Para esto se realizó el levantamiento de las condiciones de operación de cada una de las etapas de proceso productivo de café soluble en una planta localizada en Guayaquil, Ecuador. Los resultados de esta evaluación de las dos primeras etapas del proceso que son el tostado de los granos verdes de café y la extracción de sólidos solubles se encuentran en el artículo "Exergoeconomic analysis of coffee roasting and solid liquid extraction process: A case study from an instant coffee factory in Ecuador." Los resultados de la evaluación del proceso de evaporación doble efecto para la concentración del extracto de café se encuentra en el artículo "Advanced exergoeconomic analysis of a double effect evaporation process in an instant coffee plant." La última etapa de producción consiste en el secado del extracto de café para la producción de café soluble en polvo y supone una de las etapas con mayor consumo energético. Esta etapa fue analizada mediante un análisis exergoeconómico avanzado y sus resultados fueron presentados en el artículo "Conventional and Advanced Exergy and Exergoeconomic Analysis of a Spray Drying System: A Case Study of an Instant Coffee Factory in Ecuador."

Posterior al diagnóstico del proceso productivo, se diseñó el proceso de producción de biocombustibles a partir del bagazo de café el cual se desecha en la etapa de extracción. Se realizó un estudio bibliográfico sobre la valorización de bagazo de café. Además, se recopilaron los estudios experimentales que se han realizado en los últimos años para la producción de biocombustibles a partir del bagazo de café. Con los datos experimentales

encontrados se realizó la simulación del proceso de producción de biomasa, gas de síntesis y biodiesel a partir del bagazo de café en Aspen Plus. Los modelos fueron validados con datos experimentales de estudios presentes en la bibliografía. Se realizó un análisis exergético y económico de cada una de las etapas del proceso productivo de biocombustibles. Los resultados fueron presentados en el artículo "Simulation and Exergoeconomic Analysis of the syngas and biodiesel production from spent coffee ground."

Se propuso finalmente un sistema de trigeneración para la producción integrada de vapor, agua de refrigeración y potencia a base de gas de síntesis y biomasa. Este sistema permite el suministro de las utilidades necesarias a la planta de una forma más eficiente. El sistema fue simulado y validado con datos experimentales de estudios previos. Se realizó un análisis exergético y económico del sistema propuesto alimentado con combustibles fósiles y biocombustibles, para comparar su desempeño. Los resultados fueron presentados en el artículo "Simulation and exergoeconomic analysis of a trigeneration system based on biofuels from spent coffee ground."

Finalmente, se concluye que la planta de café soluble de Guayaquil, Ecuador, tiene una tasa de exergía destruída de 12.5 MJ/s y una tasa de costos operativos de $3214.9/h de los cuales el 81% se deben a la exergía destruida. Las etapas productivas que mayor tasa de exergía destruyen son la generación de vapor convencional (5.0 MJ/s) y la extracción sólido líquido de granos de café (1.8 MJ/s). Mientras que los procesos que mayores costos operativos representan a la planta son la etapa de extracción sólido líquido (952 $/h), la evaporación doble efecto (720 $/h) y el sistema de refrigeración por compresión de vapor (617 $/h). Por otro lado, se demuestra que reemplazar un sistema convencional de generación de vapor, refrigeración y generación de potencia operado con fuel oil No. 6 por un sistema de trigeneración operado con biomasa, permite reducir la tasa de exergía destruida total en un 48%. Mientras que si es operado con gas de síntesis se reducen en un 52%. Además, la eficiencia exergética incrementa en un 11 % cuando se usa biomasa y un 12% cuando se usa gas de síntesis. Los costos de las utilidades actuales se reducen hasta un 95% cuando el sistema convencional que utiliza fuel oil No.6 es reemplazado por un sistema de trigeneración a base de biomasa, y en un 93% cuando se utiliza gas de síntesis. Se estima también que el costo del producto es posible reducirlo en un 47.9% al utilizar un sistema integrado para las utilidades de la planta en lugar del sistema convencional que tienen.

Entre las líneas de investigación futuras está el estudio experimental de secado de bagazo de café y la operación de sistema de trigeneración a base de esta biomasa a escala piloto. Además, se requiere realizar un análisis exergoeconómico avanzado a todo el sistema productivo con el

fin de cuantificar los costos de exergía destruida evitables e inevitables. La optimización exergoeconómica a todo el proceso es otro tema de interés, dado que permitiría reducir aún más los costos operativos y maximizar eficiencia exergética, modificando las condiciones de operación establecidas.

ABSTRACT

The increasing demand for food lead to unsustainable process in food industries in the long term, because of the high energy consumption in heating, cooling, and cooking processes. Also, this generates large amounts of organic waste that is discarded to landfills. Specifically, the soluble coffee industry is considered one of the food industries with the highest energy consumption, and it is also estimated that 40% of its raw material is discarded as spent coffee ground to landfills [1].

These facts have been motivated to develop several studies focused on the valorization of spent coffee ground [2–5]. Given its high calorific value, several investigations have focused on experimentally studying its conversion to biofuels [1,6,7]. This has made it possible to propose alternatives to reduce the consumption of fossil fuels and thus get closer to a circular economy. However, one of the main obstacles for carrying out the large-scale production process of biofuels from this waste is its high production cost and high environmental impact [8].

The exergoeconomic analysis has been applied to different production processes [9–12]. Opportunities have been determined to reduce the environmental impact and production costs by quantifying the exergy destruction rate, operating and investment costs.

The general aim of this doctoral thesis is to increase the exergetic efficiency and reduce the operating costs of a soluble coffee production process. For which the production of biofuels from spent coffee ground is proposed. The specific objectives that will allow the fulfillment of this general objective are:

- Develop an exergoeconomic analysis of the main soluble coffee production lines from a factory located in Guayaquil, Ecuador.
- Propose a production process for the use of spent coffee ground and its conversion to biofuels by the simulation of the process.
- Integrate a renewable energy source into the process by simulating a trigeneration system.
- Develop an exergoeconomic analysis of the process redesign proposal and compare it with the base case.

The thesis topic developed is related to the renewable energy research line of the doctoral program in Chemical, Mechanical, and Manufacturing Engineering. The scientific publications executed within the subject of this doctoral thesis evaluate the current situation of the industrial process in terms of its exergetic efficiency and its impact on costs.

In addition, these publications propose alternatives for the use of their agro-industrial waste for the production of biofuels that are used within the production process. In this way, it is intended to increase the sustainability of the process together with its circular economy. Three articles have been published and there are another two that are currently under review. These articles as a whole cover the central theme of the doctoral thesis within the indicated line of research.

An exergoeconomic analysis of the entire production process was carried out for the evaluation of the plant. For this, the operating conditions of each of the stages of the soluble coffee production process were surveyed in a plant located in Guayaquil, Ecuador. The results of the first two stages of the process, which are the roasting of green coffee beans and the extraction of soluble solids, can be found in the article “Exergoeconomic analysis of coffee roasting and solid-liquid extraction process: A case study from an instant coffee factory in Ecuador." The results of the evaluation of the double effect evaporation process for the concentration of the coffee extract can be found in the article "Advanced exergoeconomic analysis of a double effect evaporation process in an instant coffee plant.". The last stage of production consists of drying the coffee extract to produce soluble coffee powder and is one of the stages with the highest energy consumption. This stage was studied through an advanced exergoeconomic analysis and its results were presented in the article "Conventional and Advanced Exergy and Exergoeconomic Analysis of a Spray Drying System: A Case Study of an Instant Coffee Factory in Ecuador."

After the evaluation of the production process, the biofuel production process was designed from spent coffee ground, which is discarded in the extraction stage. A bibliographic study was performed on the valorization of spent coffee ground. In addition, the experimental studies that have been executed in recent years to produce biofuels from spent coffee ground were compiled. With the experimental data found, the simulation of the production process of biomass, syngas, and biodiesel from spent coffee ground in Aspen Plus was carried out. The models were validated with experimental data. Exergy and economic analysis of each of the stages of the biofuel production process were developed. The results were presented in the

article "Simulation and Exergoeconomic Analysis of the syngas and biodiesel production from spent coffee ground."
A trigeneration system was finally proposed for the integrated production of steam, cooling water, and power based on syngas and biomass. This system makes it possible to supply the necessary utilities to the plant in a more efficient way. The system was simulated and validated with experimental data from previous studies. Exergy and economic analysis of the proposed system based on fossil fuels and biofuels were carried out to compare its performance. The results were presented in the article "Simulation and exergoeconomic analysis of a trigeneration system based on biofuels from spent coffee ground."

Finally, it was estimated that the soluble coffee plant in Guayaquil, Ecuador has an exergy destruction rate of 44.4 GJ/h and an operating cost rate of $ 3215/h of which 81% are due to the destroyed exergy. The productive stages that destroy the highest exergy rate are the generation of steam (18.1 GJ/h) and the solid-liquid extraction of coffee beans (6.4 GJ/h). While the processes that represent the highest operating costs for the plant are the solid-liquid extraction stage ($952/h), double effect evaporation ($ 720/h), and the vapor-compression refrigeration system ($617/h). On the other hand, it is shown that replacing a conventional steam generation, refrigeration, and power generation system operated with fuel oil No. 6 by a trigeneration system operated with biomass allows reducing the total exergy rate destroyed by 3775 kW. While if it is operated with syngas it is reduced by 7811 kW. In addition, the overall exergetic efficiency increases by 4% when using biomass and 30% when syngas is used. Current utility costs are reduced by up to 95% when the conventional system using fuel oil No.6 is replaced by a biomass-based trigeneration system, and by 93% when syngas is used. Furtheremore, it is estimated that the specific cost of the overall product of the plant could be reduced in 47.9% when using a trigeneration system that integrate all the utilities of the plant.

Future lines of research include the experimental study of spent coffee ground drying and the operation of a trigeneration system based on this biomass on a pilot scale. In addition, an advanced exergoeconomic analysis of the entire production system is required to quantify the avoidable and unavoidable costs of the destroyed exergy rate. The exergoeconomic optimization of the whole process is another topic of interest since it would allow to further reduce operating costs and maximize exergetic efficiency, modifying established operating conditions.

Nomenclature

c	unit exergy cost ($/MJ)
$\dot{C}$	cost rate associated with an exergy stream ($/h)
c_p	heat capacity (kJ/kg K)
e	specific exergy rate (kJ/kg)
$\dot{E}$	exergy rate (kJ/h)
f	exergoeconomic factor
h	specific enthalpy (kJ/kg)
$\overline{HHV}$	High heating value (MJ/kg)
i_{eff}	Interest rate
$\dot{m}$	mass flow rate (kg/h)
n	lifetime of the system (years)
P	pressure (kPa)
$\dot{Q}$	heat flow rate (kJ/h)
r	relative cost difference
R	ideal gas constant (kJ/kmol K)
r_{OM}	nominal escalation rate
s	specific entropy (kJ/kg)
T	temperature (°C)
w	mole fraction of water vapor
$\dot{W}$	power (kJ/h)
x	mole fraction
y	destruction rate
y*	relative irreversibility
$\dot{Z}$	investment cost rate ($/h)

Greek letters

η	efficiency (%)
Δ	difference
τ	annual operating hours (h)
ρ	air density (kg/m^3)
γ	specific heat ratio

Superscript

CH	chemical
CI	capital investment
e	equilibrium
KN	kinetic
OM	operating and maintenance
PH	physical
PT	potential

Subscripts

B	biodiesel process
EP	electrical power
cond	condensed
cs	cold stream
D	destruction
DB	dry biomass
elec	electric
F	fuel
gly	glycerin compound

hs	hot stream
i	ith component
in	inflow
is	isentropic
k	kth component
L	loss
min	minimum
mix	mixture
o	thermodynamic environment
out	outflow
P	product
R	reagents
S	oil extraction and biogas process
tot	overall system
x	Hydrocarbon fuels
WB	wet biomass
en	energy

Abbreviations

A	absorber
B	boiler
BT	belt
C	compressor
CE	centrifuge
CC	combustion chamber
CELF	constant-escalation levelization factor
CHX	cooler heat exchanger
CRF	capital recovery factor
D	dryer
E	heat exchanger
EV	evaporator
EX	extractor of soluble solids
F	fan
FF	vacuum pump
FFA	free fatty acids
G	mill
H	furnace
HX	heat exchanger
HXE	extract heat exchanger
HP	high pressure pump
LP	low pressure pump
MF	main fan
MHX	main heat exchanger
NIST	National Institute of Standards and Technology
OMC	operation and maintenance cost
O&M	operation and maintenance
P	pump
PEC	purchased equipment cost
PFI	plant-facilities investment
Q	furnace for afterburner

R	reactor
RC	real conditions
RFF	fine returns fan
RTI	unavoidable thermodynamic inefficiency condition
S	vibrating screen
SO	soxhlet extractor
SC	spent coffee
SCG	spent coffee ground
SD	spray dryer
SFBHX	fluidized bed heat exchanger
SFBF	fluidized bed fan
T	turbine
CS	cooling system
TDE	ThermoData Engine
TRR	total revenue requirement
UIC	unavoidable investment cost conditions
UNIQUAC	Universal quasichemical
V	expansion valve
VF1HX	vf1 heat exchanger
VF2HX	vf2 heat exchanger
VF1F	vf1 fan
VF2F	vf2 fan
WOC	worst operational conditions

INDEX

1. Introduction 1

1.1. Justification 2

1.2. State of the art 2

1.2.1. Exergoeconomic analysis in food industry 3

1.2.2. Biofuels from spent coffee grounds 4

1.2.3. Trigeneration system 6

1.3. Objectives 7

1.4. Structure of the document 8

2. Processes description 10

2.1. The production process of instant coffee powder 11

2.1.1 The roasting and coffee solid-liquid extraction process 11

2.1.2. Double effect evaporation process 13

2.1.3. Spray Drying 14

2.1.4. Steam, chilled water and power generation 16

2.2. The production process of biofuels from spent coffee grounds 17

2.2.1 System description 17

2.2.2. Process Simulation 19

2.2.3. Model Validation 20

2.3. The trigeneration process 20

2.3.1. System description 20

2.3.2. Process Simulation 22

2.3.3. Model Validation 23

3. Thermoeconomic Analysis 26

3.1. Fundamentals of Thermoeconomic Analysis 27

3.1.1. Exergy Analysis 27

3.1.2. Economic Analysis 28

3.1.3. Exergoeconomic Analysis 30

3.2. Application of thermoeconomic analysis to the processes 31

3.2.1. Roasting and solid liquid extraction 31

3.2.2. Double effect evaporation process 34

3.2.3. Spray Drying process 36

3.2.4. Biofuels production from SCG 38

3.2.5. Trigeneration system 42

4. Results and Discussion 46

4.1. Exergoeconomic Analysis of the roasting and coffee extraction process 47

4.2. Exergoeconomic analysis of the double effect evaporation process 52

4.3. Exergoeconomic analysis of the spray drying process 55

4.4. Simulation and Exergoeconomic analysis of the biofuels production process from spent coffee grounds. 61

4.5. Simulation and Exergoeconomic Analysis of the CCHP system based on biofuels 69

5. Conclusions 77

5.1. Main Conclusions 78

5.2 Future research lines 79

*7. **Anexxes** ..... Error! Bookmark not defined.*

1.Introduction

In this first chapter the justification of the work, the state of the art, the general objective, the specific objectives and the structure of the document are presented for the thesis titled "Thermoeconomic Analysis of an instant coffee plant integrated to a biofuel production unit".

1.1. Justification

The soluble coffee industry is one of the sectors with the highest energy consumption [1]. This production process consists of the roasting stage of the green coffee beans, the extraction of the soluble solids from the roasted coffee, the double effect evaporation for the concentration of the liquid extract, and finally, the spray drying of the extract to obtain the coffee powder. These stages consume large amounts of steam, cooling water, and electrical energy. Furthermore, the soluble solids extraction stage generates large amounts of spent coffee ground that are disposed to landfills [2]. The low sustainability of this process, its high carbon footprint [3], and high exergy destruction rate, lead us to seek alternatives to reduce its energy consumption and take advantage of the solid residue of this production process (spent coffee ground).

In previous studies, the exergoeconomic analysis of industrial processes has allowed the increase of exergetic efficiency and minimized the operating costs of industrial processes, thus increasing the sustainability of the process. This analysis makes it possible to identify the production stages and specific equipment that destroy the high amounts of exergy and the cost they entail. The methodology applied for this analysis begins by quantifying the exergy rate of fuel and product of each component of the system and then determines the exergy destroyed as the difference between fuel and product. In addition, an economic analysis is performed to determine the investment and operating costs, and thus the exergy destruction cost rate in each stage can be quantified [4].

The project seeks to meet the United Nations Sustainable Development Goal 7, which aims to guarantee access to affordable, safe, sustainable, and modern energy. Likewise, it wants to comply with objective 12 of Production and responsible consumption since it seeks to optimize the use of energy resources and raw materials to promote the circular economy in the industry.

1.2. State of the art

Instant coffee is one of the most commonly consumed drinks worldwide; around 118 billion dollars of it were sold in the global market in 2019. The worldwide market for instant coffee has high growth expectations: projected to grow by 11.6 % in the next 5 years [10]. Coffee

has a high concentration of antioxidants [11], vitamins B and minerals [12]. It benefits physical performance and stimulates the central nervous system [3]. Coffee is sold as whole bean, ground coffee, instant coffee, coffee pods, and capsules. Among these, instant coffee is quickly becoming popular all over the world because of cheaper transportation and convenience in preparation, which increases its demand among urban consumers [14]. Many industrial-scale plants have been established around the word to produce this kind of coffee.

The production process of instant coffee powder begins with roasting the coffee beans and grinding them. Later, they pass through a liquid solid extraction. The extracted liquid is then concentrated and, finally, it is spray dried. This process reduces the amount of water in the coffee and allows its shelf-life to be increased. The overall process is highly energy intensive. The spray drying process alone accounts for 40% of the total energy requirements of the production process, where around 90% of the energy consumed in this final process is from fossil fuels and the remaining comes from electric energy.

1.2.1. Exergoeconomic analysis in food industry

Some exergoeconomic analyses have been done on different processes of food such as maize [16], powdered milk [17], pistachios [18], mint leaves [19] and fish oil [20]. These analyses have allowed for the identification of the components with the highest exergy losses, the avoidable exergy losses, and the operational conditions which most affect the irreversibility of the systems. However, although the exergetic analysis identifies the location and magnitude of the thermal energy losses, it has limitations given that it can´t quantify the cost of those losses. Furthermore, an exergy analysis is not conclusive about which components should have investment priority in order to reduce the exergy losses.

In order to complete an exergy analysis, a thermoeconomic analysis can be applied which combines exergy and economic principles at the component level to identify the real cost sources in a thermal system. Since the thermodynamic considerations of thermoeconomics are based on the exergy concept, the term exergoeconomics can also be used to describe the combination of exergy analysis and economics [21]. Thermoeconomic methods are useful to minimize the economic losses due to irreversibility, and, consequently, provide the added benefit of reducing production costs of entire complex energy systems.

In the case of roasting and solid liquid extraction process, there is only one exergoeconomic analysis performed to a roasting process of coffee bean by Vučković, Stojiljković & Vasiljević [35], but they only determined the overall exergy destruction rate (614 kW) and the overall efficiency of 33% for the roasting system, so the components that causes the higesth destruction

of exergy were not identified. Other studies have been carried out for roasting process. Sheikhshoaei, Dowlati, Aghbashlo & Rosen [36] conducted a study in which an exergy analysis of the pistachio roasting process was carried out, where an exergy destruction of 78.3 kW was obtained, which represents an exergy efficiency of 9.96%. There was not found any exergetic or exergoeconomic analysis of solid-liquid extraction of soluble solids from coffee.
In the case of evaporation process, there is a previous study that shows that this process has low energetic and exergetic efficiencies [6], which lead to a high level of energy waste, and consequently raise production costs. In order to address these inefficiencies, it is necessary to identify and quantify the losses. Some exergy analyses have been done in food industries that have evaporation as part of their process, such as the production of tomato paste [6], powdered milk [7], and yogurt [8]. However, there are no exergoeconomic analyses performed in evaporation processes in food industries.
Finally, for drying processes, there is a study that shows that the drying process is also a highly exergy-destructive process [15]. Just a few thermoeconomic analyses of different drying technologies on both pilot and industrial scale have been found in the literature; they focused on the production of pasta [22], tea leaves [23], powdered cheese [24] and milk [25]. And only two of them refer to spray drying technology at an industrial scale [16-17].

1.2.2. Biofuels from spent coffee grounds

Currently, fossil fuels are the primary source of energy. Approximately, 80% of the word´s energy demand is supplied by them [27]. However, it's estimated that oil reserves would not be sufficient to meet the demand by 2050 [28]. To overcome this problem, it's important to look for renewable energy sources, especially in sectors that consume more energy: industries and transport [29]. Biofuels are one of the most common renewable energy sources and are considered the best option for industries especially when biofuel comes from an industrial waste [30]. During 2018, according to British Petroleum company, the United States became the first country with an annual production of 38.1 million tons of biofuel, followed by Brazil with a production of 21.4 million tons per year [31]. Nowadays there are 803 biorefineries in Europe where 45% of them produce biofuels [32]. The biofuels mostly produced are biodiesel, syngas and bioethanol [33]. In the last few years, different countries have produced biofuels from different sources, such as waste deriving from agriculture [34], agroindustry [35] and livestock [36]. These have gradually contributed to the reduction of 80% of the greenhouse emissions from landfills [37].

The agricultural wastes that have been studied to be converted to biofuels included rice bran [38], oat straw [39], fish waste [40], alga [41] and spent coffee grounds (SCG) [42], where the last one has the highest calorific value (22 MJ/kg) and oil content (29%), becoming one of the best energetic potential resources for the production of liquid and solid biofuels. There are many experimental studies about the production of biofuels from SCG at laboratory scale. Liu et al. [43] studied the biodiesel production by applying in-situ transesterification method at 70 ºC by 3 h, obtaining a yield of 98,61% greater than the 83% obtained by Haas et al. [44]. Meanwhile, Park et al. [45] applied indirect transesterification to the humidified SCG for the production of biodiesel and obtained a yield of 16.75%. Pacioni et al. [46] applied the gasification process with steam in a tubular reactor to produce syngas from SGC with a yield of 88.6%. Kibret et al. [2] applied the same process by using a semi-fluized bed and increased the yield to 95%.

In the last few years, many exergetic and exergoeconomic analyses of different biodiesel and syngas production processes have been developed in order to evaluate the sustainability of these processes. In the case of biodiesel, Antonova et al. [47] evaluated the production of biodiesel from the oil of canola seeds and found that the dryer and the transesterification reactor destroyed 7.8% and 25.2% of the fuel exergy rate, respectively. Amelio et al. [48] shows that an exergetic optimization in the biodiesel production from triolein oil achieves a higher reduction than energetic optimization, with a difference of 44.7 kW. Mancebo et al. [49] achieved an increase in the exergetic efficiency through an exergetic optimization from 10% to 22% and the reduction of exergy destruction cost rate from $0.13/h to $0.12/h. In the case of syngas, Shayan et al. [50] analyzed the gasification process of wood and determined the optimum temperature of gasification which allowed them to increase the exergetic efficiency by 24.9% and reduce the exergy destruction cost rates by 8.9%. Another similar study determined that the exergetic efficiency could be increased to 76.2% when the steam/biomass mass ratio is 1.83 [51]. Different exergetic analysis have been performed in processes that include a gasifier in combination with other treatments such as hydrotreatment, hydrocracking, steam reforming [52], direct and indirect synthesis of dimethyl ether [53], digestion plants [40] and integrated energy system [56]. In all these processes, the component with the highest exergy destruction rate was the gasifier.

As it is shown, although there are many experimental analyses on SCG that have demonstrated a high potential to be converted to biofuels, there are not exergetic and economic analyses focused on evaluating the sustainability of this process. The previous exergoeconomic analysis mentioned were only focused on evaluating specific steps such as transesterification or

gasification of other types of biomass. Therefore, an exergetic and economic analyses of an integrated process for the production of biodiesel and syngas by indirect transesterification and gasification from SCG has never been reported.

1.2.3. Trigeneration system

Around the world it is estimated that 14% of the factories use trigeneration systems (CCHP) based on fossil fuels to provide facilities to their production processes [57]. In Ecuador, non-integrated systems based on fossil fuels (vapour compression cycles and power generators) continue being used in factories, becoming a serious problem specially for processes that are energy intensive, such as instant coffee production. This mentioned process consumes large amounts of steam, chilled water, and electricity for operations such as coffee extraction, evaporation, spray drying and lyophilization. At the same time, the process discards approximately the 40% of its raw material as spent coffee grounds (SCG), which is a waste that, in previous works, has demonstrated its capability to be converted to different biofuels [58].

Efforts for a circular economy seek to replace energy sources with renewable ones, especially with biofuels from organic waste that is generated in the industrial plants [59]. Exergetic and exergoeconomic analyses have been performed on CCHP systems based on fossil fuels and biofuels [60], to make them more profitable and with less environmental impact [61].

Miar et al. [62] proposes the improvement and optimization of a CCHP system at Qom University using natural gas as fuel; where the exergetic efficiency of the system increased about 4.71%, the exergetic cost rate decreased about 0.65% and the total environmental impact rate of the system decreased about 0.01%. Ghaebi et al. [63] determined that the exergetic efficiency of a CCHP system using liquified natural gas as fuel increased 1.98% (18.52% to 20.5%) and the exergetic cost rate decreased about 1%. Marques et al. [64] determined that the exergetic efficiency of a conventional system is 40.24%; while the exergetic efficiency of the CCHP system using natural gas as fuel is 29.06%; where the equipment with the highest exergy destroyed is the combustion engine about 87.80% of the overall system. Ding et al. [65] carried out an exergy analysis of a conventional system (cogeneration) using wood biomass as fuel, where an exergetic efficiency of 41.36% was determined. Yang et al. [60] performed an exergoeconomic analysis of a CCHP system using a mixture of fuel (sugarcane bagasse and natural gas), and determined that the exergetic efficiency increased by about 5%. Through a sensitivity analysis of two types of fuel (biomass and natural gas), it was determined that the unit exergy costs of the products decreased by 2% using only biomass as fuel. Wu et al. [66]

carried out an exergoeconomic analysis of a CCHP system using biogas (biomass waste from rice paddy) as fuel together with solar energy in the gasification process, where it was determined that the exergetic efficiency increased from 27.15% to 27.70% in the thermal solar biomass gasification system; in addition, the exergy costs decreased to 0.038 $/kWh in all the facilities. Gholizadeh et al. [67] performed an exergoeconomic analysis of a trigeneration plant using biogas (biomass waste from crop straw) as fuel and toluene as coolant, where the exergetic efficiency increases from 2.58% to 13.26% and total costs decrease by 6.71%. Also, the selection of the refrigerant is essential, where it is determined that using R141b refrigerant an energy load of 172 kW and exergetic efficiency of 35.45% is achieved; while with the Toluene refrigerant and energy load of 249.8 kW, the exergetic efficiency of the process is 13%. Li et al. [68] carried out an exergy and environmental analysis to a trigeneration system using biomass (rice husk) as fuel together with solar energy, and determined the exergetic efficiency increases by 9% and the exergy cost of facilities decreased 4%. Also, the CO_2 emissions in a CCHP system decreased 2,95% than CO_2 emissions of a conventional system. Zhang et al. [61] determined that the exergy efficiency of a CCHP system using biomass (rice husk) as fuel improves about 10% when using a higher proportion of natural gas in the fuel mix ratio (biogas / natural gas) and also causes a decrease in the exergy costs of all facilities about 7.42%.

1.3. Objectives

The general objective of this doctoral thesis is to increase the exergetic efficiency and reduce the operational cost from the industrial process of instant coffee by integrating the production of biofuels from spent coffee grounds. To fulfill the aim of this work, the following specific objectives are stablished:

- Perform an exergoeconomic analysis of the main production steps of instant coffee by using real operational data from a Factory located in Guayaquil, Ecuador.
- Propose a productive process of biofuel from spent coffee grounds by the simulation of the process.
- Integrate to the current process the biofuels by the simulations of a trigeneration system that use them to provide steam, chilled water and power to the plant.
- Perform an exergoeconomic analysis to the redesign process and compare it with the base case.

1.4. Structure of the document

The structure of the document is organized as follows:

Chapter 1. Introduction

In this chapter the justification of the thesis, the state of the art, the objectives and the structure of the document are presented.

Chapter 2. Processes Description

In section 2.1 it is presented the instant coffee production process in the order it is produced:

1. Roasting and solid liquid extraction
2. Double effect evaporation process
3. Spray drying process.

In section 2.2 it is presented the system description, the methodology for the process simulation a model validation of:

1. The production process for biodiesel and biomass/syngas from SCG (Section 2.2.1)
2. The process for the trigeneration system (CCHP) operated by biofuels.

Chapter 3. Thermoeconomic Analysis

In this chapter the methodology used to perform the thermoeconomic analysis is presented in a general form (Section 3.1). Furthermore, specific information and considerations for each analyzed process are presented (Section 3.2).

Chapter 4. Results and Discussion

This chapter present the results and discussion of the thermoeconomic analysis performed for roasting and solid liquid extraction process (Section 4.1), double effect evaporation process (Section 4.2), spray drying process (Section 4.3), the biofuel production process (Section 4.4) and the trigeneration system (Section 4.5).

Chapter 5. Conclusions

The main conclusions are presented in this chapter. Also future research lines are presented.

Chapter 6. References

The references used in the different chapters are presented in this section.

2. Processes description

2.1. The production process of instant coffee powder

The production process of instant coffee powder is shown on Figure 2.1. The process begins with roasting the green coffee beans and grinding them. Later, they pass through a liquid solid extraction. The extracted liquid is then concentrated by an evaporation process and, finally, it is spray dried to produce soluble powder. Each step of the process consumes steam, chilled water and electricity that are provided by boiler, a steam compression cycle and a diesel engine. In the following sections, each process is explained in detail and it is presented the real operational data obtained from the plant located in Guayaquil, Ecuador.

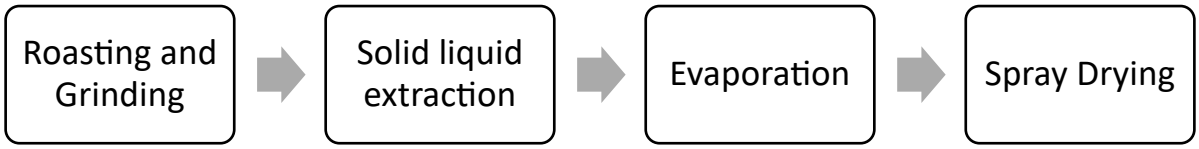

Figure 2.1. General production process of instant coffee powder

2.1.1 The roasting and coffee solid-liquid extraction process

Figure 2.2. shows the diagram of the system. Air with 15% excess (stream R-3) and of 0.02131 kg/s of Diesel (stream R-7) are pumped into a combustion chamber to carry out a combustion reaction and thus generate hot flue gases. The furnace charges a flow of 0.5722 kg/s of green coffee beans (stream R-12) with a moisture of 11.42%.

The coffee beans undergo the roasting process by contacting the flue gases (stream R9) from the combustion chamber, and this is where this process releases multiple volatile organic compounds "VOC's", among which are CO_2, CO and H_2O [12]. The roasting process is carried out at an approximate temperature of 232°C, with a residence time inside the furnace is about 7 minutes.

In order to reduce the possible environmental pollution, the gases that leave the furnace (stream R-10) are sent to an afterburner for the VOC's and CO present in the stream. The gases resulting from this process (stream R-11) are released to. The outlet temperature of these gases is 283°C.

At the outlet of the furnace, coffee beans (stream R-13) have an average moisture around 1% and are at 360.1°C. Roasted coffee beans are led to a cooling system in which a stream of water is used to decrease the temperature of these beans to the ambient temperature. A flow of 0.09803 kg/s is used to achieve cooling. Once the beans (stream R-16) leave the cooling system they have a moisture of 5.2%.

The roasted coffee beans (stream R-16) pass through a mill to obtain (stream R-18). For the extraction process only 0.2453 kg/s (stream E-11) are fed to the extractor, the rest of the roasted coffee obtained in the previous process is used to produce other products that the plant commercializes. The extraction happens in a semi-continuous system consisting of 6 countercurrent batteries. One of the batteries is charged with the coffee beans from the grinder, here the passage of water is allowed so that the extract of the previous battery enters the same from the bottom, causing the air to be expelled through the interstices when opening the purge. This stays up to a pressure between 200 and 500 kPa with temperature between 118°C to 120°C. Simultaneously, another battery is isolated for spent coffee ground discharge (residue), by a pipe to a hydro cyclone to separate the water and then deposit the waste in a hopper for disposal in the landfill. The coffee extract (stream E-5), is cooled in multiple heat exchangers until reaching a temperature of 12 °C. The cold extract (stream E-8) is passed to a centrifuge to separate the insoluble solids (stream E-10) from the desired product (stream E-9).

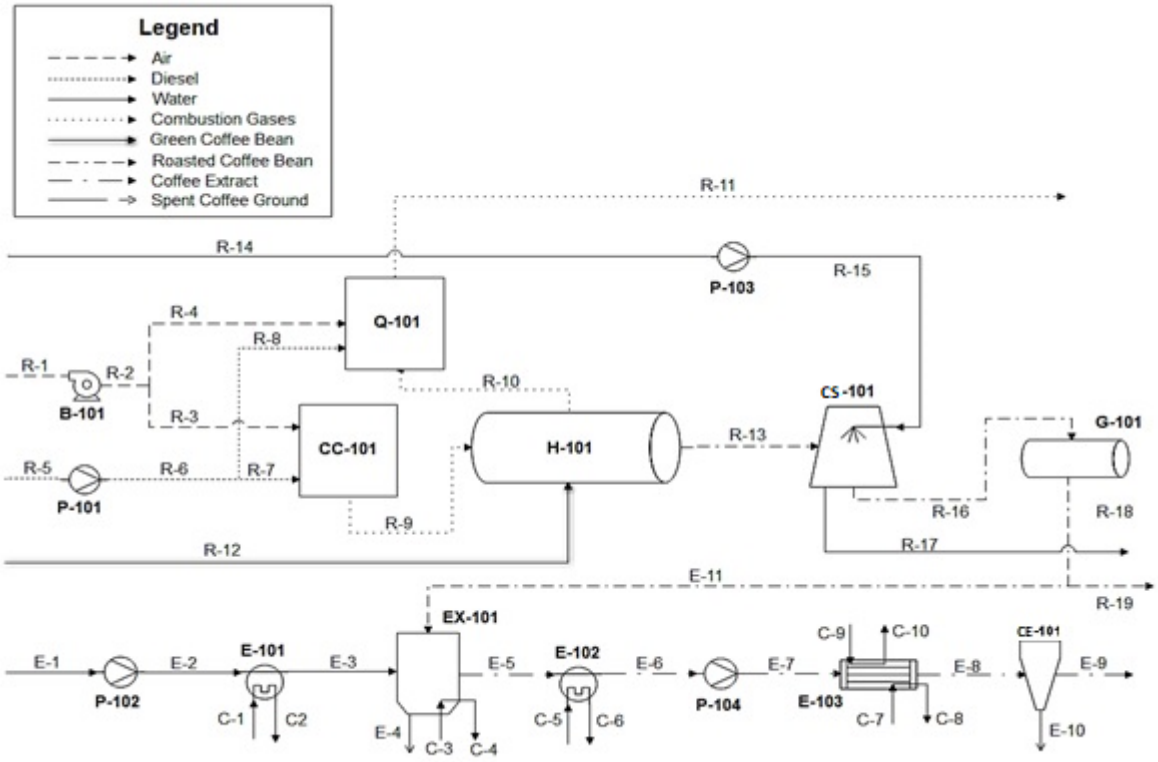

Figure 2.2. Process flow diagram for roasting and extraction of coffee.

To develop the model of the roasting process and coffee extraction, some assumptions were made.

- The process was at a steady state.

- The dead state conditions are 298 K and 101 kPa.
- The values for temperature and reference pressure are 273 K and 101 kPa.
- It is considered a complete combustion in the CC-101 and Q-101.
- In heat exchangers pressure drop is neglected.
- Kinetic exergy and potential exergy are negligible.
- Chemical exergy for pure substances are considered according to Model I [42].
- The average molecular formula for VOC's is considered C_2H_6O taking into account the main compounds that are released in the roasting process [13].

2.1.2. Double effect evaporation process

Figure 2.3 describes the double effect evaporation process of coffee extract in a factory located in Ecuador. Coffee extract (stream 1) is an aqueous solution with an initial concentration of soluble solids of 18 w/w%, from *Robusta* and *Arabica* beans. This extract is pumped to a heat exchanger (E-102) for pre-heating it up to 50ºC by using steam. The steam is generated in the boiler (B-201) by using fuel oil Nº6. Meanwhile, an already concentrated extract (stream 7) leaves the second effect (EV-102); part of it is mixed with the heated extract and recirculated to EV-102.The other part is sent to the first effect (EV-101). The evaporated water (stream 11) in EV-102 enters the condenser (E-101), where the temperature is reduced from 50°C to 32°C. The condensate water (stream 15) is mixed with condensate from de EV-102 (stream 16) and then it is discarded. The concentrated coffee (stream 8) that leaves the EV-101 reaches a concentration of 50 w/w% and then it is cooled from 66°C to 11°C in a heat exchanger of multiple flow (E-103), where cooling-tower water (C1) and chilled water (W3) are used.

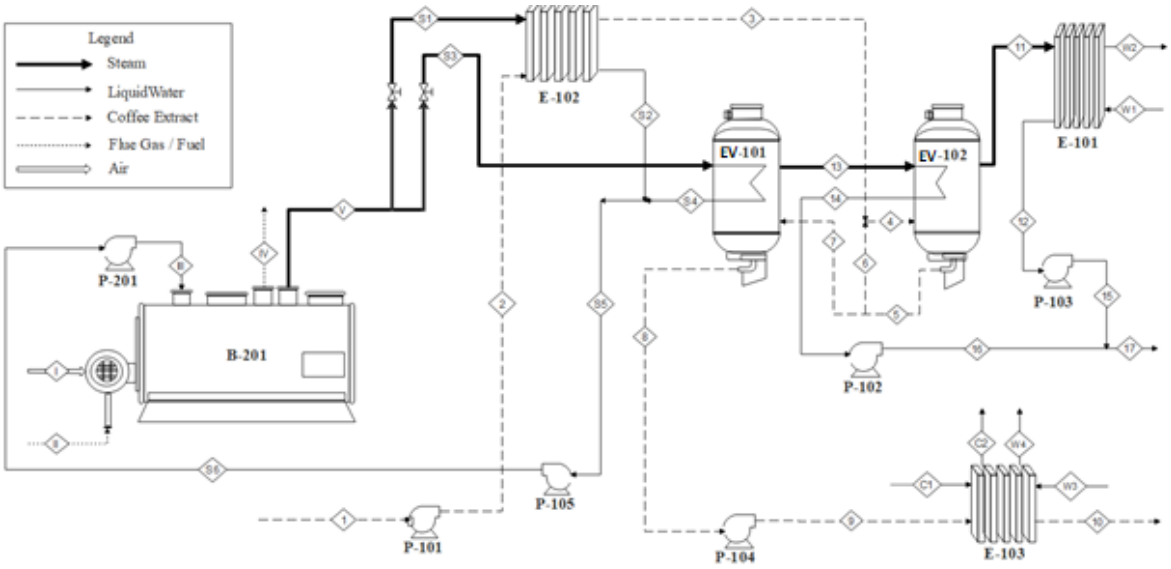

Figure 2.3. Process flow diagram of the double effect evaporation of coffee extract and the steam generation unit.

The process simulation was developed taking into account the following assumptions:

- The system was at steady state and the elevation in the coffee extract boiling point, due to concentration of solution, was assumed to be negligible.
- The heat loss rate and the pressure lost in all the components were negligible.
- A complete combustion was assumed in the combustion chamber.
- The steam and gases were considered as ideal gases when the pressure was below 1000 kPa. For higher pressures, the SRK-Equation was used as the equation of state.
- The coffee extract and liquid water were considered as ideal solutions.

2.1.3. Spray Drying

The instant coffee is dried in an industrial scale spray drying system. Figure 2.4 illustrates a schematic diagram of the process. The coffee extract (44% m/m of soluble coffee) comes from a storage tank that has a temperature of 12 ºC. A flow rate of 528 kg/h of coffee extract (stream 2) is pumped by a low-pressure pump (LP) and mixed with 7.4 kg/h of carbon dioxide (stream 1). Then it is pumped by a high-pressure pump (HP) into a heat exchanger unit (HXE) where steam increases its temperature to 32 ºC. The coffee extract (stream 6) is sprayed by a nozzle into the drying unit (SD), which is at vacuum pressure. A flow rate of 9922 kg/h of ambient air (stream 7) is heated by the main heat exchanger (MHX) using steam until it reaches the temperature of

180 ºC. A flow rate of 4002 kg/h of ambient air (stream 10) with an absolute humidity of 0.02 kg water/kg dry air is dehumidified to $8x10^{-3}$ kg water/kg dry air by a cooler (CHX) and then a fraction of it (stream 11) is heated and distributed in order to maintain a fluidized bed in the bottom of the spray dryer. The dried instant coffee produced with a humidity of about 3% m/m (stream 23) is then collected on a belt (BT), where two streams of dehumidified air at 85 ºC (stream 16) and 27 ºC (stream 20) are used to gradually cool the coffee and prevent it from agglomerating. Then the instant coffee (stream 25) is passed through vibratory screen (S) in order to obtain the required particle size. The fraction of instant coffee with the smallest particle size (stream 28) is recirculated to the process using dried air at 27 ºC (stream 22) while the biggest particle size of instant coffee (stream 27) is considered waste. The humidified air (stream 29) that exits the spray dryer is passed through a cyclone separator (FF) to remove solid coffee particles. These solid particles (stream 32) are recirculated into the process and the humidified air (stream 31) is released to the environment.

To develop the process modeling, the following assumptions were made:

- The process was at a steady state condition.
- The coffee extract was modeled as a solution with a constant concentration of soluble solids from Coffea arabica beans.
- The heat losses from the components were neglected.
- The pressure losses in the pipes, heat exchangers, bag filter and spray dryer were neglected.
- The properties of the incoming air were considered as constants.

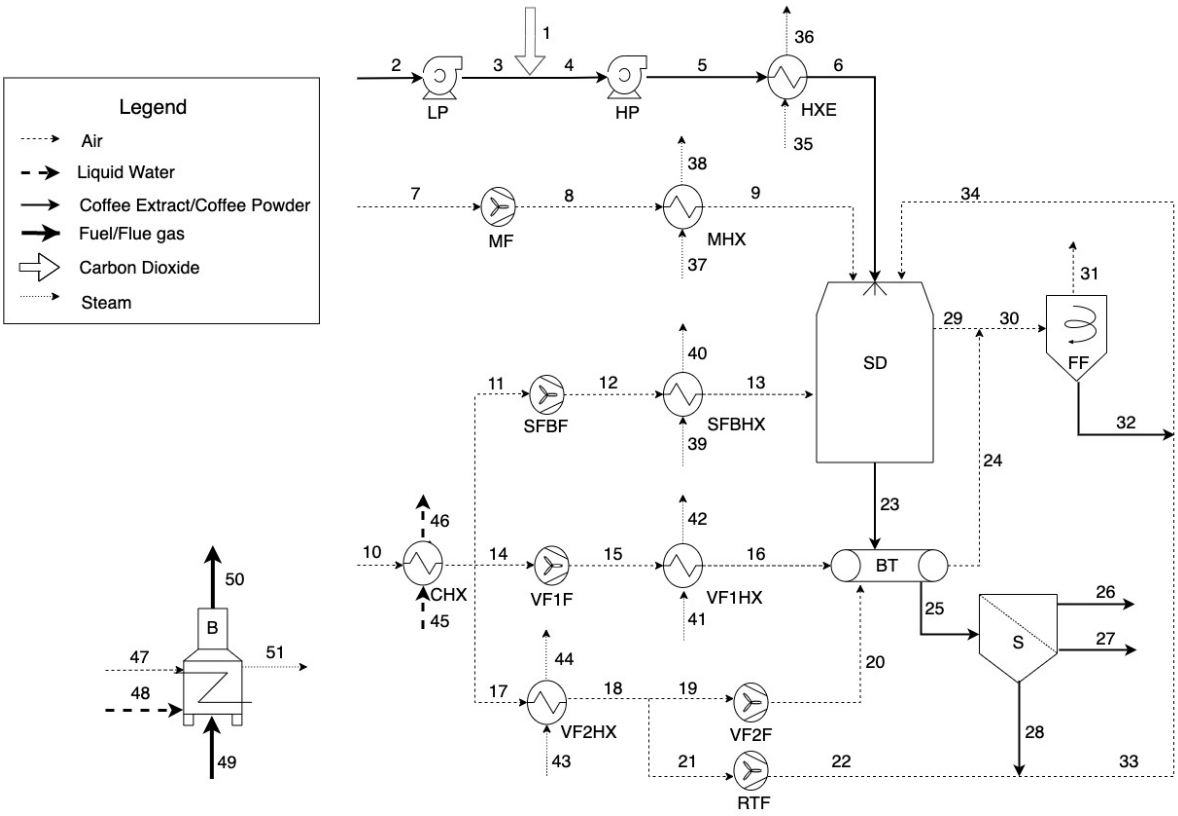

Figure 2.4. Process flow diagram of the spray dryer system

2.1.4. Steam, chilled water and power generation

The steam generation system is a boiler system traditionally used, in which fuel oil No. 6 is fed as fuel to the equipment, on the other hand, it is also fed a stream of water, which is recommended to go through a previous treatment to avoid possible incrustations in the equipment and thus not lose efficiency in the equipment. Finally, we will obtain a stream of greenhouse gases, which is the result of the combustion of the fuel together with the steam stream generated that will be the product that will be used in the production processes of soluble coffee.

For the power generation, the plant has a diesel generator. The plant needs 558.6 kW of power for supply their process with electricity.

The refrigeration system shown in Figure 2.5 is a vapor compression refrigeration system, which consists of three important stages: vapor compression, evaporator, and condenser. Through the S2 stream flows ammonia in gas phase which enters a flash separator to separate the stream into two phases (liquid and gas). The liquid phase exits through stream 3 and enters the evaporator (HX-101), where it will exchange heat with stream S5 (water) to obtain the ice water we are looking for through stream S6, the ammonia that exits this evaporator (stream S7)

increases its temperature due to the heat gained in the evaporator, this ammonia stream is recirculated and re-enters the flash separator (FS-101).

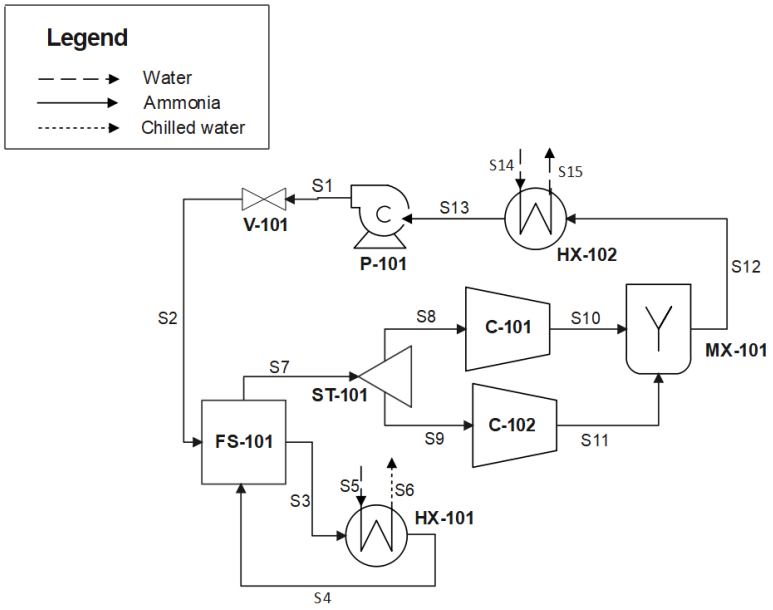

Figure 2.5. The vapor compression system used as conventional refrigeration.

The gas phase that leaves the flash separator (stream S7), will pass through a compression stage to obtain ammonia gas at a high temperature and pressure (stream S12), then this stream will enter a condenser where it will transfer heat to a water stream (stream S14) that enters the heat exchanger, the ammonia that leaves the condenser (stream S13) at a low temperature will be taken to a pump (P-101) where its pressure will be increased even more, finally the ammonia that circulates through stream S1 will be throttled in a valve in order to lower the ammonia temperature to saturation so that it enters the flash separator and the cycle continues.

2.2. The production process of biofuels from spent coffee grounds

2.2.1 System description

Figure 2.6 shows the production of syngas and biodiesel from SCG with initial moisture of 61.1% w/w. Air (stream S3) is heated up to 150 ºC (stream S4) in a heat exchanger (E-101), then it enters a dryer (D-101) to reduce the SCG´s moisture to 12.4% w/w. The dried biomass (Stream S5) enters the soxhlet extractor (SO-101), where it is in contact with hexane (stream S6) to extract 15% of the lipids from the SCG. The oil stream enters into a flash evaporator (EV-101) to recover the hexane (stream S8) and separate it from the lipids (stream S9). Traces of solvent in the spent biomass are evaporated in the dryer (D-102) with air preheated to 100

ºC (stream S12). Then, the dried SCG enters a gasifier at 900 ºC with carbon dioxide as the gasifying agent (stream S15) and produces syngas (stream 16), with a relative molar composition of 0.02, 0.43, 0.10, 0.37 for H_2, CH_4, CO, and CO_2, respectively [71]. In addition, the gasifier produces a solid stream with 95% char and 5% ash (stream 17). SCG oil (stream S9) is heated in a heat exchanger (E-202) with steam (stream B21) to 54 ºC (stream B6). A mixture of methanol (stream B4) and hydrogen chloride (stream B3) is heated in a heat exchanger (E-201) with steam (stream B19) up to 54 ºC. The heated mixture enters into a reactor (R-201) where the esterification reaction occurs to obtain methyl esters from free fatty acids. The methyl esters and the triglycerides of the oils leave the reactor (steam B8). Other products like excess reagent and produced water leave the reactor separately (stream B7). The product is decanted before going into the second reactor to eliminate the residues of methanol, water and HCl. In the second transesterification reactor (R-202), triglycerides from SCG oil (stream B10) react with methanol and KOH (stream B12) to produce water as a by-product (stream B14) and a mixture of glycerin and biodiesel as a product (stream B15). The product from the second reactor is cooled to room temperature (stream B16) and decanted to separate the glycerin (stream B17) from the biodiesel (stream B18).

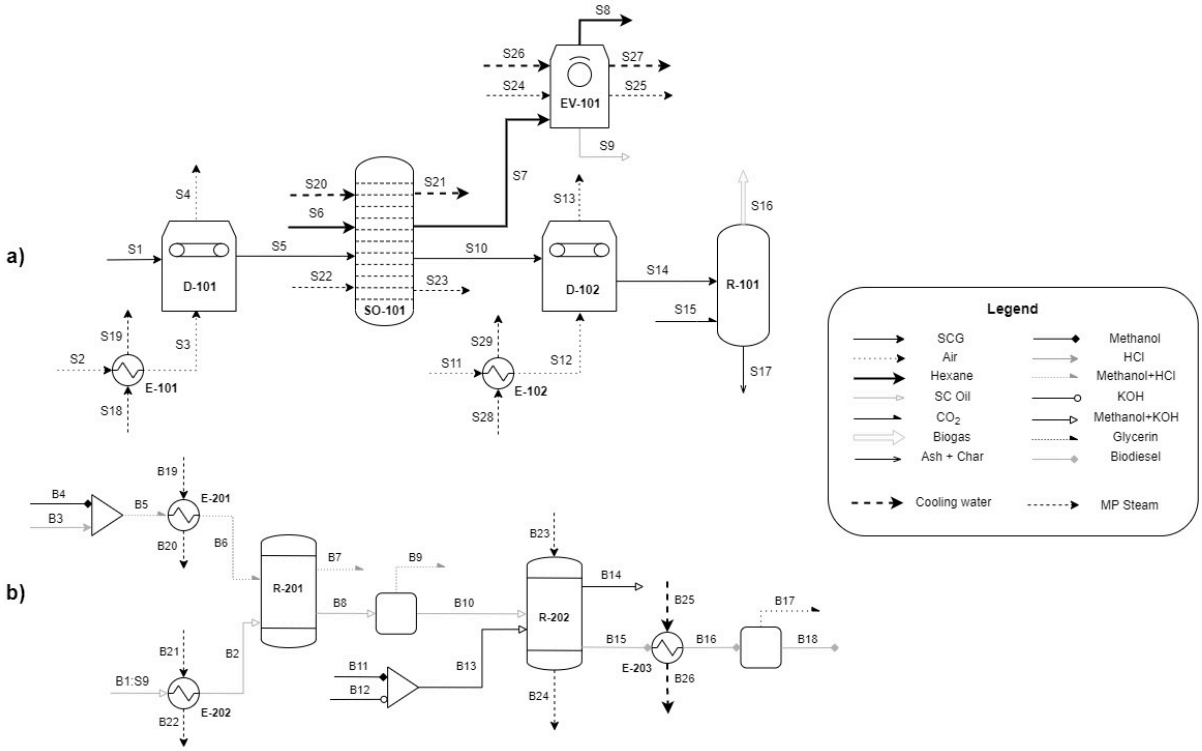

Figure 2.6. Process flow diagram of the integrated process to produce a) syngas and b) biodiesel

2.2.2. Process Simulation

The simulation of the process was performed in Aspen Plus V12.1. The SCG and the ash were simulated as unconventional components. Proximate and ultimate analyses were defined by applying the enthalpy and density model of the unconventional components (HCOALGEN and DCOALIGT) [72]. The oil chemical composition extracted from the SCG was obtained from a previous study [73], therefore the chemical compounds were simulated as conventional components using the NIST ThermoData Engine (TDE) database [74].

The conditions of the D-101 such as air/SCG mass ratio and initial and final humidity were established from experimental data in a convective dryer [75]. The EV-101 was simulated as a flash separator and a total solvent recovery was assumed. The ideal thermodynamic model was used for the gasification process because the pseudo-components were at a low pressure of 101.3 kPa [76]. The gasifier was simulated by the use of the RYIELD and the RGIBBS reactors [77]. Tar formation was not considered [78] and char was defined as pure coal, which was determined by the mass of fixed coal in the biomass.

For the esterification and transesterification processes, the UNIQUAC thermodynamic model was used, because the studied system has two liquid phases, some strong polar compounds and

is at a low pressure of 101.3 kPa [79]. A yield of 100% and 85% were considered for the esterification and transesterification reactions occurring in R-201 and R-202, respectively, according to previous studies [80].

2.2.3. Model Validation

The final moisture obtained in the dryers, the syngas composition obtained in the gasifier, the yield achieved in the oil extraction process, and the yield and composition of the biodiesel produced in the transesterification reactor were compared with the results obtained experimentally by previous studies using the same operational conditions, to ensure the validity of the modeled processes. For the esterification and the transesterification reactors, the operating conditions of Haile et al. [80] were used. The esterification reactor was operated at atmospheric pressure, with a methanol/FFA molar ratio of 20:1 and HCl at 10% w/w free fatty acids. The transesterification reactor had a methanol/oil molar ratio of 9:1 and KOH and 1% w/w of oil content. The D-101 was operated with the conditions presented in the experimental study of Gómez et al. [75].

The drying air temperature was 150 ºC, and its relative humidity was 50%. The SCG initial moisture was 61.1% w/w. The inlet air flow was 524.8 kg wet air per kg of wet biomass.

For the soxhlet extraction the solvent/biomass mass ratio was 9.87 as used by De Melo et al. [81]. The gasifier was operated at 900 ºC, with a CO_2/SCG molar ratio of 0.17 and with initial biomass moisture of 2.89% w/w, which are the conditions proposed by Kibret et al. [2].

2.3. The trigeneration process

2.3.1. System description

The CCHP system shown below consists essentially of three parts that have an established functionality: electric power generation, steam generation and cooling water generation. Figure 2.7 represents the process flow diagram of the CCHP system. The CCHP process begins with the stages of electric power production, immediately following the generation of steam. First, the fuel (bunker, natural gas, syngas, or dry biomass) (Stream 1) enters the P-101 pump and then into the combustion chamber CC-101. Air (Stream 3) that takes the oxidizer paper enters a compressor C-101 and then into the chamber CC-101. It should be noted that in the combustion chamber, complete combustion of the fuel takes place. The flue gas stream obtained in the combustion chamber (Stream 5) enters a gas turbine T-101 where electrical energy is produced. Then the flue gas stream coming out of the turbine (Stream 6) is directed

to a heat exchanger HX-101, which would function as a boiler to produce steam (Stream 9) from a mixture of plant recirculation water stream and fresh water (Stream 8). The exhaust flue gases of the heat exchanger (Stream 7) are directed to the desorber or generator HX-102, where it initiates the absorption cycle to produce chilled water.

Regarding the absorption system, the mixture of LiBr / H_2O (Stream 14) enters the pump P-102 and then goes to the heat exchanger HX-103 where it gains temperature. Then, the mixture goes into the generator or desorber HX-102 where the separation of water (Stream 11) and LiBr (Stream 12) is made through the heat supplied by the flue gases of Stream 7 that leaves the HX-101 exchanger. In exchanger HX-103, there is another high temperature outlet stream with a higher concentration of the LiBr / H_2O mixture than stream 15.

The generator outlet stream containing only water vapor (Stream 17) enters condenser HX-104 where it is fully condensed using water from the cooling tower (Stream 18). Then the water (Stream 20) passes to a V-102 expansion valve to reduce its pressure (Stream 21) prior entering the evaporator.

The output stream of the generator containing only water steam (Stream 17) enters the condenser HX-104 where it is completely condensed using water from the cooling tower (Stream 18). The water then passes into a V-102 expansion valve to reduce its pressure (Stream 21) prior to its entry into the evaporator. In the evaporator HX-105 the water of the cycle (Stream 21) absorbs heat from a stream of hot water (Stream 22), vaporizing completely. The stream of water that loses heat (Stream 23) corresponds to the chilled water provided by the CCHP system. The stream of water from the cycle that leaves the evaporator (Stream 24), enters the absorber AB-101, where it is mixed with the LiBr / H_2O solution that has a higher concentration of LiBr (Stream 13). The stream leaving the absorber has lower Concentration of LiBr because it is diluted with stream 24. Because absorption is an exothermic process, cooling water (Stream 25) which exits the absorber at a higher temperature (Stream 26) is used.at a higher temperature (Stream 26).

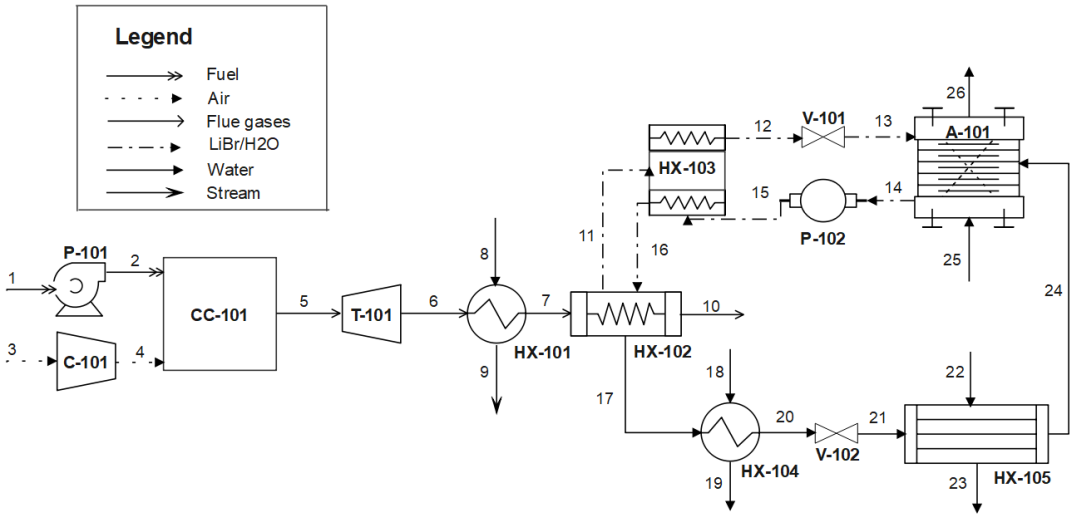

Figure 2.7. CCHP system based on biofuel from SCG

2.3.2. Process Simulation

The simulation of the process was performed in Aspen Plus V12. Biomass was defined as an unconventional component using the enthalpy and density model known as HCOALGEN and DCOALIGT where Proximate and Ultimate analysis were specified. This data was obtained from previous studies [82]. Natural gas and syngas contains a mixture of components of known chemical composition like methane, nitrogen, carbon dioxide, hydrogen, and carbon monoxide [83,84]. Therefore, they were simulated as conventional components using the ThermoDataEngine (TDE) database of NIST simulator Aspen Plus, achieving an approximation of the properties of natural gas and syngas from the molecular structure of the components that compose them. Bunker was defined as a pseudocomponent, adding characterization data like density and molecular weight, obtained from literature [85].

For the CCHP system, the ELECNRTL thermodynamic model was used, since it is specifically designed for electrolyte solutions, in this case, for the lithium bromide solution. For this model, it is necessary to use an electrolyte wizard to generate relevant reactions for the electrolyte solution which are the association/dissociation of lithium bromide [86]. The following conditions were considered in certain components: In the CC-101 combustion chamber, a complete combustion of the fuel operating at specific temperatures and pressures was considered. These conditions were obtained from previous studies for each fuel: biomass [87], fuel oil No. 6 [83], natural gas [88] and syngas [85]. In the T-101 turbine, an isentropic efficiency of 70% and an expansion ratio of 1:15 were considered according to previous studies [86]. The HX-101 boiler was simulated as a shell and tube heat exchanger since the combustion

gases obtained from the combustion chamber heat the feed water producing steam and therefore lowering the temperature of the flue gases. This component operates at specific pressures and temperatures of cooling water and combustion gases according to the fuel used: biomass [87], bunker [83], natural gas [88] and syngas [85].

For the absorption chiller system, conditions of temperature, pressure and lithium bromide concentration were considered according to Somers et al. [84]. In the pump (P-102) a pressure of 7.461 kPa was considered with a lithium bromide concentration of 57.4%. The generator was simulated as a heat exchanger (HX-102) to separate the components in the solution, in this case, the lithium bromide from water, through the heat supplied by the flue gases from the cogeneration system. For the condenser (HX-104), evaporator (HX-105) and absorber (A-101), the temperatures were considered according to Somers et al. [84]. For valves V-101 and V-102 a pressure of 7.461 kPa was considered. It should be noted that cooling water was used in the condenser and absorber, while in the evaporator hot water was used as heating medium.

Throughout the study, the following assumptions were made: All components belonging to the systems were considered to operate under stationary conditions, so the dead temperature and pressure were 293.15 K and 101.3 kPa respectively for the conventional cooling system and 298.15 k and 101.3 kPa for the other systems and the reference temperature for the calculation of enthalpy and entropy is 298.15 K and 101.3 kPa; in this case, variations in ambient temperature were ignored. Regarding the calculations for the combustion chamber, complete combustion is assumed and heat losses to the environment are considered negligible. For the exergy analysis, the kinetic and potential exergies of the flows are negligible so their contribution to the general exergy was excluded and calculations of chemical exergy in the conventional cooling system were not considered since the compositions of the flows remain the same throughout the process.

2.3.3. Model Validation

To ensure the validity of the modeled processes using different fuels, the same operational conditions were used, data obtained from previous studies for the combustion chamber and boiler of the steam generation system and the lithium bromide/water absorption chiller system for each CCHP system shown in Table 2.14.

Table 2.14. Initial conditions for the steam generation system using different fuels

Component	Parameter	**Biomass** [82]	**Fossil Fuel** [85]	**Natural Gas** [83]	**Syngas** [89]
CC-101	Mass Ratio Air:Fuel	12	15.4	18.1	1.53
	Air Inlet Pressure (bar)	15	15	15	15
	Air Inlet Temperature (°C)	25	25	20	25
HX-101	Feed relation (kg water/kg flue gas)	2.5	2.75	2	2.46
	Water Inlet Pressure (bar)	12.5	12.5	12.5	12.5
	Water Inlet Temperature (°C)	25	25	25	25
	Flue Gas Inlet Pressure (bar)	7.95	8.02	8.20	10.14
	Flue Gas Inlet Temperature (°C)	1711	2118	2044	1799.7

Table 2.15. Initial conditions for the absorption chiller system [84]

Component	Parameter	Value
P-102	Output Pressure (kPa)	7.461
	Refrigerant mass flow (kg/s)	3.53
HX-102	Relation mass Refrigerant/Flue gas	0.1
HX-103	Output Temperature Diluted Refrigerant (°C)	89.9
HX-104	Output Temperature (°C)	40.2
	Cold water mass flow (kg/s)	7.07
	Inlet cooled water Temperature (°C)	25
HX-105	Output Temperature (°C)	2
	Inlet Temperature water	25

Component	Parameter	Value
A-101	Water mass flow (kg/s)	7.07
	Inlet Temperature (°C)	43.1
	Inlet Concentration LiBr (%)	0.574
	Cold water mass flow (kg/s)	7.07
	Inlet cooled water Temperature (°C)	25
V-101	Output Pressure (kPa)	0.672
V-102	Output Pressure (kPa)	0.672

3. Thermoeconomic Analysis

3.1. Fundamentals of Thermoeconomic Analysis

The thermoeconomic analysis is used in this work as an equivalent of exergoeocnomic analysi. It includes exergetic and economic analyses, in order to determine the cost of the irreversibilities of the process. The fundamentals of each analysis are explained in detail on the following sections.

3.1.1. Exergy Analysis

The exergy analysis was performed by using the engineering equation solver (EES) software for the formulation of mass, energy, and exergy balances for each component. In their general form, they are Eq. (1), Eq. (2), and Eq. (3), respectively:

$$\sum_{in} \dot{m}_{in} - \sum_{out} \dot{m}_{out} = 0 \tag{1}$$

$$\sum_{in} h_{in}\dot{m}_{in} - \sum_{out} h_{out}\dot{m}_{out} + \dot{W}_k + \dot{Q}_k = 0 \tag{2}$$

$$\sum_{k} \dot{E}_{q,k} + \dot{W}_k + \sum_{in} \dot{E}_{in} - \sum_{out} \dot{E}_{out} - \dot{E}_{D,k} = 0 \tag{3}$$

The enthalpies, entropies, molecular weights and densities of the pure substances in the process were determined using the functions in the EES software. For the streams that had soluble coffee solids as part of their compositions, Eq. (4) and Eq. (5) were used to determine the thermodynamic properties such as enthalpy and entropy. The C_p value was obtained from Burmester et al. [90]. The dead state conditions have been taken as T_0 = 27.5 ºC and P_0= 101.13 kPa.

$$h - h_0 = c_p(T - T_0) \tag{4}$$

$$\Delta S = \int_{T\,ref}^{T} \frac{Cp}{T} dT - \int_{P\,ref}^{P} \left(\frac{\partial V}{\partial T}\right)_P dP \tag{5}$$

The exergy rate, specific exergy, physical exergy, kinetic exergy and potential exergy are calculated using Eqs. (6) – (10).

$$\dot{E} = \dot{m} \cdot e \tag{6}$$

$$e = e^{PH} + e^{CH} + e^{KN} + e^{PT} \tag{7}$$

$$e^{PH} = (h - h_0) - T_0(s - s_0) \tag{8}$$

$$e^{PT} = gz \tag{9}$$

$$e^{KN} = \frac{v^2}{2} \tag{10}$$

Where h and s are the enthalpy and entropy values to a given state, while h_o and s_o are the enthalpy and entropy of the dead state, respectively.

The standard chemical exergies were obtained from the Model II [91]. The velocities of different streams were estimated by the Bernoulli relationship, Eq. (11), where γ is the specific heat ratio and ρ is the density of the stream.

$$\frac{\Delta v^2}{2} + \left(\frac{\gamma}{\gamma-1}\right) * \frac{P}{\rho} = \left(\frac{\gamma}{\gamma-1}\right) * \frac{P_0}{\rho_0} \tag{11}$$

The exegetic balance is developed through the following Eq. (12). Where $\dot{E}_F$, $\dot{E}_P$, $\dot{E}_D$, $\dot{E}_L$ are fuel exergy, product exergy, destroyed exergy and lost exergy respectively.

$$\dot{E}_{F,k} - \dot{E}_{P,k} = \dot{E}_{D,k} - \dot{E}_{L,k} \tag{12}$$

The exergetic efficiencies for each equipment present in the process are determined by relating the product and fuel exergy according to the following expression Eq. (13).

$$\eta_{e,k} = \left(\frac{E_{P,k}}{E_{F,k}}\right) \tag{13}$$

The exergetic factor presented in Eq. (14) is used to determine the amount of exergy destroyed on each component with respect to the total destroyed exergy.

$$y^*_{D,k} = \frac{\dot{E}_{D,k}}{\dot{E}_{D,tot}} \tag{14}$$

The exergetic factor presented in Eq. (15) is used to determine the destroyed equipment exergy with respect to the total fuel exergy.

$$y_{D,k} = \frac{\dot{E}_{D,k}}{\dot{E}_{F,tot}} \tag{15}$$

3.1.2. Economic Analysis

The economic analysis was developed following the methodology TRR (total revenue requirement) [22]. The investment cost rate and the operation and maintenance cost rate were determined for each component of the system.

The variable $\dot{Z}_k$ is calculated as the sum of capital investment ($\dot{Z}_k^{CI}$) and operation and maintenance costs ($\dot{Z}_k^{OM}$) for each component, as is shown in Eq. (16) [93].

$$\dot{Z}_k = \dot{Z}_k^{OM} + \dot{Z}_k^{CI} \tag{16}$$

The capital investment for each component can be calculated by using Eq. (17) [93]:

$$\dot{Z}_k^{CI} = \frac{PEC_k \cdot CRF}{\tau} \tag{17}$$

where PEC_k is the purchase price of the kth component, τ is the number of annual operating hours (24 hours per day, 365 days per year). It is assumed that the ordinary annuities transaction occurs at the end of each time interval, thus the CRF (capital recovery factor) can be obtained using Eq. (18) [93], where i_{eff} is the interest rate and n is the lifetime of the system (20 years).

$$\mathrm{CRF} = \frac{\mathrm{i_{eff}}\cdot(1+\mathrm{i_{eff}})^{\mathrm{n}}}{(1+\mathrm{i_{eff}})^{\mathrm{n}}-1} \tag{18}$$

The rate of operation and maintenance costs ($\dot{Z}_k^{OM}$) can be calculated by using Eq. (19). The operation and maintenance cost ($\mathrm{OMC_k}$) of each component is determined by using Eq. (20) which is a close approximation used by Bejan et al [93]. The constant-escalation levelization factor (CELF) was determined by using Eq. (21), which depends on the factor k_{OMC} defined by Eq. (22) [93]. For the nominal escalation rate (r^{OM}), it was assumed that all costs except fuel costs and the values of by-products change annually with the constant average inflation rate [93].

$$\dot{Z}_k^{OM} = \frac{OMC_k \cdot CELF^{OM}}{\tau} \tag{19}$$

$$OMC_k = 0{,}2 \cdot PEC_k \tag{20}$$

$$CELF^{OM} = \frac{k_{OMC}\cdot(1-{k_{OMC}}^{n})\cdot CRF}{(1-k_{OMC})} \tag{21}$$

$$k_{OMC} = \frac{1+r^{OM}}{1+i_{eff}} \tag{22}$$

The economic indicators [22] that were assumed for the analysis are described in Table 3.1.

Table 3.1. Economic indicators

Parameter	Value
Average general inflation rate	0.05
Average nominal escalation of all costs	0.05
Average nominal escalation of fuel costs	0.06
Plant economic life in years (n)	20
Plant life for tax purposes in years	15
Average combined income tax rate	0.38
Average property tax rate (%PFI)	0.015
Average insurance rate (%PFI)	0.5
Average capacity factor	0.85
Labor positions for O&M	20
Average labor rate ($/h)	18

3.1.3. Exergoeconomic Analysis

The exergoeconomic analysis consists of the formulation of a cost balance and its auxiliary equations at a component level, for each component of the process, proposed by Bejan et. al [22].. The general cost balance [93] is shown in Eq. (23) where c_{out} and c_{in}represent the costs of the outflows and inflows respectively, $c_{w,k}$ represents the cost rate related with the work and $\dot{Z}_k$ represents the investment cost of each component.

$$\sum_k c_{q,k}\dot{E}_{q,k} + c_{w,k}\dot{W}_k + \sum_{in} c_{in}\dot{E}_{in} - \sum_{out} c_{out}\dot{E}_{out} - c_{D,k}\dot{E}_{D,k} + \dot{Z}_k = 0 \quad (23)$$

The cost balance can be written in terms of the fuel and product formulation [94] as is shown in Eqs. (24) - (25).

$$\dot{C}_{F,k} + \dot{Z}_k = \dot{C}_{P,k} \quad (24)$$

$$c_{P,k}\dot{E}_{P,k} = c_{F,k}\dot{E}_{F,k} + \dot{Z}_k - \dot{C}_{D,k} \quad (25)$$

where $\dot{C}_{P,k}$ is the product cost rate, $\dot{C}_{F,k}$ is the fuel cost rate for each component.

The exergy destroyed in the k-th component has an associated cost rate $\dot{C}_{D,k}$ that can be calculated in terms of the cost of the additional fuel ($c_{F,k}$) that needs to be supplied to this component to cover the exergy destruction and to generate the same exergy flow rate of the product, when $\dot{E}_{P,k}$ stay constant (Eq. (26)) [93].

$$\dot{C}_{D,k} = c_{F,k}\dot{E}_{D,k} \quad (26)$$

where $\dot{C}_{D,k}$ is the cost rate associated with the destroyed exergy for each component.

For a better interpretation of the results, the exergoeconomic factor (f_k) and relative cost difference (r_k) were determined. The first factor represents the relationship between the investment cost and the total operating cost rate, while the r_k represents the increase of the specific exergy cost in a component divided by the specific exergy cost of the fuel.

$$f_k = \frac{\dot{Z}_k}{\dot{Z}_k + \dot{C}_{D,k}} \quad (27)$$

$$r_k = \frac{c_{P,k} - c_{F,k}}{c_{F,k}} \quad (28)$$

3.2. Application of thermoeconomic analysis to the processes

3.2.1. Roasting and solid liquid extraction

The following information was used for perform the exergoeconomic analysis of the roasting and solid liquid extraction process of coffee beans:

- The enthalpy of green and roasted coffee beans, extract, and spent coffee ground, as well as fuel and combustion gases were calculated by integrating the equation from the text by Felder & Rousseau [21]. This expression depends on the calorific capacity of each of the compounds and the change in temperature.
- For the entropy of streams of green and roasted coffee beans, extract, and spent coffee grounds, as well as fuel and combustion gases were calculated by integrating the Eq. (2).
- The molecular weight of the Diesel was determined using the Maxwell chart where 100 samples were used, later given a statistical treatment to obtain the approximate value of the molecular weight, the work was done by Hidalgo[15]. Diesel density was provided by Hidalgo [15], where using API density the relative density of 100 samples was determined.
- The calorific capacity of the green coffee bean was obtained from a study provided by Cardoso, de Andrade, Calderón, Rabelo, de Almeida Dias & Lemos [16]. The calorific capacity of roasted coffee beans was determined from a study by Schwartzberg [17]. The calorific capacities of the coffee extract and spent coffee grounds were obtained from Tellis-Romero, Gabas, Polizelli, & Telis [18].
- The specific heat of the Diesel was obtained from work done by Elijah, Olurunnishola, & Enyejo [20]. To determine the chemical exergy of diesel, the following Eq. (29). developed in the Bejan, Tsatsaronis, & Moran text [22] is used which is useful to calculate the chemical exergy of fuels that are pure hydrocarbons, although it can also be adapted to calculate the chemical exergy of any fuel.

$$e_{fuel}^{CH} = \overline{HHV}\,(T_o, P_o) - T_o\left[\bar{s}_{fuel} + \left(a + \frac{b}{4}\right)\bar{s}_{O_2} - a\bar{s}_{CO_2} - \frac{b}{2}\bar{s}_{H_2O}\right](T_o, P_o) + \left[a\bar{e}_{CO_2} + \frac{b}{2}\bar{e}_{H_2O} - \left(a + \frac{b}{4}\right)\bar{e}_{O_2}\right] \qquad where:\ C_aH_b \qquad (29)$$

where HHV is the heating higher value of the fuel at dead state conditions, this value was taken from literature [23]. The LHV or lower heating value for the case of Diesel was taken from previous studies [23].

- The molecular formula and the average molecular weight of the VOC's was determined by monitoring the VOC's during coffee roasting by mass spectrometry testing by Yeretzian, Jordan, Badoud, & Lindinger [24], selecting the compounds with the highest relative intensity of explosions.
- The chemical exergy for VOC's is determined following the methodology proposed by Bejan et al. text [22], which was developed to find the exergy of any substance not found in the environment. The chemical exergy for the streams of green and roasted coffee beans are estimated according to Eq. (30), it is obtained experimentally through the relationship between energy and exergy developed by Özilgen [25]. This expression includes all the contributions made by the nutrients present in the green and roasted coffee bean. The symbols P, F and C represent the dry-based fraction of proteins, carbohydrates, and lipids respectively.

$$e^{CH} = 25.4P + 39.6F + 17.5C \quad (30)$$

- The mass compositions of the compounds present in the roasted coffee bean were obtained by experimentation by Wei & Tanokura [26], subjecting green coffee beans to a roasting process, and by nuclear magnetic resonance to determine the concentration of the most abundant compounds. The compositions presented below are defined on a dry basis.

Table 3.2. Nutritional composition of green and roasted coffee beans

Component	Green Coffee Bean	Roasted Coffee Bean
Proteins	11.0 - 13.0 %	13.0 - 15.0 %
Carbohydrates	56.0 - 63.0 %	24.0 - 42.5 %
Lipids	12.0 - 18.0 %	14.5 - 20.0 %

- The chemical exergy of spent coffee ground is using a previous study from Song, Shen, & Xiao [27], which considered the elemental analysis.

Table 3.3. Elemental chemical composition of coffee bagasse.

Component	Green Coffee Bean
Carbon	52.24%
Hydrogen	6.95%
Oxygen	34.82%
Nitrogen	3.46%
Sulphur	0.1%

Ash	2.39%

- Coffee extract is a substance that can be assumed as a mixture, which has soluble solids, insolube solids and water. Therefore, the appropriate expression to determine the chemical exergy value of the extract is the Eq. (31). Where x_i is the molar fraction of the component, e_i^{CH} is the chemical exergy per component and R is the constant of the ideal gases.

$$e^{CH} = \sum x_i e_i^{CH} + RT_o \sum x_i \ln(x_i) \quad (31)$$

- Table 3.4 shows the expressions used for the calculation of fuel and product exergy rates.

Table 3.4. Fuel and product exergy for each system component.

Component	$\dot{E}_{F,k}$	$\dot{E}_{p,k}$
B-101	$\dot{W}_{B-101}$	$\dot{E}_{R-2} - \dot{E}_{R-1}$
P-101	$\dot{W}_{P-101}$	$\dot{E}_{R-6} - \dot{E}_{R-5}$
CC-101	$\dot{E}_{R-7}$	$\dot{E}_{R-9} - \dot{E}_{R-3}$
H-101	$\dot{E}_{R-10} - \dot{E}_{R-9} + \dot{Q}_{reaction}$	$\dot{E}_{R-13} - \dot{E}_{R-12}$
CS-101	$\dot{E}_{R-13} - \dot{E}_{R-15} - \dot{E}_{R-17}$	$\dot{E}_{R-16}$
Q-101	$\dot{E}_{R-8}$	$\dot{E}_{R-11} - \dot{E}_{R-4} - \dot{E}_{R-10}$
P-103	$\dot{W}_{P-103}$	$\dot{E}_{R-15} - \dot{E}_{R-14}$
P-102	$\dot{W}_{P-102}$	$\dot{E}_{E-2} - \dot{E}_{E-1}$
E-101	$\dot{E}_{C-1} - \dot{E}_{C-2}$	$\dot{E}_{E-3} - \dot{E}_{E-2}$
EX-101	$\dot{E}_{E-3} + \dot{E}_{E-11} - \dot{E}_{E-5}^{PH}$	$\dot{E}_{E-5}^{CH} - \dot{E}_{E-4} + (\dot{E}_{C-4} - \dot{E}_{C-3})$
E-102	$\dot{E}_{E-5} + \dot{E}_{C-5}$	$\dot{E}_{C-6} + \dot{E}_{E-6}$
P-104	$\dot{W}_{P-104}$	$\dot{E}_{E-7} - \dot{E}_{E-6}$
E-103	$\dot{E}_{C-7} + \dot{E}_{C-9} + \dot{E}_{E-7}$	$\dot{E}_{C-10} + \dot{E}_{C-8} + \dot{E}_{E-8}$

- For the economic analysis the following costs were considered: The green coffee beans used in the process have a price of \$3.09 per kg. The steam has a value of \$0.039 per kg. The Diesel 2 which is the fuel used by industry in Ecuador has a value of \$0.6381 per kg [29]. The cost of electric power is \$0.0765 per kWh [30], while the cost of water for industries in Guayaquil is \$0.72 per m^3 [31].
- Table 3.5 shows the fuel and product cost rates for the system under analysis.

Table 3.5. Cost balance equations for exergy costs.

Component	Fuel cost expression	Product cost expression	Auxiliary Equations
B-101	$\dot{W}_{B-101} \cdot c_{EP}$	$\dot{C}_{R-2} - \dot{C}_{R-1}$	$c_{R-1} = 0$ $c_{R-4} = c_{R-2}$ $c_{R-3} = c_{R-2}$
P-101	$\dot{W}_{P-101} \cdot c_{EP}$	$\dot{C}_{R-6} - \dot{C}_{R-5}$	$c_{R-7} = c_{R-6}$ $c_{R-8} = c_{R-6}$
CC-101	$\dot{C}_{R-7}$	$\dot{C}_{R-9} - \dot{C}_{R-3}$	-
H-101	$\dot{C}_{R-10} - \dot{C}_{R-9}$	$\dot{C}_{R-13} - \dot{E}_{R-12}$	$c_{R-9} = c_{R-10}$
CS-101	$\dot{C}_{R-13} - \dot{C}_{R-15} - \dot{E}_{R-17}$	$\dot{C}_{R-16}$	$c_{R-15} = c_{R-17}$
Q-101	$\dot{C}_{R-8}$	$\dot{C}_{R-11} - \dot{C}_{R-4} - \dot{C}_{R-10}$	-
P-103	$\dot{W}_{P-103} \cdot c_{EP}$	$\dot{C}_{R-15} - \dot{C}_{R-14}$	-
P-102	$\dot{W}_{P-102} \cdot c_{EP}$	$\dot{C}_{E-2} - \dot{C}_{E-1}$	-
E-101	$\dot{C}_{C-1} - \dot{C}_{C-2}$	$\dot{C}_{E-3} - \dot{C}_{E-2}$	$c_{C-1} = c_{C-2}$
EX-101	$\dot{C}_{E-3} + \dot{C}_{E-11} - \dot{E}^{PH}_{E-5} \cdot c_{E-5}$	$\dot{E}^{CH}_{E-5} \cdot c_{E-5} - \dot{C}_{E-4} - (\dot{C}_{C-4} - \dot{C}_{C-3})$	$c_{E-4} = 0$ $c_{C-3} = c_{C-4}$
E-102	$\dot{C}_{C-5} + \dot{C}_{E-5}$	$\dot{C}_{C-6} + \dot{C}_{E-6}$	$c_{C-5} = c_{C-6}$
P-104	$\dot{W}_{P-104} \cdot c_{EP}$	$\dot{C}_{E-7} - \dot{C}_{E-6}$	-
E-103	$\dot{C}_{C-7} + \dot{C}_{C-9} + \dot{C}_{E-7}$	$\dot{C}_{C-10} + \dot{C}_{C-8} + \dot{C}_{E-8}$	$c_{C-7} = c_{C-8}$ $c_{C-9} = c_{C-10}$

3.2.2. Double effect evaporation process

The following information was used for perform the exergoeconomic analysis of the double effect evaporation process of coffee extract:

- Table 3.6 shows the expressions used for the calculation of fuel and product exergy rates.

Table 3.6. Fuel and product exergy for each system component.

Component	$\dot{E}_{F,k}$	$\dot{E}_{P,k}$
EV-101	$\dot{E}_{S3} - \dot{E}_{S4} + \dot{W}_{D-101}$	$\dot{E}_8 + \dot{E}_{13} - \dot{E}_7$
EV-102	$\dot{E}_{13} - \dot{E}_{14} + \dot{W}_{D-102}$	$\dot{E}_7 + \dot{E}_{11} - \dot{E}_3$
P-101	$\dot{W}_{P-101}$	$\dot{E}_2 - \dot{E}_1$
P-102	$\dot{W}_{P-102}$	$\dot{E}_{16} - \dot{E}_{14}$
P-103	$\dot{W}_{P-103}$	$\dot{E}_{15} - \dot{E}_{12}$
P-104	$\dot{W}_{P-104}$	$\dot{E}_9 - \dot{E}_8$
P-105	$\dot{W}_{P-105}$	$\dot{E}_{S6} - \dot{E}_{S5}$

E-101	$\dot{E}_{11} - \dot{E}_{12}$	$\dot{E}_{W2} - \dot{E}_{W1}$
E-102	$\dot{E}_{S1} - \dot{E}_{S2}$	$\dot{E}_3 - \dot{E}_2$
E-103	$\dot{E}_{C1}^{PH} - \dot{E}_{C2}^{PH} + \dot{E}_9^{PH} + \dot{E}_{W3}^{PH}$	$\dot{E}_{10}^{PH} + \dot{E}_{W4}^{PH}$
B-201	$\dot{E}_I + \dot{E}_{II} - \dot{E}_{IV}$	$\dot{E}_V - \dot{E}_{III}$
M-201	$\dot{E}_V$	$\dot{E}_{VI} + \dot{E}_{VII}$
V-201	$\dot{E}_{VI}$	$\dot{E}_{S1}$
V-202	$\dot{E}_{VII}$	$\dot{E}_{S3}$
TK-201	$\dot{E}_{S6}$	$\dot{E}_{S7}$
P-201	$\dot{W}_{P-201}$	$\dot{E}_{III} - \dot{E}_{S7}$

The cost balance estimation requires the simultaneous resolution of a system equation. The components exergoeconomic equations as well the auxiliary relations are shown in Table 3.7 and definitions are obtained from literature [29][28].

Table 3.7. Cost balance equations for exergy costs

Component	**Fuel cost expression**	**Product cost expression**	**Auxiliary Equations**
EV-101	$\dot{C}_7 + \dot{C}_{S3} + \dot{C}_{W-D101}$	$\dot{C}_8 + \dot{C}_{13} + \dot{C}_{S4}$	$\frac{\dot{C}_{S4}}{\dot{E}x_{S4}} = \frac{\dot{C}_{S3}}{\dot{E}x_{S3}}$ $\frac{\dot{C}_7}{\dot{E}x_7} = \frac{\dot{C}_8}{\dot{E}x_8}$
EV-102	$\dot{C}_3 + \dot{C}_{13} + \dot{C}_{W-D102}$	$\dot{C}_7 + \dot{C}_{14} + \dot{C}_{11}$	$\frac{\dot{C}_{14}}{\dot{E}x_{14}} = \frac{\dot{C}_{13}}{\dot{E}x_{13}}$ $\frac{\dot{C}_7}{\dot{E}x_7} = \frac{\dot{C}_3}{\dot{E}x_3}$
P-101	$\dot{C}_1 + \dot{C}_{W-P101}$	$\dot{C}_2$	-
P-102	$\dot{C}_{14} + \dot{C}_{W-P102}$	$\dot{C}_{16}$	-
P-103	$\dot{C}_{12} + \dot{C}_{W-P103}$	$\dot{C}_{15}$	-
P-104	$\dot{C}_8 + \dot{C}_{W-P104}$	$\dot{C}_9$	-
P-105	$\dot{C}_{S5} + \dot{C}_{W-P105}$	$\dot{C}_{S6}$	-
P-201	$\dot{C}_{S7} + \dot{C}_{W-P201}$	$\dot{C}_{III}$	-
E-101	$\dot{C}_{11} + \dot{C}_{W1}$	$\dot{C}_{12} + \dot{C}_{W2}$	$\frac{\dot{C}_{12}}{\dot{E}x_{12}} = \frac{\dot{C}_{11}}{\dot{E}x_{11}}$

E-102	$\dot{C}_{S1} + \dot{C}_2$	$\dot{C}_3 + \dot{C}_{S2}$	$\frac{\dot{C}_{S2}}{\dot{E}x_{S2}} = \frac{\dot{C}_{S1}}{\dot{E}x_{S1}}$
E-103	$\dot{C}_9 + \dot{C}_{W3} + \dot{C}_{C1}$	$\dot{C}_{C2} + \dot{C}_{W4} + \dot{C}_{10}$	$\frac{\dot{C}_{10}}{\dot{E}x_{10}} = \frac{\dot{C}_{W4}}{\dot{E}x_{W4}}$ $\frac{\dot{C}_{C2}}{\dot{E}x_{C2}} = \frac{\dot{C}_{C1}}{\dot{E}x_{C1}}$
B-201	$\dot{C}_I + \dot{C}_{II} + \dot{C}_{III}$	$\dot{C}_V + \dot{C}_{IV}$	$\frac{\dot{C}_{II}}{\dot{E}x_{II}} = \frac{\dot{C}_{IV}}{\dot{E}x_{IV}}$
M-201	$\dot{C}_V$	$\dot{C}_{VI} + \dot{C}_{VII}$	$\frac{\dot{C}_{VI}}{\dot{E}x_{VI}} = \frac{\dot{C}_{VII}}{\dot{E}x_{VII}}$
V-201	$\dot{C}_{VI}$	$\dot{C}_{S1}$	-
V-202	$\dot{C}_{VII}$	$\dot{C}_{S3}$	-
TK-201	$\dot{C}_{S6}$	$\dot{C}_{S7}$	-

3.2.3. Spray Drying process

The following information was used for perform the exergoeconomic analysis of the spray drying process of concentrated coffee extract:

- The composition for the different states of the system are shown in Table 3.8. This information was used to calculate the different thermodynamic properties.

Table 3.8. Composition of the different states.

State	Description	Soluble solids (kg/kg)	Water (kg/kg)	Dried air (kg/kg)
2	Coffee extract	0.440	0.560	-
23	Soluble Coffee powder	0.970	0.030	-
24	Mixture BT	0.001	0.009	0.990
29	Mixture SD	0.004	0.040	0.955
33	Mixture S	0.038	0.008	0.954
34	Mixture FF	0.117	0.001	0.882

- For the calculation of chemical exergy of each state point that has soluble coffee solids and water, Eq. (32) [93] was used. The concentration of water and coffee in equilibrium with the environment (x_i^e) was chosen as the dead state of reference. Those values were

obtained from previous studies on Arabica coffee by Yao et al. [109]. For the calculation of the chemical exergy of each state point that has soluble coffee solids, water, and air, Eq. (31) [93].

$$e^{CH} = -RT_0 \sum x_i \ln\left(\frac{x_i^e}{x_i}\right) \tag{32}$$

- The chemical exergy of air for the different moisture content in air was calculated using an expression from Wepfer et al. [110], according to Eq. (33), where w_o and w are mole fraction of water vapor at environmental conditions and operational conditions, respectively.

$$e_{air}^{CH} = 0.2857 c_{p,air} T_o ln\left[\left[\frac{1+1.6078w_o}{1+1.6078w}\right]^{(1+1.6078w)}\left[\frac{w}{w_o}\right]^{1.6078w}\right] \tag{33}$$

- The exergy of the fuel and the exergy of the product for each single component have been formulated following Lazzareto and Tsatsaronis rules [94] and they are shown in Table 3.9.

Table 3.9. Definitions of fuel and product exergy for each component.

Component	$\dot{E}_{F,k}$	$\dot{E}_{P,k}$
LP	$\dot{W}_{LP}$	$\dot{E}_3 - \dot{E}_2$
HP	$\dot{W}_{HP}$	$\dot{E}_5 - \dot{E}_4$
HXE	$\dot{E}_{35} - \dot{E}_{36}$	$\dot{E}_6 - \dot{E}_5$
MHX	$\dot{E}_{37} - \dot{E}_{38}$	$\dot{E}_9 - \dot{E}_8$
SFBHX	$\dot{E}_{39} - \dot{E}_{40}$	$\dot{E}_{13} - \dot{E}_{12}$
VF1HX	$\dot{E}_{41} - \dot{E}_{42}$	$\dot{E}_{16} - \dot{E}_{15}$
VF2HX	$\dot{E}_{43} - \dot{E}_{44}$	$\dot{E}_{18} - \dot{E}_{17}$
MF	$\dot{W}_{MF}$	$\dot{E}_8 - \dot{E}_7$
SFBF	$\dot{W}_{SFBF}$	$\dot{E}_{12} - \dot{E}_{11}$
VF1F	$\dot{W}_{VF1F}$	$\dot{E}_{15} - \dot{E}_{14}$
VF2F	$\dot{W}_{VF2F}$	$\dot{E}_{20} - \dot{E}_{19}$
RFF	$\dot{W}_{RFF}$	$\dot{E}_{22} - \dot{E}_{21}$
FF	$\dot{W}_{FF}$	$\dot{E}_{32} + \dot{E}_{31} - \dot{E}_{30}$
SD	$\dot{E}_{13} + \dot{E}_9 - \dot{E}_{29}$	$\dot{E}_{23} - \dot{E}_6 - \dot{E}_{34}$
BT	$\dot{E}_{20} + \dot{E}_{16} - \dot{E}_{24}$	$\dot{E}_{25} - \dot{E}_{23}$
S	$\dot{E}_{27} + \dot{W}_S$	$\dot{E}_{26} + \dot{E}_{28} - \dot{E}_{25}$
B	$(\dot{E}_{49} + \dot{E}_{47}) - \dot{E}_{50}$	$\dot{E}_{51} - \dot{E}_{48}$
CHX	$\dot{E}_{45} - \dot{E}_{46}$	$\dot{E}_{14} + \dot{E}_{17} + \dot{E}_{11} - \dot{E}_{10}$

- Table 3.10 shows the equations used for the calculation of fuel and product cost rates.

Table 3.10. Cost balance equations and auxiliary equations for exergy costs of the system.

Component	Fuel cost expression	Product cost expression	Auxiliary equations
LP	$\dot{C}_3 + \dot{W}_{LP}$	$\dot{C}_2 + \dot{Z}_{LP}$	-
HP	$\dot{C}_5 + \dot{W}_{HP}$	$\dot{C}_4 + \dot{Z}_{HP}$	$c_4 = c_3 + c_1$
HXE	$\dot{C}_6 + \dot{C}_{36}$	$\dot{C}_5 + \dot{C}_{35}$	$c_{36} = c_{35} = c_{51}$
MHX	$\dot{C}_9 + \dot{C}_{38}$	$\dot{C}_8 + \dot{C}_{37}$	$c_{38} = c_{37} = c_{51}$
SFBHX	$\dot{C}_{13} + \dot{C}_{40}$	$\dot{C}_{12} + \dot{C}_{39}$	$c_{40} = c_{39} = c_{51}$
VF1HX	$\dot{C}_{16} + \dot{C}_{42}$	$\dot{C}_{15} + \dot{C}_{41}$	$c_{42} = c_{41} = c_{51}$
VF2HX	$\dot{C}_{18} + \dot{C}_{44}$	$\dot{C}_{17} + \dot{C}_{43}$	$c_{44} = c_{43} = c_{51}$
MF	$\dot{C}_8 + \dot{W}_{MF}$	$\dot{C}_7$	$c_7 = 0$
SFBF	$\dot{C}_{12} + \dot{W}_{SFBF}$	$\dot{C}_{11}$	-
VF1F	$\dot{C}_{15} + \dot{W}_{VF1F}$	$\dot{C}_{14}$	-
VF2F	$\dot{C}_{20} + \dot{W}_{VF2F}$	$\dot{C}_{19}$	$c_{19} = c_{18}$
RFF	$\dot{C}_{22} + \dot{W}_{RFF}$	$\dot{C}_{21}$	$c_{21} = c_{18}$
FF	$\dot{C}_{31} + \dot{C}_{32} + \dot{W}_{FF}$	$\dot{C}_{30}$	$c_{31} = c_{32}$
SD	$\dot{C}_{29} + \dot{C}_{23}$	$\dot{C}_6 + \dot{C}_9 + \dot{C}_{13} + \dot{C}_{34}$	$c_{29} = c_9$
BT	$\dot{C}_{24} + \dot{C}_{25}$	$\dot{C}_{16} + \dot{C}_{23}$	$c_{24} = c_{16}$
S	$\dot{W}_S$	$\dot{C}_{26} + \dot{C}_{27} - \dot{C}_{25} - \dot{C}_{28}$	$c_{28} = c_{30}; c_{29} = c_{31}$
B	$\dot{C}_{50} + \dot{C}_{51}$	$\dot{C}_{47} + \dot{C}_{48} + \dot{C}_{49}$	$c_{47} = 0; c_{49} = c_{50}$
CHX	$\dot{C}_{11} + \dot{C}_{14} + \dot{C}_{17} + \dot{C}_{46}$	$\dot{C}_{10} + \dot{C}_{45}$	$c_{10} = 0; c_{45} = c_{46}$ $c_{11} = c_{14} = c_{17}$

- There are some non-energetic costs used in the calculations of the cost balance of each component. In the boiler, the fuel used to generate vapor is fuel oil 6. The price of the liquid fuel (stream 49) is 1.07 $ per gallon [114]. The potable water (stream 48) has a cost of 0.53 $ per cubic meter [115] . The price of carbon dioxide (stream 1) injected into the coffee extract was 24.22 $ per kg.

3.2.4. Biofuels production from SCG

The following information was used for perform the exergoeconomic analysis of the syngas, biodiesel and biomass production process from SCG:

- The specific heat capacity expressions for substances were not included in the EES database, such as SCG [116], lipids [117], ash [118], char [119] and glycerin [120], they were found in the literature.

- The exergy of wet biomass was calculated by using Eq. (34) [121] where x_{DB} is the composition of SCG in a dry free ash basis.

$$e_{WB}^{CH} = x_{DB} \cdot e_{DB}^{CH} + \sum x_i \cdot e_i^{CH} \tag{34}$$

- The chemical exergy of the ashes was calculated by using the model proposed by Song et al. [122] which is based on a statistical study of ash in 86 varieties of biomass and depends on the total concentration of different minerals. For SCG, this total concentration was obtained from a study conducted on coffee waste [123]. The chemical exergies of SCG, defatted SCG, oil, char and the biodiesel were determined by using Eq. (35) applied to pure hydrocarbon fuels [121]. The molecular formula of each of these substances was estimated based on their respective ultimate analysis.

$$e_x^{CH} = \overline{HHV}(T_o, P_o) - T_o\left[\sum_R v_R \bar{s}_R - \sum_P v_P \bar{s}_P\right](T_o, P_o) - \left[\sum_P v_P \bar{e}_P^{CH} - \sum_R v_R \bar{e}_R^{CH}\right] \tag{35}$$

  Where $\overline{HHV}$ represents the higher heating value at the dead state conditions; v is the stochiometric coefficient of each combustion compound, and $\bar{s}$ the standard entropy of each compound. The higher heating values of SCG oil [80], biodiesel [124], SCG and defatted SCG [72], and char [46] were obtained from literature.

- For the calculation of the chemical exergy of glycerin, a reaction involving reference substances has been considered:

$$C_3H_8O_3 + 5\ O_2 \rightarrow 3CO_2 + 4H_2O$$

- Eq. (36) was used for the determination of the chemical exergy of glycerin [121]; where ΔG is the change in the Gibbs function at dead state conditions.

$$e_{gly}^{CH} = \Delta G - \left[\sum_P v_P\, \bar{e}_P^{CH} - \sum_R v_R \bar{e}_R^{CH}\right] \tag{36}$$

- Table 3.11 presents the definitions of the fuel and product exergy for each component of the process. For the overall system, the $\dot{E}_{heating}$ is the sum of the changes of exergy rates of the streams of steam used in the heating processes. $\dot{E}_{cooling}$ is the sum of the change of exergy rates of the streams of cooling water used in the cooling processes.

Table 3.11. Definitions of fuel and product exergy for each component.

Component	$\dot{E}_{F,k}$	$\dot{E}_{P,k}$
E-101	$\dot{E}_{S18} - \dot{E}_{S19}$	$\dot{E}_{S3} - \dot{E}_{S2}$
D-101	$\dot{E}_{S1} + \dot{E}_{S3}$	$\dot{E}_{S5}$
SO-101	$(\dot{E}_{S22} - \dot{E}_{S23}) - (\dot{E}_{S21} - \dot{E}_{S20}) + (\dot{E}_{S5} - \dot{E}_{S10})$	$\dot{E}_{S7} - \dot{E}_{S6}$
EV-101	$(\dot{E}_{S24} - \dot{E}_{S25}) + \dot{E}_{S7} - (\dot{E}_{S27} - \dot{E}_{S26})$	$\dot{E}_{S8} + \dot{E}_{S9}$
E-102	$\dot{E}_{S28} - \dot{E}_{S29}$	$\dot{E}_{S12} - \dot{E}_{S11}$
D-102	$\dot{E}_{S10} + \dot{E}_{S12}$	$\dot{E}_{S14}$
R-101	$\dot{E}_{S14} + \dot{E}_{S15} - \dot{E}_{S17}$	$\dot{E}_{S16}$
E-201	$\dot{E}_{B19} - \dot{E}_{B20}$	$\dot{E}_{B6} - \dot{E}_{B5}$
E-202	$\dot{E}_{B21} - \dot{E}_{B22}$	$\dot{E}_{B2} - \dot{E}_{B1}$
E-203	$\dot{E}_{B15} - \dot{E}_{B16}$	$\dot{E}_{B26} - \dot{E}_{B25}$
R-201	$\dot{E}_{B6} + \dot{E}_{B2} - \dot{E}_{B7} - \dot{E}_{B9}$	$\dot{E}_{B10}$
R-202	$(\dot{E}_{B13} - \dot{E}_{B14}) + (\dot{E}_{B23} - \dot{E}_{B24}) + \dot{E}_{B10}$	$\dot{E}_{B15}$
Overall system	$\dot{E}_{heating} - \dot{E}_{cooling} + \dot{E}_{S6} - \dot{E}_{S8} + \dot{E}_{S1} + \dot{E}_{S15} + \dot{E}_{B5} - (\dot{E}_{B7} - \dot{E}_{B9}) + \dot{E}_{B13} - \dot{E}_{B14}$	$\dot{E}_{B16} + \dot{E}_{S16}$

- The purchase equipment cost (PEC) for each component of the process was obtained from vendors based on the required characteristics and are presented in the results section. The costs of steam and carbon dioxide were considered as \$0.03/kg and \$24.22/ kg, respectively [125]. The cost of cooling water [126] is \$0.72/m^3. The cost of n-hexane, methanol, hydrogen chloride and sodium hydroxide were \$0.03/kg, \$1.15/kg, \$0.50/kg, \$0.04/kg, respectively, which were obtained from vendors.

- The cost rates were determined following the expressions from Table 3.12.

Table 3.12. Cost balance equations and auxiliary equations for exergy costs of the system.

Component	Fuel cost expression	Product cost expression	Auxiliary Equations
E-101	$\dot{C}_{S18} - \dot{C}_{S19}$	$\dot{C}_{S3} - \dot{C}_{S2}$	$c_{S2} = 0$
			$c_{S19} = c_{S18}$
D-101	$\dot{C}_{S1} + \dot{C}_{S3}$	$\dot{C}_{S5}$	$c_{S1} = 0$
SO-101	$(\dot{C}_{S22} - \dot{C}_{S23}) - (\dot{C}_{S21} - \dot{C}_{S20}) + (C_{S5} - \dot{C}_{S10})$	$\dot{C}_{S7} - \dot{C}_{S6}$	$c_{S21} = c_{S20}$
			$c_{S23} = c_{S22}$
			$c_{S10} = c_{S7}$
EV-101	$(\dot{C}_{S24} - \dot{C}_{S25}) + \dot{C}_{S7} - (\dot{C}_{S27} - \dot{C}_{S26})$	$\dot{C}_{S8} + \dot{C}_{S9}$	$c_{S25} = c_{S24}$
			$c_{S27} = c_{S26}$
			$c_{S8} = c_{S9}$
E-102	$\dot{C}_{S28} - C_{S29}$	$\dot{C}_{S12} - \dot{C}_{S11}$	$c_{S11} = 0$
			$c_{S29} = c_{S28}$
D-102	$\dot{C}_{S10} + \dot{C}_{S12}$	$\dot{C}_{S14}$	-
R-101	$\dot{C}_{S14} + \dot{C}_{S15} - \dot{C}_{S17}$	$\dot{C}_{S16}$	$c_{S17} = c_{S16}$
E-201	$\dot{C}_{B19} - \dot{C}_{B20}$	$\dot{C}_{B6} - \dot{C}_{B5}$	$c_{B19} = c_{B20}$
E-202	$\dot{C}_{B21} - \dot{C}_{B22}$	$\dot{C}_{B2} - \dot{C}_{B1}$	$c_{B21} = c_{B22}$
E-203	$\dot{C}_{B15} - \dot{C}_{B16}$	$\dot{C}_{B26} - \dot{C}_{B25}$	$c_{B26} = c_{B25}$
			$c_{B17} = c_{B18}$
R-201	$\dot{C}_{B6} + \dot{C}_{B2} - \dot{C}_{B7} - \dot{C}_{B9}$	$\dot{C}_{B10}$	$c_{B7} = c_{B6}$
			$c_{B9} = c_{B6}$
R-202	$(\dot{C}_{B13} - \dot{C}_{B14}) + (\dot{C}_{B23} - \dot{C}_{B24}) + \dot{C}_{B10}$	$\dot{C}_{B15}$	$c_{B23} = c_{B24}$
			$c_{B14} = c_{B13}$

Overall System	$\dot{C}_{heating} - \dot{C}_{cooling} + \dot{C}_{S6} - \dot{C}_{S8} + \dot{C}_{S1} + \dot{C}_{S15} + \dot{C}_{B5} - (\dot{C}_{B7} - \dot{C}_{B9}) \quad \dot{C}_{B16} + \dot{C}_{S16} + \dot{C}_{B13} - \dot{C}_{B14}$

3.2.5. Trigeneration system

The following information was used for perform the exergoeconomic analysis of trigeneration system based on biofuels:

- The heat capacities of substances that are not defined in the EES database, such as diesel [127], biodiesel [128], fuel oil No. 6 [129], SCG [116], were taken from the literature.
- The composition of the natural gas [88], syngas [130], as well as the molecular weights were obtained from an estimate based on an ultimate analysis taken from previous studies.
- The standard chemical exergy of lithium bromide [131] and ammonia [132] were obtained from literature. The chemical exergy of diesel and fuel oil 6 were obtained using Eq. (4), which is only useful for pure hydrocarbons, where a represents the number of carbon atoms and b represents the number of hydrogen atoms in the molecule. The molecular weight of the Diesel was determined using the Maxwell chart where 100 samples were used, later given a statistical treatment to obtain the approximate value of the molecular weight, the work was done by Hidalgo [95]. The molecular weight of the fuel oil 6 was obtained from an estimation of an elementary analysis performed by Park et al. [83].
- In the case of biodiesel, Eq. (43) was used, which can be used for any type of fuel, both equations were obtained from Bejan, Tsatsaronis, & Moran [121]. The composition of the biodiesel was estimated based on their respective ultimate analysis [80].
- $\overline{HHV}$ represents the higher heating value at dead state conditions, and for diesel [133] and biodiesel [134] and fuel oil 6 [135] were taken from literature. The lower heating value for SCG [72], syngas [136], natural gas [137], diesel [133], biodiesel [138] and fuel oil No. 6 [135] were obtained from previous studies.
- The chemical exergy of dry biomass is evaluated by Eq. (37), which is obtained from a study carried out by Song, Shen, & Xiao [101]. In the expression H, C, N, O, S, A they represent the mass fraction on dry basis of hydrogen, carbon, oxygen, sulfur, and ash

respectively. The composition of the SCG was determined according to the results of a previous study conducted by Vardon et al. [72].

$$e_{SCG}^{CH} = 1812.5 + 295.606 \cdot C + 587.354 \cdot H + 17.506 \cdot O + 17.735 \cdot N + 95.615 \cdot S - 31.8 \cdot A \quad (37)$$

- Table 3.13 shows the equations used to determine the fuel and product exergy in each of the system components.

Table 3.13. Exergy of fuel and product.

Component	$\dot{E}_{F,k}$	$\dot{E}_{P,k}$
P-101	$\dot{W}_{P-101}$	$\dot{E}_2 - \dot{E}_1$
C-101	$\dot{W}_{C-101}$	$\dot{E}_4 - \dot{E}_3$
CC-101	$\dot{E}_2$	$\dot{E}_5 - \dot{E}_4$
T-101	$\dot{E}_5 - \dot{E}_6$	$\dot{W}_{T-101}$
HX-101	$\dot{E}_6 - \dot{E}_7$	$\dot{E}_9 - \dot{E}_8$
HX-102	$(\dot{E}_7 - \dot{E}_{10}) + \dot{E}_{12}$	$\dot{E}_{15} - \dot{E}_{17}$
HX-103	$\dot{E}_{12} - \dot{E}_{13}$	$\dot{E}_{15} - \dot{E}_{14}$
HX-104	$\dot{E}_{17} + \dot{E}_{18}$	$\dot{E}_{19} + \dot{E}_{20}$
HX-105	$\dot{E}_{24} - \dot{E}_{21}$	$\dot{E}_{23} + \dot{E}_{22}$
P-102	$\dot{W}_{P-102}$	$\dot{E}_{15} - \dot{E}_{14}$
A-101	$(\dot{E}_{26} - \dot{E}_{25}) + \dot{E}_{13} + \dot{E}_{24}$	$\dot{E}_{14}$

- The purchase equipment cost (PEC) was determined based on certain specific characteristics of each of the equipment present in the system. For the case of evaporators, pumps and exchangers we used Eq. (38) proposed by Towler & Sinnott [39].

$$PEC = a + b \cdot S^n \quad (38)$$

Where a and b represent cost constants, n is an exponent and S is the size parameter, each of these values are specific to each type of equipment. Table 3.14 shows the values of constants and parameters for these components.

Table 3.14. Cost constants, exponent and size parameter

Components	a	b	n	S
Evaporators	330	36000	0.55	0.36 [m^2]
Pumps	8000	240	0.9	2.22 [L/s]
Heat exchangers	28000	54	1.2	3.15 [m^2]

- The purchase equipment cost of the turbine was determined using Eq. (39) provided by Kolahi, Yari, Mahmoudi & Mohammadkhani [40].

$$log(PEC) = k_1 + k_2 \cdot log_{10}(A_i) + k_3 \cdot [log_{10}(A_i)]^2 \quad (39)$$

where k_1, k_2 and k_3 represent constants while $A_i$the power produced by the equipment in kW.

- The purchase equipment cost for compressor is determined by Eq. (40) proposed by Bejan et al. [29], which depends on the flow rate entering the equipment in kg/s, the inlet and outlet pressure in MPa and the isentropic efficiency of the equipment.

$$PEC_{c-101} = \left(\frac{71.1 \cdot \dot{m}}{0.9 - \eta_{is}}\right)\left(\frac{P_{out}}{P_{in}}\right) ln\left(\frac{P_{out}}{P_{In}}\right) \quad (40)$$

- In the case of the combustion chamber, we used the Eq. (41) proposed by Amidpour, Hasan & Man [41], which depends on the mass flow of air entering the combustion chamber in kg/s, as well as the air inlet pressure in kPa, the pressure and outlet temperature of the combustion gases in K. For the condenser we used the Eq. (42) proposed by Abam, Briggs, Ekwe & Effiom [42], which depends on the inlet and outlet temperatures of the cold and hot streams in K, the mass flow of the hot stream in kg/s, as well as the condenser heat in MW units.

$$PEC_{CC-101} = \frac{28.98 \cdot \dot{m}_{air}}{0.995\left(\frac{P_{out}}{P_{in}}\right)} \cdot (1 + e^{(0.015(T_{out}-1540))}) \quad (41)$$

$$PEC_{HX-104} = 280.74 \frac{Q_{cond}}{22000\left[\frac{(T_{in,hs} - T_{out,cs}) - (T_{out,hs} - T_{in,cs})}{ln\left(\frac{T_{in,hs} - T_{out,cs}}{T_{out,hs} - T_{in,cs}}\right)}\right]} + 746 \cdot \dot{m}_{out,cs} \quad (42)$$

- The cost of natural gas [36], diesel [43] were considered as 0.0894 $/kg and 0.6381 $/kg respectively. The cost of water is 0.72 $/m3 [43]. The cos of the power electricity in Guayaquil, Ecuador is 0.0756 $/kWh [44]. The cost of syngas, SCG, fuel oil No. 6, lithium bromide and ammonia were 0.326 $/kg, 2.46 $/kg, 0.257 $/kg, 0.3 $/kg and 0.6 $/kg respectively, which were obtained from different suppliers.
- Table 3.15 shows the fuel and product cost equations for the proposed system.

Table 3.15. Fuel and product cost rates

Component	Fuel cost expression	Product cost expression	Auxiliary Equations
P-101	$\dot{W}_{P-101} \cdot c_{EP}$	$\dot{C}_2 - \dot{C}_1$	c_1

C-101	$\dot{W}_{C-101} \cdot c_{EP}$	$\dot{C}_4 - \dot{C}_3$	c_3
CC-101	$\dot{C}_2$	$\dot{C}_5 - \dot{C}_4$	-
T-101	$\dot{C}_5 - \dot{C}_6$	$\dot{W}_{T-101}$	-
HX-101	$C_6 - \dot{C}_7$	$\dot{C}_9 - \dot{C}_8$	$c_6 = c_7$
HX-102	$(\dot{C}_7 - \dot{C}_{10}) + \dot{C}_{12}$	$\dot{C}_{15} - \dot{C}_{17}$	$c_7 = c_{10}$
HX-103	$\dot{C}_{12} - \dot{C}_{13}$	$\dot{C}_{15} - \dot{C}_{14}$	$c_{14} = c_{15}$
HX-104	$\dot{C}_{17} + \dot{C}_{18}$	$\dot{C}_{19} + \dot{C}_{20}$	$c_{18} = c_{19}$
HX-105	$\dot{C}_{24} - \dot{C}_{21}$	$\dot{C}_{23} + \dot{C}_{22}$	$c_{22} = c_{23}$
P-102	$\dot{W}_{P-102} \cdot c_{EP}$	$\dot{C}_{15} - \dot{C}_{14}$	c_{14}
A-101	$(\dot{C}_{26} - \dot{C}_{25}) + \dot{C}_{13} + \dot{C}_{24}$	$\dot{C}_{14}$	$c_{25} = c_{26}$

4. Results and Discussion

4.1. Exergoeconomic Analysis of the roasting and coffee extraction process

Table 4.1 contains the data of the operating conditions (T, P), as well as the data of enthalpy (h), entropy (s), physical exergy ($\dot{E}^{PH}$), chemical exergy ($\dot{E}^{CH}$) and total exergy of each of the process currents.

Table 4.1 Thermodynamics properties of the stream process.

Stream	m (kg/h)	T (ºC)	P (kPa)	h (kJ/kg)	s (kJ/kg-K)	$\dot{E}^{PH}$ (kW)	$\dot{E}^{CH}$ (kW)	$\dot{E}$ (kW)
R-1	1256.4	25	101	237	5.24	0	0	0
R-2	1256.4	196	500	411	5.24	61	0	61
R-3	1242.0	196	500	411	5.24	60	0	60
R-4	15.0	196	500	411	5.24	1	0	1
R-5	79.6	25	101	44	0.15	0	1080	1080
R-6	79.6	35	500	62	0.15	0	1080	1080
R-7	76.7	35	500	62	0.15	0	1050	1050
R-8	2.7	35	50	62	0.15	0	37	37
R-9	1321.2	232	500	598	5.47	80	15	94
R-10	1551.6	232	500	932	5.71	128	52	179
R-11	1569.6	283	500	1010	5.84	143	47	190
R-12	2059.2	25	101	48	0.17	0	11700	11700
R-13	1828.8	360	101	1310	3.06	204	11900	12100
R-14	352.8	25	101	105	0.37	0	0	0
R-15	352.8	25	300	105	0.37	0	0	0
R-16	1908.0	25	101	37	0.13	0	11900	11900
R-17	271.8	80	101	335	1.08	1	0	2
R-18	1908.0	50	101	82	0.27	1	11900	11900
R-19	1026.0	50	101	82	0.27	0	6390	6390
E-1	5004.0	40	101	168	0.57	2	3	6
E-2	5004.0	41	138	173	0.59	4	3	8
E-3	5004.0	179	1383	761	2.13	180	3	183
E-4	3412.8	72	101	103	0.34	5	1970	1970
E-5	2473.2	120	200	457	1.39	33	6110	6150
E-6	2473.2	64	200	236	0.78	6	6110	6120
E-7	2473.2	65	318	240	0.79	6	6110	6120

E-8	2473.2	12	196	45	0.16	1	6110	6110
E-9	2469.6	12	196	45	0.16	1	6100	6100
E-10	4.9	12	196	18	0.06	0	3	3
E-11	882.0	50	101	82	0.27	0	5490	5490
C-1	1965.6	190	125	2790	6.51	464	262	726
C-2	1965.6	18	1250	807	2.23	79	262	341
C-3	86760.0	30	155	126	0.44	5	60	66
C-4	86760.0	40	155	168	0.57	38	60	98
C-5	31896.0	30	155	126	0.44	2	22	24
C-6	31896.0	40	155	168	0.57	14	22	36
C-7	6084.0	30	155	126	0.44	0	4	5
C-8	6084.0	40	155	168	0.57	3	4	7
C-9	5544.0	5	500	22	0.08	5	4	9
C-10	5544.0	14	500	59	0.21	2	4	6

Table 4.2 shows the fuel and product exergy rates, the exergy destroyed, the exergy efficiency, as well as the exergy destruction ratios of each of the system components. For the roasting process, the equipment with the highest fuel exergy rate are CS-101 and CC-101, while EX-101 and E-101 have the most significant fuel exergy rate in the extraction process. CS-101 and P-101 are the components with the highest exergy efficiency in the roasting process with 98.45 and 72.20% respectively, while E-102 and E-103 are in the extraction process with 99.76 and 99.89% respectively.

The roasting process presents an exergy destruction of 1555 kW, resulting in an exergy efficiency of 88.88%, while the liquid-solid extraction process destroys 1774 kW of exergy, resulting in an exergy efficiency of 90.32%. In a previous study [35], the real coffee roasting process was thermodynamically evaluated, where an exergy destruction of 614 kW and an exergy efficiency of 33.26% was obtained, while in another study [36], where pistachio roasting was performed, an exergy destruction of 78.3 kW and an exergy efficiency of 9.96% was obtained. In different studies on oil extraction processes from organic solids using different routes, energy efficiencies between 24 and 55% were obtained [37, 39].

Table 4.2 Exergetic analysis in system equipment.

Component	$\dot{E}_{F,k}$ (kW)	$\dot{E}_{P,k}$ (kW)	$\dot{E}_{D,k}$ (kW)	$\eta_{e,k}$ (%)	$y^*_{D,k}$	$y_{D,k}$
B-101	87	61	26	69.8	0.008	0.001
P-101	1	0	0	72.2	0.000	0.000
CC-101	1050	34	1010	3.3	0.304	0.031
H-101	659	356	303	54.1	0.091	0.009
CS-101	12100	11900	188	98.5	0.056	0.006
Q-101	37	10	27	26.8	0.008	0.001
P-103	0	0	0	23.2	0.000	0.000
P-102	11	2	8	19.6	0.003	0.000
E-101	385	176	209	45.7	0.063	0.006
EX-101	5640	4110	1530	72.9	0.460	0.048
E-102	6170	6160	15	99.8	0.005	0.000
P-104	4	0	3	8.0	0.001	0.000
E-103	6130	6130	7	99.9	0.002	0.000

Figure 4.1 and Figure 4.2 show the fuel and product exergy rate of the roasting process and the solid-liquid extraction respectively. The combustion chamber "CC-101" and the extractor "EX-101" are the equipment that have the greatest impact on the exergy destruction for the roasting and extraction process. This is because these components use heat as the most important supply for the exergy rate of the fuel, and in these equipments there are processes where significant amounts of heat are transferred, which makes them have a greater tendency to destroy exergy. On the other hand, components such as pumps and compressors where the main source of fuel exergy is electrical energy have the lowest impact on the exergy destroyed in the system. Similar results can be observed in a study carried out by Sadreddini, Fani, Ashjari Aghdam & Mohammadi [40] where an exergy analysis and optimization of a CCHP system was performed, in which it was found that the combustion chamber was the equipment with the highest exergy destruction rate, while pumps and compressors were the ones that destroyed the least exergy.

Additionally, the CC-101 and EX-101 components have the highest exergy destruction ratio compared to the fuel exergy ratio, in contrast to the P-101 and P-104 components, which have the lowest amount.

In the green coffee bean roasting process, the equipment that destroys the most exergy are the combustion chamber "CC-101" and the furnace "H-101" with 30.39% and 9.09% respectively of the total exergy destroyed in the overall system, while for the liquid solid extraction process, the extractor "EX-101" and the heat exchanger "E-101" are the equipment that destroy the most exergy with 46.01% and 6.28% respectively of the overall total of the system.

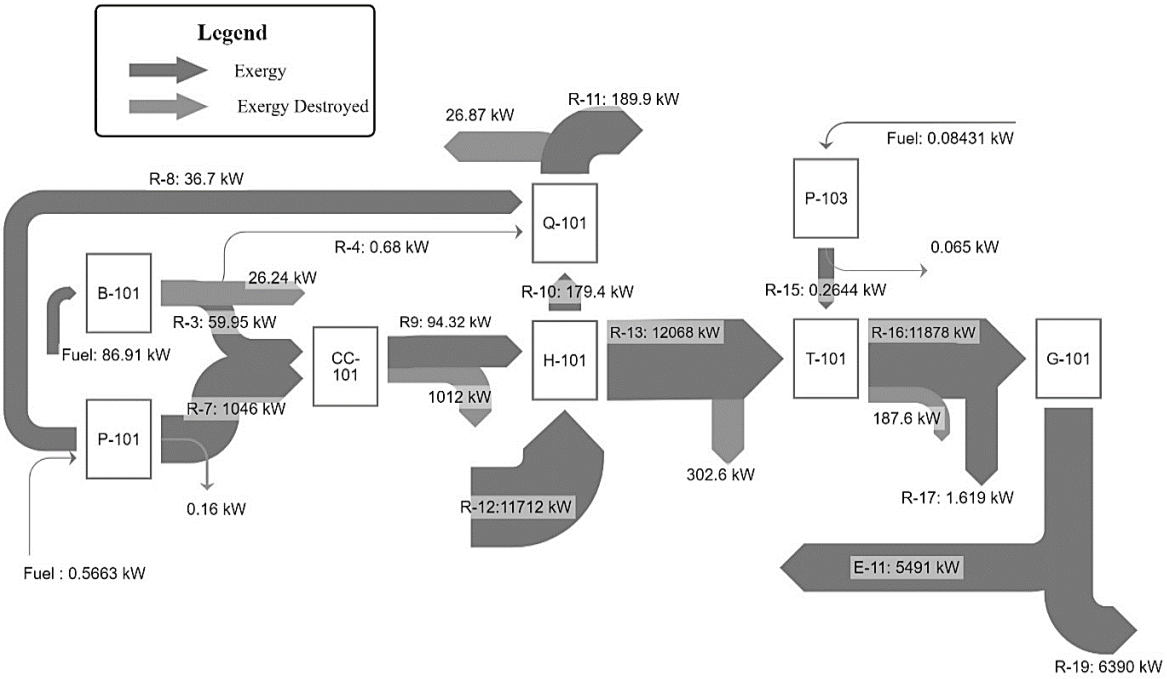

Figure 4.1. Grassman diagram of the coffee roasting process

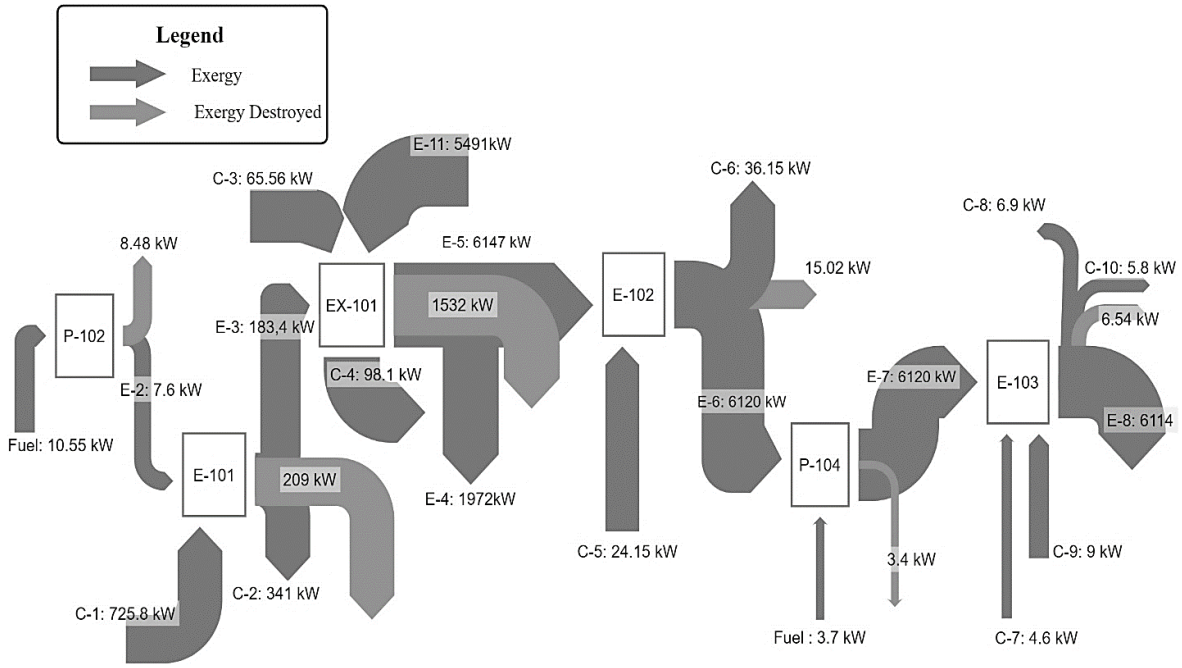

Figure 4.2. Grassman diagram of the solid-liquid extraction coffee process

The C-101 equipment has a high exergy destruction because it is an equipment where chemical reactions are carried out, which are characterized by having a large amount of irreversibilities, in addition to a large energy transfer because the combustion gases leave at a high temperature, to this is added that it converts high quality energy from the fuel into low quality energy. In a previous study [41] where a combustion chamber was used to generate gases at high temperature, similar results were obtained since this equipment represented the highest energy loss of the system with 76% of the total.

For the furnace "H-101" a similar analysis can be made regarding the causes of the high exergy destruction. The chemical reactions that take place in this equipment between the combustion gases and the green coffee beans fed to the process generate high irreversibilities, in addition to the heat transfer and the loss of heat in the exhaust gases generate a high destruction of exergy.

Table 4.3 contains the data of the cost of fuel ($\dot{C}_{F,k}$), cost of product ($\dot{C}_{P,k}$), operation cost ($\dot{Z}_k + \dot{C}_{D,k}$), destroyed exergy cost ($\dot{C}_{D,k}$), exergoeconomic fator (f_k), and relative cost differnecia (r_k) of each of the process components.

Table 4.3 Results of the exergoeconomic analysis of the coffee roasting and extraction process

Component	$\dot{C}_{F,k}$ **(\$/h)**	$\dot{C}_{P,k}$ **(\$/h)**	$\dot{Z}_k + \dot{C}_{D,k}$ **(\$/h)**	$\dot{C}_{D,k}$ **(\$/h)**	f_k **(%)**	r_k
B-101	6.66	8.39	3.74	2.01	46.3	0.81
P-101	0.04	0.19	0.16	0.01	92.3	4.99
CC-101	49.32	50.76	49.32	47.52	3.6	30.50
H-101	53.28	77.40	48.60	24.55	49.5	1.68
CS-101	6444	6480	129.96	100.08	22.9	0.02
Q-101	1.72	1.76	1.30	1.26	2.8	2.81
P-103	0.01	0.15	0.15	0.00	96.7	99.70
P-102	0.81	7.31	7.16	0.65	91.0	45.20
E-101	40.68	60.48	42.12	22.07	47.5	2.27
EX-101	3045	3092	874.80	828	5.4	0.39
E-102	3164	3175	19.44	7.70	60.4	0.01
P-104	0.29	2.98	2.96	0.26	91.1	129.00
E-103	3315	3330	17.21	3.54	79.5	0.01

The components with the highest operating cost $\dot{Z}_k + \dot{C}_{D,k}$ for the roasting process are the CS-101 and CC-101 components, while for the extraction process they are the EX-101 and E-101 equipment, which means that this equipment contributes significantly to the costs of the overall process.

The components with the highest exergoeconomic factor for the roasting process and for the extraction process are P-103 and P-104 with 96.7 and 91.1% respectively, while those with the lowest f_k are Q-101 and EX101 for the roasting and extraction processes respectively. The results obtained for this parameter for each of the components present in the system are within the typical values for this parameter [22].

The increase of capital investment in the components with the highest exergoeconomic factor in the system would generate a significant increase in the exergy efficiency of the components in question and of the overall process, likewise it is possible to find ways to reduce capital investment in equipment with a high exergoeconomic factor without affecting the profitability of the process but sacrificing exergy efficiency.

4.2. Exergoeconomic analysis of the double effect evaporation process

Table 4.4 contains the data of the operating conditions (T, P), as well as the data of enthalpy (h), entropy (s), specific physical exergy (e^{PH}), chemical exergy (e^{CH}) and total exergy of each of the process currents.

Table 4.4 Thermodynamic values of the streams

Stream	T (ºC)	P (kPa)	m (kg/h)	SS %	e^{PH} (kJ/kg)	e^{CH} (kJ/kg)	Ė (kW)
1	23	101	4598	22.0	0.0	4072	5201
2	23	2698	4598	22.0	2.4	4072	5204
3	50	2698	4598	22.0	5.3	4072	5208
4	50	677	20190	28.9	3.2	5333	29925
5	50	12	18901	30.6	2.6	5639	29622
6	50	677	15579	30.6	3.2	5639	24418
7	50	677	3309	30.6	3.2	5639	5186
8	65	25	1905	53.1	5.2	9756	5165
9	66	7284	1905	53.1	11.4	9756	5168
10	11	7284	1905	53.1	6.5	9756	5166
11	50	12	1289	0.0	189.1	50	86

12	32	12	1289	0.0	0.2	50	18
13	65	25	1404	0.0	287.5	50	132
14	65	25	1404	0.0	10.2	50	23
15	32	4892	1289	0.0	5.1	50	20
16	65	8046	1404	0.0	18.3	50	27
17	51	4892	2693	0.0	9.2	50	44
S1	155	101	184	0.0	515.6	50	29
S2	100	101	184	0.0	33.9	50	4
S3	155	101	1464	0.0	515.6	50	230
S4	100	101	1464	0.0	33.9	50	34
S5	100	101	1648	0.0	33.9	50	38
S6	100	2512	1648	0.0	36.7	50	40
S7	100	130	1648	0.0	34.3	50	39
W1	27	101	329712	0.0	0.0	50	4574
W2	30	101	329712	0.0	0.2	50	4584
W3	26	317	4984	0.0	0.2	50	69
W4	33	317	4984	0.0	0.7	50	70
C1	5	101	8400	0.0	3.0	50	123
C2	10	101	8400	0.0	1.6	50	120

The exergy rate of the fuel ($\dot{\mathbf{E}}_{F,k}$) and the product ($\dot{\mathbf{E}}_{P,k}$), the exergetic ($\boldsymbol{\eta}_{\mathbf{e,k}}$) and the exergy destruction ratio ($\boldsymbol{y}^{*}_{\boldsymbol{D,k}}$) were calculated for each component in the system. The results are summarized in Table 4.5. The components with the highest exergy fuel rates are the evaporators EV-101 and EV-102. The components with the lowest exergy efficiency are the heat exchanger E-101, E-102 and E-103.

Table 4.5 Results of the exergy analysis of all the components of the double effect evaporation process.

Component	$\dot{\mathbf{E}}_{\mathbf{F,k}}$ **(kW)**	$\dot{\mathbf{E}}_{\mathbf{P,k}}$ **(kW)**	$\dot{\mathbf{E}}_{\mathbf{D,k}}$ **(kW)**	$\boldsymbol{\eta}_{\mathbf{e,k}}$ **(%)**	$\mathbf{y}^{*}_{\mathbf{D,k}}$ **(%)**
EV-101	210.7	110.3	100.4	52	7.37
EV-102	115.9	64.5	51.4	56	3.77
P-101	4.0	3.1	0.9	77	0.07
P-102	4.0	3.2	0.8	79	0.06
P-103	2.2	1.8	0.4	80	0.03

P-104	4.0	3.3	0.7	82	0.05
P-105	1.5	1.2	0.3	83	0.02
E-101	67.6	10.4	57.3	15	4.21
E-102	24.6	3.6	20.9	15	1.54
E-103	9.4	4.3	5.0	46	0.37
P-201	0.7	0.6	0.1	79	0.01

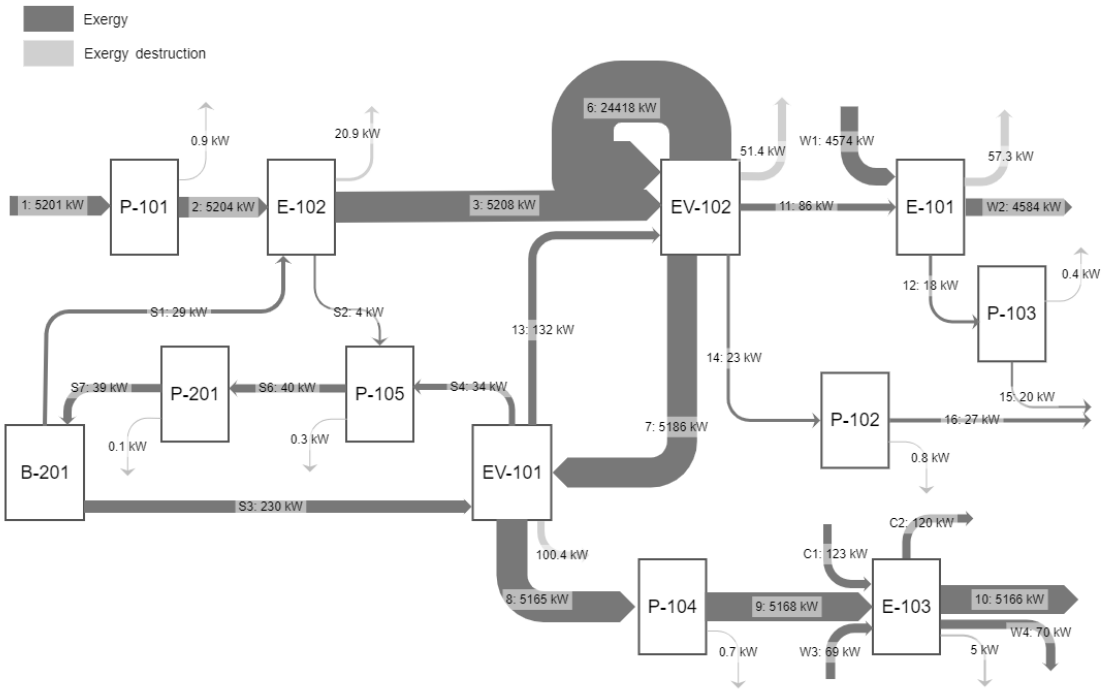

Figure 4.3. Grassmann's diagram of the double effect evaporation process

Figure 4.3 shows the diagram of Grassmann for the process, it shows that 77% of the fuel exergy is available on the product, and the total exergy destruction rate of this process is 1362 kW.

Table 4.6 shows the exergoeconomic indicators obtained from the analysis of the process. The heat exchanger E-101 has de highest exergy destruction cost rat, with an exergoeconomic factor of 2%, which mean that the capital investment cost are negligible.

Table 4.6 Results of the Exergoeconomic Analysis

Component	$\mathbf{f_k}$ **(%)**	$\mathbf{r_k}$	$\mathbf{\dot{C}_{D,k}}$ **(\$/h)**	$\mathbf{\dot{Z}_k + \dot{C}_{D,k}}$ **(\$/h)**
E-101	2.0	4.5	302.5	360.07
EV-102	55.0	1.5	83.4	212.00

EV-101	86	6.4	13.6	101.57
E-103	8	$8x10^{-4}$	29.6	44.62
E-102	23	7.4	3.3	4.78
P-101	89	2.8	0.1	0.81
P-102	90	2.7	0.1	0.81
P-104	91	2.9	0.04	0.80
P-103	91	2.6	0.1	0.49
P-105	93	3.0	9.92	0.36
P-201	93	3.8	0.01	0.19

The required modifications should be focused to reduce the exergy destruction cost rate (even if this results in a higher investment cost), because the components that have the highest operating cost, also have the lowest exergoeconomic factor (less than 10%).

4.3. Exergoeconomic analysis of the spray drying process

The parameters of the exergetic analysis were calculated for each state throughout the entire studied system. Table 4.7 shows the flow rate ($\dot{m}$), temperature (T), pressure (P), specific chemical exergy (e^{CH}), specific physical exergy (e^{PH}), specific kinetic exergy (e^{KN}) and exergy rate ($\dot{E}$) of each stream.

Table 4.7 Thermodynamic values of the streams.

Stream	ṁ (kg/h)	T (ºC)	P (kPa)	e^{CH} (kJ/kg)	e^{PH} (kJ/kg)	e^{KN} (kJ/kg)	Ė (kJ/h)
1	7.4	12	101	322	0.22	0.0	2383
2	528	14	101	2.25	10.8	0.0	6891
3	528	15	750	2.25	9.70	0.5	6593
4	528	16	750	1.56	8.84	0.5	5776
5	528	18	5400	1.56	4.73	4.0	5470
6	528	39	5400	1.56	13.4	4.0	10045
7	9922	28	101	0.00	0.00	0.0	0
8	9922	28	105	0.01	0.00	1.0	10286
9	9922	178	105	0.01	29.9	1.0	307205
10	4002	28	101	0.00	0.00	0.0	0
11	1626	15	101	0.002	0.27	0.0	436

Stream	ṁ (kg/h)	T (ºC)	P (kPa)	e^{CH} (kJ/kg)	e^{PH} (kJ/kg)	e^{KN} (kJ/kg)	Ė (kJ/h)
12	1626	15	105	0.012	0.27	1.0	2126
13	1626	96	105	0.012	6.97	1.0	13031
14	1100	15	101	0.002	0.27	0.0	295
15	1100	15	105	0.012	0.27	1.0	1438
16	1100	85	105	0.012	5.02	1.0	6665
17	1276	15	101	0.002	0.27	0.0	342
18	1276	26	101	0.002	0.00	0.0	6
19	1101	26	101	0.002	0.00	0.0	6
20	1101	27	105	0.012	0.00	1.0	1146
21	175	26	101	0.002	0.00	0.0	1
22	175	27	105	0.012	0.00	1.0	182
23	209	80	101	5.80	8.24	6.0	4202
24	2203	58	101	0.002	1.49	0.0	3298
25	207	35	101	5.80	0.18	1.0	1450
27	0.04	30	101	4.18	0.07	0.0	0.04
26	200	30	101	5.80	0.02	0.0	1163
28	6.96	30	101	5.80	0.02	0.0	40
29	12065	96	100	0.001	7.45	2.1	114790
30	14268	94	100	0.003	6.94	0.0	99094
31	14252	94	105	0.003	6.94	0.9	111685
32	16	94	100	1647	11.2	0.0	26942
33	182	30	101	1647	0.01	0.0	26763
34	198	40	101	1647	0.26	0.9	27009
35	20	90	70	480	418	0.0	18231
36	20	90	70	2.50	23.9	0.0	537
37	806	190	1250	480	499	0.0	789231
38	806	190	1250	2.50	29.0	0.0	25387
39	80	165	700	480	753	0.0	98620
40	80	165	700	2.50	104	0.0	8507
41	43	165	700	480	753	0.0	53008
42	43	165	700	2.50	104	0.0	4581

Stream	ṁ (kg/h)	T (°C)	P (kPa)	e^{CH} (kJ/kg)	e^{PH} (kJ/kg)	e^{KN} (kJ/kg)	Ė (kJ/h)
43	10	165	700	480	753	0.0	12328
44	10	165	700	2.50	104	0.0	1063
45	25438	2	500	2.50	5.13	0.0	194111
46	25438	6	500	2.50	3.71	0.0	157878
47	959	190	1250	480	499	0.0	938861
48	959	104	1250	2.50	39.3	0.0	40075
49	2217	28	101	0.00	0.00	0.0	0
50	77	28	101	43293	0.00	0.0	3332277
51	2294	650	101	26.0	331	0.0	817815

The exergy rate of the fuel ($\dot{E}_{F,k}$) and the product ($\dot{E}_{P,k}$), the exergetic ($\eta_{e,k}$) and energetic ($\eta_{en,k}$) efficiencies and the exergy destruction ratios ($y^*_{D,k}$ and $y_{D,k}$) were calculated for each component in the system. The results are summarized in Table 4.8. The components with the highest exergy fuel rates are the B, the MHX and the SD. The MHX is the component with the highest exergetic efficiency (38.9%), followed by the boiler (37%). There is a big difference between the exergetic and the energetic efficiencies of the majority of the components, consequently the overall system also exhibits the same behavior. Therefore, despite the energy efficiency of the system (the conservation of the quantity of energy) being 67.8%, the overall exergy efficiency (the quality of that energy) is only 33.3%. Similar results were obtained in a study on the spray drying process in an industrial scale ceramic factory, in which the energetic efficiency was found to be between 43% and 87 % [139], and the exergetic efficiency was between 12% and 64% [140]. However, in a pilot-scale study of spray drying of cherry puree the energetic and exergetic efficiencies were only 3.2% and 0.7%, respectively [141]. This, along with laboratory-scale studies [142–144], demonstrates that pilot-scale and laboratory-scale studies don`t accurately represent the energectic and exergetic performances of the industrial-scale spray drying process.

Table 4.8 Results of the exergy analysis of all the components of the spray drying system.

Component	$\dot{E}_{F,k}$ (kJ/h)	$\dot{E}_{P,k}$ (kJ/h)	$\eta_{e,k}$ (%)	$\eta_{en,k}$ (%)	$y^*_{D,k}$	$y_{D,k}$
SD	205446	32852	16.0	93.9	0.058	0.040
LP	7920	298	3.8	27.2	0.003	0.002
HP	19800	307	1.5	34.2	0.007	0.005

Component	$\dot{E}_{F,k}$ (kJ/h)	$\dot{E}_{P,k}$ (kJ/h)	$\eta_{e,k}$ (%)	$\eta_{en,k}$ (%)	$y^*_{D,k}$	$y_{D,k}$
HXE	17694	4576	25.9	76.4	0.005	0.003
MHX	763844	296918	38.9	79.4	0.174	0.116
SFBHX	90114	10906	12.1	81.4	0.030	0.020
VF1HX	48427	5227	10.8	88.6	0.016	0.011
VF2HX	11264	336	3.0	69.2	0.004	0.003
MF	66600	10286	15.4	46.3	0.021	0.014
SFBF	19800	1690	8.5	24.0	0.007	0.005
VF1F	14400	1143	7.9	22.4	0.005	0.003
VF2F	14400	1140	7.9	23.3	0.005	0.003
RFF	1980	181	9.2	29.4	0.001	0.001
FF	108000	39534	36.6	51.5	0.026	0.017
CHX	36233	1072	3.0	27.8	0.013	0.009
B	2514427	898786	35.7	73.3	0.611	0.374
BT	7920	546	6.9	69.9	0.003	0.002
S	3600	247	6.9	n.a	0.001	0.001

Figure 4.4 shows the fuel and product exergy rate of the overall system, as well as the destroyed exergy rate of each component. The results show that the components that have electric energy as the main fuel exergy source such as the vibrating screen, belt, and fans have the lowest impact on the exergetic destruction. This occurs because the electric energy is used for mechanical operations, instead of being used as a heat source. The exergy destruction ratio (y_D) is lower than 5% for these components. These results are similar to other studies that determined an exergy destruction ratio lower than 2% for the compressors and pumps in a CCHP system [145]. Furthermore, in a yogurt plant the devices that required electric energy accounted for less than 5% of the total exergy destruction [146].

Conversely, the boiler destroyed 39.4% of the overall fuel exergy rate. This percentage is similar to other plants where the boiler is used as an auxiliary supply of steam. For instance, in a factory which produces ghee, the boiler has the highest exergy destruction ratio 39% [147]. This is because the main purpose of this component is to convert a high-quality energy (chemical energy of fuel oil) to a low-quality energy (heat).

The MHX also has a high exergy destruction rate, despite having one of the highest exergetic efficiencies. The air heater used in this process is a steam-heated type, which is one

of the most used in food industry, it has an exergy efficiency of 38.9% and a high specific exergy destruction of 287 kJ per kg of heated air, with a minimum temperature difference of 12 ºC. There are other types of air heaters that could reduce the exergy destruction rate and the minimum temperature difference such as a system with a heat exchanger that uses geothermic fluid. A previous study showed that this kind of heat exchanger has an exergy efficiency of 42% and specific destruction exergy of 57.5 kJ per kilogram of heated air with a minimum temperature difference of 5ºC [17]. Another type of air heater is one that uses electric energy as the source of heat. A previous study on the spray drying of photochromic dyes determined that the exergy efficiency of this kind of heater was 16.4% [142], this has the lowest exergy efficiency because it is transforming high quality energy (electric energy) to low quality energy (heat).

The SD also affects the performance of the overall system, since it has one of the highest rates of exergy destruction at 595 kJ/kg of evaporated water. Previous studies by Bühler et al. [113], found that the spray dryer is a highly exergy- destructive component in a powdered milk factory. Similarly in a large dairy factory producing primarily milk powder, they obtained an exergy destruction rate of 1345 kJ/kg of evaporated water [7] . In a ceramic plant, the exergy destruction rate was 1111.4 kJ/kg of evaporated water [140].

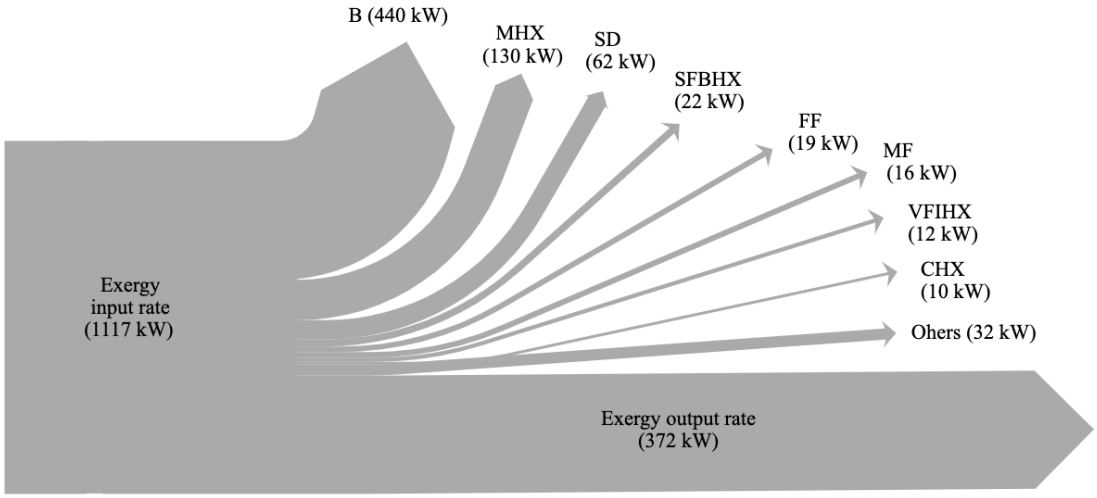

Figure 4.4. Grassmann's diagram of the spray drying process

The exergoeconomic analysis was carried out at a level component and it is presented in Table 4.9 different indicators such as the specific fuel cost ($c_{F,k}$), the destruction exergy cost

rate ($\dot{C}_{D,k}$), the exergoeconomic factor (f_k), the relative cost difference (r_k) and the total operating cost rate ($\dot{C}_{D,k} + \dot{Z}_k$) in descending order.

Table 4.9 Results of the thermoeconomic analysis

Component	$c_{F,k}$ ($/kJ)	$\dot{C}_{D,k}$ ($/h)	$\dot{Z}_k + \dot{C}_{D,k}$ ($/h)	r_k	f_k (%)
SD	6.2E-04	106.8	109.6	0.02	2.50
MHX	1.3E-04	60.5	61.6	0.01	1.73
B	6.7E-06	13.1	14.4	0.07	9.03
SFBHX	1.0E-04	8.2	8.3	0.02	2.06
VF1HX	1.0E-04	4.4	4.6	0.02	2.61
BT	5.7E-04	4.2	4.5	0.06	5.71
CHX	7.0E-05	2.4	3.0	0.20	17.43
HXE	1.4E-04	1.9	1.9	0.01	1.37
VF2HX	1.0E-04	1.1	1.2	0.03	3.17
FF	2.6E-05	1.8	1.9	0.05	7.83
MF	2.6E-05	1.5	1.6	0.08	9.00
HP	2.6E-05	0.5	1.1	1.14	53.73
RTF	2.6E-05	0.05	0.2	3.30	78.42
SFBF	2.6E-05	0.5	0.6	0.33	26.52
VF2F	2.6E-05	0.3	0.5	0.45	33.02
VF1F	2.6E-05	0.3	0.5	0.45	33.03
LP	2.6E-05	0.2	0.4	1.21	55.73
S	2.6E-05	0.1	0.4	8.16	78.49

The results show that the two highest total operating cost rates ($\dot{Z}_k + \dot{C}_D$) are from the SD followed by the MHX, meaning that the influence of these components on the total costs associated with the overall system is significant. Interesting results are presented, because although the B has a higher avoidable exergy destruction rate than the SD and MHX, the specific cost rate is higher in the SD than in the B, thus making the SD the component that has the greatest influence on the total operating cost rate. In contrast, the fans, the pumps, and the vibrating stream are the three components which contributed least to the total operating cost rate. Similar results were obtained by an exergoeconomic analysis in a corn dryer, where the drying chamber represented more than 98% of the total operational costs [149].

Furthermore, although the percentage relative cost differences for components such as the B (7%), SD (2%) and MHX (1%) are found to be low, their exergy destruction cost rates are high. The MHX and the SD have exergoeconomic factors of 1.6% and 3.3%, respectively, which means that the exergetic efficiency of these components must increase in order to reduce the overall system cost. Similar results were found in other drying technologies such as gas engine-driven heat pump dryer and a ground-source heat pump food dryer which had exergoeconomic factors of 25% [150] and 14.6% [151], respectively. Another previous study on a pilot-scale spray dryer for the production of cheese powder, concluded similarly that in order to reduce the operational cost in spray drying systems, the exergy efficiency in the drying chamber should be increased even though this would require an increment in the capital investment [24].

4.4. Simulation and Exergoeconomic analysis of the biofuels production process from spent coffee grounds.

In order to verify the validity of each component's calculation models, the values of the main operating parameters obtained in this work have been compared with those reported in experimental studies from other literature. On Table 4.10, the final moisture obtained in the dryer (D-101), the yield of the Soxhlet extractor (SO-101), the syngas composition that is produced in the gasifier (R-101) and the yield and biodiesel composition produced in the reactor (R-202) were presented and compared. It can be observed that the results of the model are close to the results reported in the experimental studies, with a maximum absolute error of 5.3, which represents a 6% relative error. Therefore, it is concluded that the models can be used to represent the syngas and biodiesel production process from SCG oil under the established operating conditions.

Table 4.10 Validation of the models

Component	Parameter	This work	Literature	Absolute Error
D-101	Final moisture (%, wb)	12.4	12.4[75]	0
SO-101	Yield (%, db)	15.0	15.0[81]	0
R-101	CO_2	0.370	0.373[2]	0.003
	CO	0.100	0.040[2]	0.060
	CH_4	0.430	0.526[2]	0.096
	H_2	0.020	0.061[2]	0.041
R-202	Yield	82.0	87.3[80]	5.3
	Linoleic Acid	0.37	0.41[80]	0.04

	Palmitic Acid	0.36	0.36[80]	0.00
	Oleic	0.14	0.14[80]	0.00
	Stearic	0.08	0.08[80]	0.00

Table 4.11 shows the mass flow rate ($\dot{m}$), the temperature (T), the pressure (P), the specific enthalpy (h), the specific entropy (s), the physical exergy ($\dot{E}^{PH}$), the chemical exergy ($\dot{E}^{CH}$) and the total exergy ($\dot{E}$) of each material stream. It can be observed that the chemical exergy is higher than the physical exergy in most of the states, especially in the streams that have lipids, hexane, biomass, and its derivatives. Therefore, this production process is focused on using the chemical exergy of biomass through chemical reactions, for the transformation into biofuels.

Table 4.11 Thermodynamic values of the streams.

Stream	$\dot{m}$ **(kg/h)**	**T (ºC)**	**P (bar)**	**h (kJ/kg)**	**s (kJ/kg-K)**	$\dot{E}^{PH}$ **(kW)**	$\dot{E}^{CH}$ **(kW)**	$\dot{E}$ **(kW)**
S1	1071	30	1	197	0.5905	6.2	3630	3636
S2	562075	25	1	0	0.0000	0.0	0	0
S3	562075	150	1	151	0.4206	4010.0	0	4010
S4	562670	80	1	57	0.1763	730.3	2	732
S5	476	80	1	159	0.4873	1.9	3622	3624
S6	4570	25	1	0	0.0000	0.0	60608	60608
S7	4586	68	1	71	0.2238	6.0	61127	61133
S8	4524	69	1	72	0.2264	6.1	60001	60008
S9	62.5	30	1	11	0.0350	0.0	1126	1126
S10	459	68	1	113	0.3517	1.0	3094	3095
S11	50651	25	1	0	0.0000	0.0	0	0
S12	50651	100	1	78	0.2330	118.0	0	118
S13	50746	60	1	36	0.1156	27.4	578	605
S14	365	60	1	94	0.2967	0.6	2240	2240
S15	0.01	25	1	0	0.0000	0.0	0	0
S16	289	425	1	876	1.9150	24.5	1334	1358
S17	75.8	900	1	981	1.5350	11.4	596	608
S18	34874	190	13	2681	6.1420	8234.0	5108	13342
S19	34874	190	13	702	1.8670	1408.0	484	1891
S20	7550	25	1	0	0.0000	0.0	105	105

S21	7550	68	1	179	0.5596	24.5	105	129
S22	976	190	13	2681	6.1420	230.5	143	374
S23	976	190	13	702	1.8670	39.4	14	53
S24	745	190	13	2681	6.1420	175.8	109	285
S25	745	190	13	702	1.8670	30.1	10	40
S26	7680	25	1	0	0.0000	0.0	107	107
S27	7680	69	1	184	0.5750	26.3	107	133
S28	1882	190	13	2681	6.1420	444.3	276	720
S29	1882	190	13	702	1.8670	76.0	26	102
B1	63	30	1	11	0.0350	0.0	1126	1126
B2	63	54	1	61	0.1959	0.1	1126	1126
B3	6	30	1	12	0.0391	0.0	2	1909
B4	6	30	1	13	0.0424	0.0	39	39
B5	12	25	1	0	0.0000	0.0	37	37
B6	12	54	1	72	0.2306	0.0	37	37
B7	1	54	1	61	0.1958	0.0	0	0
B8	71	54	1	64	0.2036	0.1	1125	1125
B9	11	54	1	93	0.2963	0.0	39	39
B10	63	53	1	57	0.1824	0.0	1095	1095
B11	26	30	1	13	0.0424	0.0	159	159
B12	1	30	1	17	0.0580	0.0	0	0
B13	26	30	1	13	0.0428	0.0	159	159
B14	0	54	1	77	0.2464	0.0	0	0
B15	89	54	1	46	0.1471	0.1	881	881
B16	89	30	1	7826	0.0260	0.0	881	881
B17	34	30	1	11	0.0352	0.0	343	343
B18	55	30	1	6607	0.0220	0.0	767	767
B19	0	190	13	2681	6.1420	0.1	0	0
B20	0	190	13	703	1.8690	0.0	0	0
B21	2	190	13	2681	6.1420	0.4	0	1
B22	2	190	13	703	1.8690	0.1	0	0
B23	0	190	13	2681	6.1420	0.0	0	0
B24	0	190	13	703	1.8690	0.0	0	0

B25	156	27	1	8366	0.0280	0.0	2	2
B26	156	40	1	63	0.2053	0.1	2	2

Table 4.12 shows the exergy of the fuel ($\dot{E}_{F,k}$), the exergy of the product ($\dot{E}_{P,k}$), the exergy destruction ($\dot{E}_{D,k}$) and the exergetic efficiency ($\eta_{e,k}$) for each component and for the overall system. The components E-201, E-202 and E-203 have an exergy destruction rate lower than 0.5 kW, therefore they were excluded from the table. It can be observed that the E-101 and D-101 are the main sources of irreversibility, they cause 53% and 28% of the overall exergy destruction rate, respectively. Similar results were found in a spray drying process of instant coffee [125] where the dryer was responsible for 23% of the exergy destruction. Similarly, Mehrpooya et al. [38] reported that air heat exchangers based on steam were the components with the lowest exergetic efficiency in the drying process of wood chips because a great amount of high quality energy was destroyed when the air was discharged.

Some studies show that the heat source in heat exchangers significantly affects the exergy destruction rate. When the heat source is flue gases, the exergy destruction rate is reduced [156]. Singh et al. [157] found that the use of solar energy for heating air increased the exergetic efficiency of the heat exchanger and the dryer from 15.3% to 24%. Another reason for a low exergetic efficiency is the high drying temperature. Beigi et al. [158] identified that an increase in the air temperature, increases the rate of heat and mass transfer and thus, increases the exergy of the exhaust air and the exergy losses.

Additionally, other components such as the R-202 and the R-101 destroy 5% of the overall destroyed exergy. Ofori-Boateng et al. [159] identified that transesterification reactors have a high exergy destruction rate because the reaction produces glycerin as a by-product and it has a high chemical exergy. Some factors that reduced the exergetic efficiency of these reactors were a high concentration of the catalyst, a high methanol/oil ratio and a high temperature of reaction [160]. Regarding the gasifier, Ji-chao et al. [161] found that unwanted products in the reaction such as char, increase the exergy destruction rate of this component, because it has a high chemical exergy. Another study identified that parameters such as a high initial humidity of the biomass [162] and a low gasifying agent/biomass mass ratio [163] decreased the exergetic efficiency of the gasifier.

Table 4.12 Results of the exergetic analysis of all the main components of the process

Component	$\dot{E}_{F,k}$ (kW)	$\dot{E}_{P,k}$ (kW)	$\dot{E}_{D,k}$ (kW)	$\eta_{e,k}$ (%)	$y^*_{D,k}$	$y_{D,k}$
E-101	11451	4010	7441	35	0.526	0.050
D-101	7646	3624	4022	47	0.285	0.027
SO-101	61433	61133	300	99	0.021	0.002
EV-101	61351	61133	217	99	0.015	0.001
E-102	617	118	499	19	0.035	0.003
D-102	3213	2240	972	69	0.069	0.006
R-101	1633	1358	274	83	0.019	0.002
R-201	1125	1095	30	97	0.000	0.000
R-202	1254	877	376	70	0.000	0.000
Overall System	149725	135588	14135	91	1.000	1.000

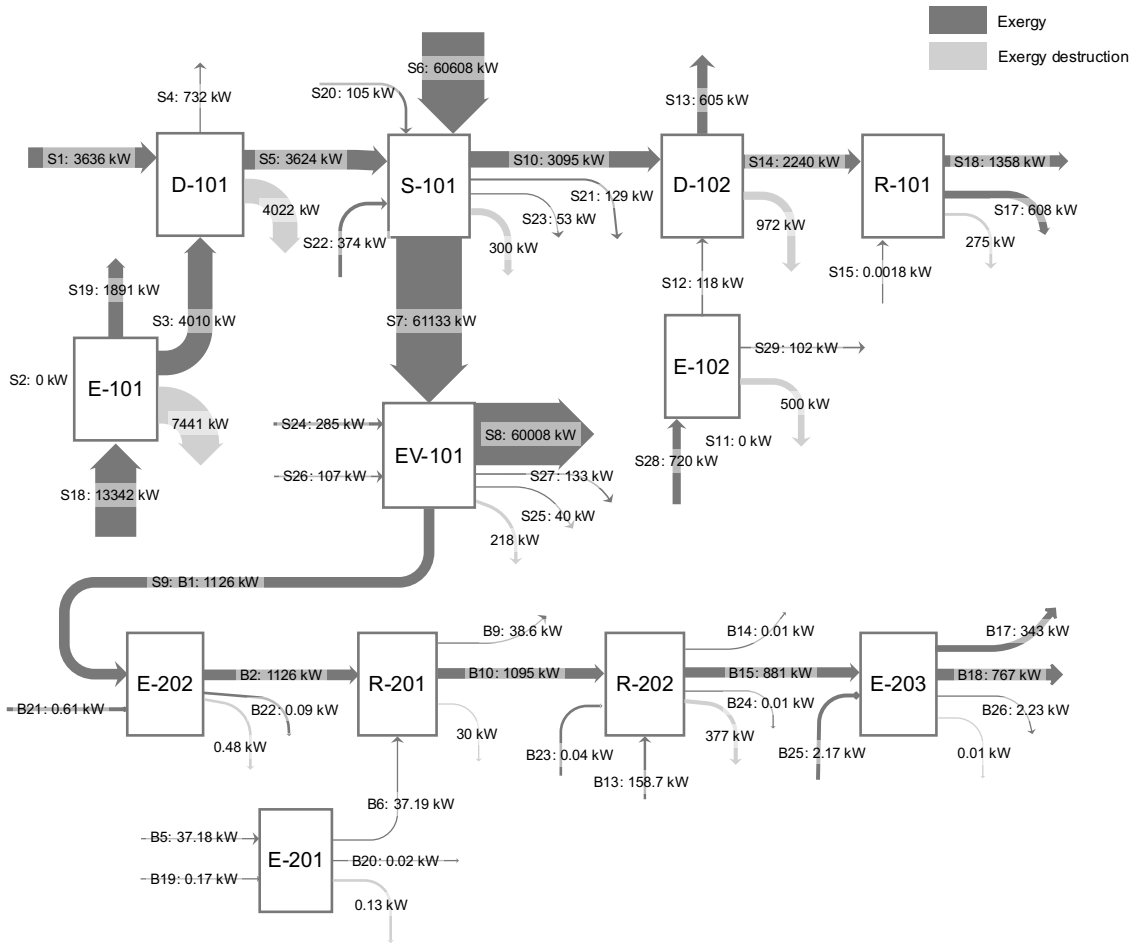

Figure 4.5. Grassmann's diagram of the process.

Furthermore, the components with the least impact on the overall exergy destruction rate are the E-201 and E-202 because they destroy less than 1%. Figure 4.5 shows the exergy flows rates across the process. It can be observed that the SO-101 and EV-101 have an input exergy rate higher than 60 MW. This occurs because the input solvent has the highest chemical exergy rate. That is why the recuperation of the solvent in the EV-101 is so important in order to reduce the exergy destruction rate and the operating costs. A previous experimental study showed that the use of a recycled solvent in the extraction process did not affect the extraction yield of SCG oil [164].

The total investment cost for the plant of syngas and biodiesel from SCG is estimated to be $13.2 million. The annual fuel cost and the operation and maintenance costs are $375,100 and $49,820 dollars, respectively, for a production of 289 kg/h of syngas and 55 kg/h of biodiesel, from processing a mass flow of 41,500 kg/h of SCG.

Table 4.13 shows the purchase equipment cost (PEC_k), the specific fuel costs ($c_{f,k}$), the capital investment cost rate ($\dot{Z}_k^{CI}$), the operational and maintenance cost rate ($\dot{Z}_k^{OM}$), the total operational cost rates ($\dot{Z}_k + \dot{C}_D$), the exergy destruction cost rate ($\dot{C}_D$), the exergoeconomic factor (f_k), and the relative difference (r_k) for each component. It can be observed that the components with the highest purchased costs such as R-201 and R-202 are not the components with the highest operational cost rates. Also there are other components with lower investment costs that have higher exergy destruction cost rates, such as the heat exchangers and the dryers.

Table 4.13 Results of exergoeconomic analysis

Component	PEC_k ($)	$c_{f,k}$ ($/MJ)	$\dot{Z}_k^{CI}$ ($/h)	$\dot{Z}_k^{OM}$ ($/h)	$\dot{Z}_k + \dot{C}_{D,k}$ ($/h)	$\dot{C}_{D,k}$ ($/h)	f_k	r_k
E-101	1415	0.028	0.44	0.25	759.20	758.50	0.09	1.86
D-101	6000	0.042	1.87	1.08	617.40	614.40	0.48	1.12
SO-101	15000	0.005	4.69	2.69	12.94	5.56	57.02	0.01
EV-101	5000	0.006	1.56	0.90	7.06	4.60	34.85	0.01
E-102	1415	0.028	0.44	0.25	51.65	50.96	1.35	4.29
D-102	6000	0.011	1.87	1.08	41.73	38.78	7.07	0.47
R-101	10000	0.015	3.12	1.79	19.95	15.03	24.66	0.27
E-201	3000	0.028	0.82	0.42	1.25	0.01	98.93	1121.00
E-202	3000	0.028	0.82	0.42	1.29	0.05	96.22	269.00
R-201	25000	0.001	6.80	3.49	10.44	0.14	98.67	2.10

Component	PEC_k ($)	$c_{f,k}$ ($/MJ)	$\dot{Z}_k^{CI}$ ($/h)	$\dot{Z}_k^{OM}$ ($/h)	$\dot{Z}_k + \dot{C}_{D,k}$ ($/h)	$\dot{C}_{D,k}$ ($/h)	f_k	r_k
R-202	20000	0.003	5.44	2.79	12.90	4.66	63.87	1.20
E-203	4000	0.014	1.09	0.56	1.65	0.00	99.96	628.00

Figure 4.6 shows that the E-101 and the D-101 are the components with the highest operating costs rates ($Z_k + \dot{C}_{D,k}$), followed by the E-102 and the D-102. This means that the air heater and the dryer influence significantly the overall costs of the system. These components have an exergoeconomic factor (f_k) of less than 10%, which means that the predominant cost is related to the destruction of exergy. At the same time, these components have the highest exergy destruction rate. Similar results have been found in a study related to a food drying process [155], where the dryer and the air heat exchanger presented an exergoeconomic factor of less than 5%.

A previous study had demonstrated that the avoidable exergy destruction cost rate could be more than 50% in components such as dryers or heat exchangers. Therefore, if the exergy destruction cost rate is reduced by at least 50% in D-101 and E-101, the overall operational cost of the process can be reduced by 45% and the overall exergetic efficiency could increase from 90.6% to 94.4%.

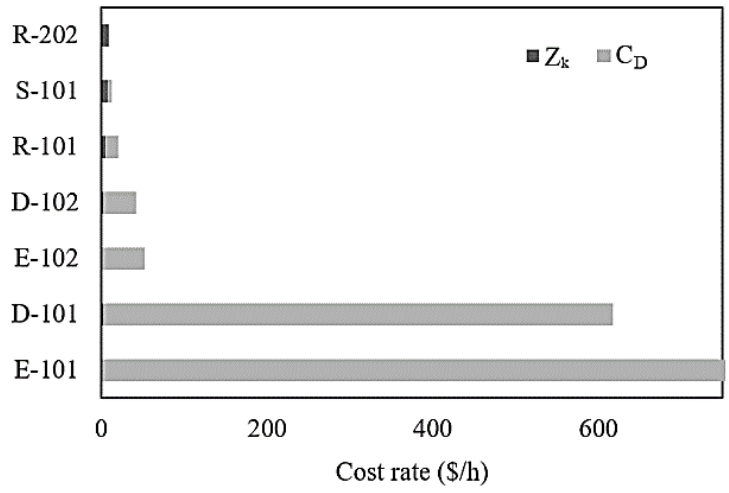

Figure 4.6. Main operational cost rates

In order to reduce costs, it is possible to optimize the operational conditions of the process and to analyze the different factors that significantly affect the exergy destruction cost rate. A previous study [165] proposed solar heat pump dryers, which allowed the reduction of the

exergy destruction cost rate from \$0.06/h to \$0.0044/h and the increase in the f_k from 5% to 51%; so that a balance is reached between the investment cost and exergy destruction cost rate with this structural change. Another study identified that recycling the drying air in continuous dryers has an economic and exergetic benefit for the process [166]. S. Zohrabi et al. [167] studied the recirculation of air in a convective dryer and achieved an increase of the exergetic efficiency from 55% to 95%.

According to different studies, the gasifier is one of the components that has the highest exergy destruction cost rate. Fakhimghanbarzadeh et al. [168] determined that this component was responsible for 11% of the operational cost rate and that it could be reduced 10% by increasing the temperature of the reaction and reducing the biomass/gasifying agent mass ratio. Fani et al. [169] found that the decrease of pressure in the reactor also reduces the cost rate. In addition, there are other important factors that are more dependent on the fuel used to operate the plant´s facilities [170]. In a previous study, the specific cost of the gasifying agent was found to be key in this cost rate [171].

The specific cost of biomass, syngas and biodiesel was determined by the economic analysis, and it was calculated in \$0.007/kg, \$0.037/kg and \$0.71\$/kg, respectively.

The dead state temperature is also another important factor because it is determined by the initial condition of the air and the water used in the system and influences the exergy rates of each process stream. This variable changes over time, as it depends on climatic changes. Figure 4.7 shows the effect of the dead state temperatures between 15 ºC and 35 ºC on the exergy destruction rate and the cost of exergy destruction rate. The results are favorable for high dead state temperatures, and a 10ºC change reduces the process cost rate by \$150/h.

a 10ºC change reduces the process cost rate by \$150/h.

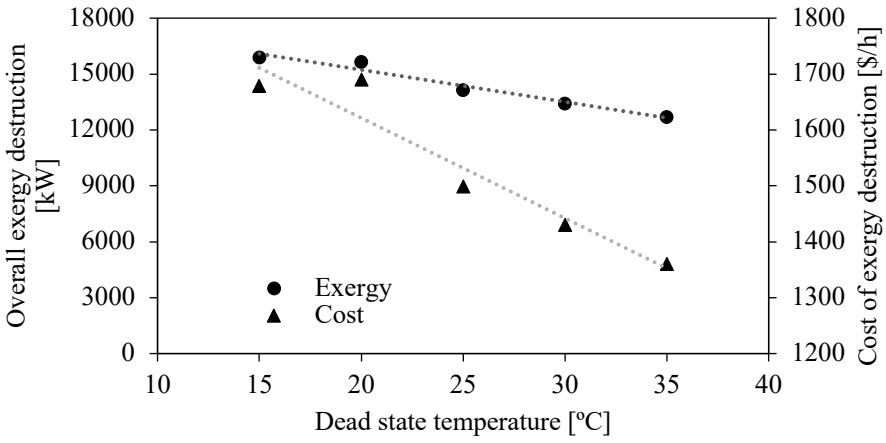

Figure 4.7. Effect of dead state temperature on a) overall exergy destruction and cost of exergy destruction and b) specific biofuels cost

Figure 4.8 shows the components of the process that are most affected by the change of the dead state temperature; in this case, they are the components with the highest exergy destruction cost rate. This means that the overall operational cost rate could be reduced by $300/h when the temperature of the environment is increased. Erbay et al. [151] presented similar results when they analyzed the effect of the dead state temperature between 0 – 20 °C in the exergetic efficiency and total exergy costs of a ground-source heat pump food dryer. Other components such as the R-101 are not significantly affected by the change of the dead state temperature, because they do not have inputs from the environment. Dryers and heat exchangers require ambient air, which means that environmental conditions strongly affect the performance of these components.

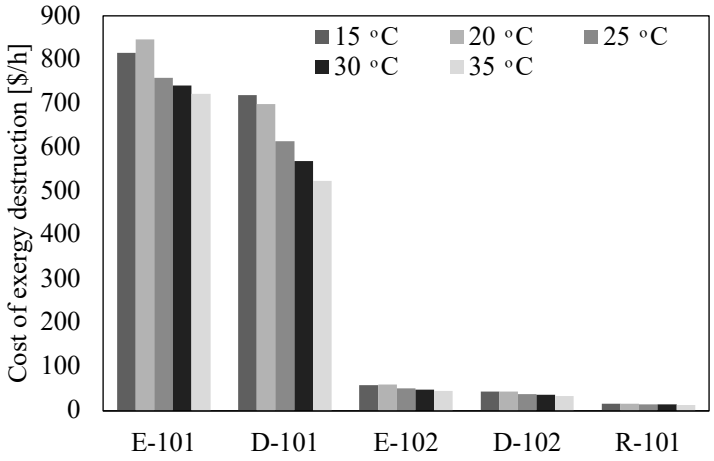

Figure 4.8. Effect of the dead state temperature on the costs of exergy destruction of the main components.

4.5. Simulation and Exergoeconomic Analysis of the CCHP system based on biofuels

To verify the validity of the proposed model, the absolute errors between the results of the model for each fuel and the ones obtained by experimental data from previous studies are presented in Table 4.14 to 4.18. Through the results and errors for each fuel, it is perceived that the results of the model are close to the results reported in the experimental studies. Hence, it is concluded that the model can be used successfully to describe the CCHP system applying different fuels like natural gas, bunker, syngas, and biomass under the established operating conditions.

Table 4.14 Comparison with data from previous experimental studies using Natural Gas [83].

Component	Parameter	Model	Experimental	Absolute Error
CC-101	Outlet Temperature flue gas (°C)	2252	2248	4.0
	CO_2 (%mol)	8.7	8.5	0.2
	O_2 (%mol)	0.18	0.16	0.02
HX-101	Mass Flow rate flue gas (kg/s)	1.85	1.90	0.05
	Temperature flue gas (°C)	774.7	770	4.7
	Steam generation (kg/s)	1.27	1.75	0.48

Table 4.15 Comparison with data from previous experimental studies using Fuel Oil No. 6 [85].

Component	Parameter	Model	Experimental	Absolute Error
CC-101*	Outlet Temperature flue gas (°C)	2338	2340	2.0
	CO_2 (%mol)	13	12	1.0
	O_2 (%mol)	1.7	2.1	0.4
HX-101*	Mass Flow rate flue gas (kg/s)	1.82	2.01	0.19
	Temperature flue gas (°C)	775.7	780	4.3
	Steam generation (kg/s)	1.27	1.75	0.48

Table 4.16 Comparison with data from previous experimental studies using Syngas [89].

Component	Parameter	Model	Experimental	Absolute Error
CC-101	Outlet Temperature flue gas (°C)	1987	1985	2.0
	CO_2 (%mol)	16.4	13	3.4
	O_2 (%mol)	0.20	0.1	0.1
HX-101	Mass Flow rate flue gas (kg/s)	2.11	1.47	0.64
	Temperature flue gas (°C)	645	649.5	4.5
	Steam generation (kg/s)	1.27	1.75	0.48

Table 4.17 Comparison with data from previous experimental studies using Biomass [82].

Component	Parameter	Model	Experimental	Absolute Error
CC-101*	Outlet Temperature flue gas (°C)	1908	1910	2.0
	CO_2 (%mol)	9.2	10.5	1.3
	O_2 (%mol)	14	17.8	3.8
HX-101*	Mass Flow rate flue gas (kg/s)	2.17	1.50	0.67
	Temperature flue gas (°C)	508.6	512	3.4
	Steam generation (kg/s)	1.27	1.75	0.48

Table 4.18 Comparison with data from previous experimental studies of an absorption chiller system [84].

Component	Parameter	Model	Experimental	Absolute Error
A-101**	Temperature (°C)	32.7	32.7	0.0
	Concentration LiBr (%)	0.574	0.574	0.0
	Concentration H_2O (%)	0.426	0.426	0.0

The exergetic analysis was performed to the conventional system using fuel oil No.6 as fuel (base case) and to the CCHP systems using different fuels. The exergy destruction rate of each case is presented in Fig. 3, and it is shown that the CCHP based on syngas has the lowest exergy destroyed, while the base case has the highest. The CCHP system based on biomass has also a low exergy destruction rate compared with the same system using fossil fuels. Ghaebi et al. [63] indicated that the exergy destruction rate of the CCHP system with liquified natural gas is 2273 kW; however, Gholizadeh et al. [67] determined that the exergy destruction rate of the CCHP system with biomass as fuel is 1670 kW, lower value than the exergy destruction rate of a CCHP system using fossil fuel.

Figure 4.9 (b) shows the exergetic efficiency of the conventional system (base case) and CCHP systems with different fuels; where, it is revealed that the CCHP systems applying biofuels (syngas and biomass) have the highest exergetic efficiency due to low rates of exergy destroyed; unlike CCHP systems using fossil fuels which have the lowest exergetic efficiency. Similar results were found in previous works. Yang et al. [60] determined that the exergetic efficiency of a CCHP system using a mixture of fuel (sugarcane bagasse and natural gas) increased by about 4.1%. and that the exergy costs decreased by 2%.

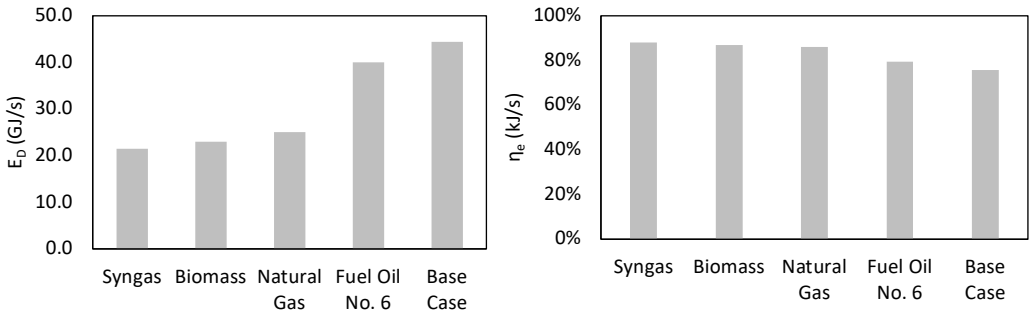

(a) **(b)**

Figure 4.9. Effect of different fossil fuels and biofuels on (a) the exergy destruction rate (b) exergy efficiency.

Figure 4.10 (a) shows the exergy destruction for each component of the system. It is shown that the combustion chamber (CC-101) that use fuel oil No. 6 has the highest exergy destruction rate. Miar et al. [62] determined that the component with the highest exergy destroyed of a CCHP system using a fossil fuel (natural gas) is the combustion chamber with a value of 3892.6 kW. Marques et al. [64] determined that the combustion engine in the CCHP system with natural gas is the component of high irreversibilities around 87.80% of the overall system. It is observed that the component HX-101 (boiler) and HX-102 (generator) employing fuel oil No.6 have high values of exergy destroyed around 400 – 1500 kJ/s unlike other fuels, where the exergetic losses in these components are around 500 - 900 kJ/s. Similar results show that the boiler is a component with high rate of exergy destroyed. Miar et al. [172] determined that the boiler presents a greater exergy destroyed of 104.4 kW, representing around 61.57% of exergy destroyed in the overall CHP system using sugarcane bagasse (biomass) as fuel. The components with low values of exergy destroyed are the absorber and the condenser around 140 – 150 kJ/s in the absorption chiller. Yang et al. [60] indicated that the exergy destroyed of the absorber and the condenser in the absorption chiller are 135 and 145 kJ/s respectively.

Figure 4.10 (b) shows exergy destruction cost rate ($\dot{C}_{D,k}$), for each component of each CCHP system using different fuels. It is observed that the components with the highest total operational cost rates, regardless the type of fuel, are T-101, A-101 and P-102; however, components T-101 and P-102 have low exergy destruction cost rate; unlike component A-101 have an exergy destruction cost rate over 143 $/h, higher than the components mentioned before in all the types of fuel. It should be mentioned that the components CC-101 and HX-102 have the highest exergy destruction cost rate using fuel oil No.6; while the exergy destruction cost rate of these components using the other fuels is lower around 136 - 795 $/h

for the CC-101 and 728 - 816 $/h for the HX-102. In addition, the component HX-102 has the highest exergy destruction cost rate in any CCHP system.

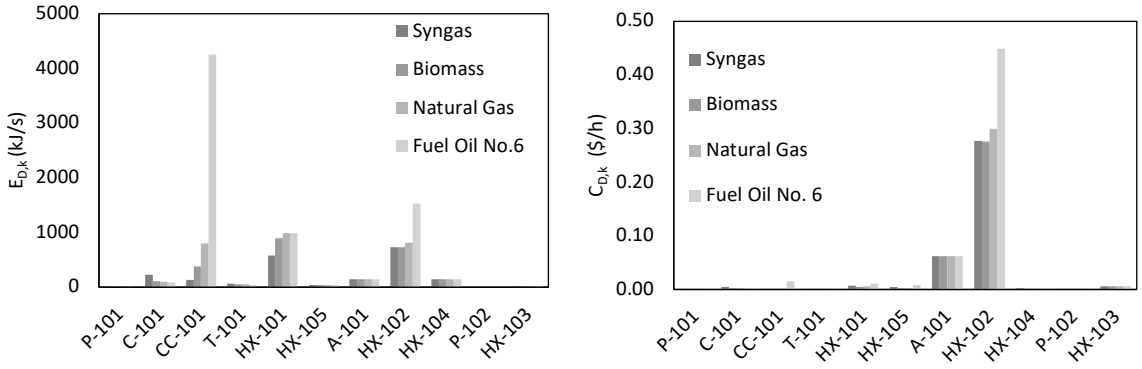

Figure 4.10 Exergoeconomic analysis of the CCHP system based on different fuels at a component level (a) Exergy destruction rate; (b) Exergy destruction cost rate

Table 4.19 shows the steam cost, the cold water cost, the power cost, the exergy destruction ($\dot{E}_D$), the exergy destruction cost rate ($\dot{C}_D$), the total operational cost rates ($\dot{C}_D + Z$), exergetic efficiency (n_{ex}) and footprint for each CCHP system using different fuels. CCHP system with fuel oil No.6 has higher cost for steam, cold water and electricity than the other CCHP systems with different fuels; unlike the base case, which has the highest cold water cost and CCHP system with syngas is the second one that has higher steam cost than the CCHP system with natural gas and biomass. Similar results have been found in previous studies where the costs of steam, cooling water and electricity are high when fossil fuels are used in a CCHP system. Ghaebi et al. [63] carried out an exergoeconomic analysis of a CCHP system using liquified natural gas and geothermal heat where it was obtained that the cost of cooling output and heating output is 26 $/ton, 35 $/ton and the power output is 45.62 $/GJ. In addition, it determined that the highest cost per exergy destroyed is for the absorber (235 543 $/yr.). Marques et al. [64] determined in a CCHP system with natural gas hat the component with the highest C_D is the internal combustion engine (63.73%) followed by the steam generator (19.83%). Also, the cost of chilled water is 17 $/ton, and the cost of hot water is 22 $/ton. As shown, the facility cost for CCHP system using biomass are lower than other systems. Jia et al. [173] determined that the cost of heating is 0.074 $/ton, the cost of cooling water is 0.066 $/ton, and the cost of electricity is 0.0084 $/GJ for a CCHP system using wood as biomass. In addition, it indicates that the component with the highest exergy destroyed is the gasifier (15%), followed by the combustion chamber (10%). Wu et al. [66] used wheat straw as

biomass in a CCHP system and a gasifier, where he determined that 0.065 $/ton is the cost of cooling water, 0.024 $/ton is the cost of hot water and 0.0045 $/GJ is electricity. Wang et al. [174] used wood chips as biomass in a trigeneration system where it determined that the equipment that generates the most costs per exergy destroyed is the HX-03, which is the exchanger that transfers heat with the combustion gases at high temperature, followed by the HX-01, which is the exchanger after the gasifier. He also obtained as a result that the cost of chilled water is 0.65 $/ton, the cost of hot water is 0.40 $/ton, and the cost of power electricity is 0.0016 $/GJ. As mentioned before, adding equipment, or even optimizing the operating conditions of the system can lead to cost reduction or even maximize system efficiency [65]. Regarding the footprint, it is observed that the CCHP system with fuel oil No. 6 has a high carbon footprint value of around 11,320 ton/year; while low carbon footprint values occur in CCHP systems that use natural gas and biomass as fuel. Similar results have been found in previous studies where high values of greenhouse gas emissions are observed when using fossil fuels in a CCHP system. Cavalcanti E. [175] carried out an exergy and environmental analysis of a trigeneration system using a diesel engine, where an exergetic efficiency of 87% in cycle was determined and that the diesel engine presents a greater destroyed exergy of 3.051 MW, with a NO emission of 92%.

Table 4.19 Comparative table of the results obtained for CCHP systems with different fuels.

Fuel	**Steam cost ($/t)**	**Cold water cost ($/t)**	**Power cost ($/GJ)**	$\dot{\mathbf{E}}_{\mathbf{D,k}}$ (**MW**)	$\dot{\mathbf{C}}_{\mathbf{D,k}}$ ($/**h**)	$\dot{\boldsymbol{Z}}_{\boldsymbol{k}} + \dot{\boldsymbol{C}}_{\boldsymbol{D,k}}$ ($/**h**)	$\boldsymbol{\eta}_{\mathbf{e,k}}$ (%)	**Foot print (t/year)**
Fuel Oil No.6	24.1	2.8	24.1	40007	3645	4135	79.6	11320
Natural Gas	15.5	1.5	19.1	25082	2973	3460	86.2	8116
Syngas	23.6	1.9	21.3	21490	2946	3447	88.0	9056
Biomass	13.9	1.4	21.3	22951	2869	3356	87.0	9501

Table 4.20 shows the fuel, product and destroy exergy rate of the integrated process that includes the instant coffee production process, the biofuel production process and the system for the production of the utilities for the plant. The Base Case refers to the conventional process for generation of steam, chilled water and power using fiuel oil No.6. The TS refers to the overall process integrated to the trigeneration system, and the results for this system using different fuels is presented in the table.

It is shown that the trigeneration system allows to reduce the specific cost of the overall product in 47.9%. Also it is shown that using biofuels instead of fuel oil No-6 allows to reduce the exergy cost rate in to 61.8%. This could occur because when using biofuels from SCG the exergy destruction rate from the solid liquid extraction is reduced because the SCG is not discarded but is used to produce syngas or biomass.

Table 4.20 Comparative table of for the integrated system proposed with CCHP and the base case

System	$\dot{E}_F$ (kW)	$\dot{E}_P$ (kW)	$\dot{E}_D$ (kW)	n_{ex} (%)	Coffee powder Cost ($/t)
Base Case	23399	10849	12550	46.3	12
TS Fuel Oil No.6	22113	7878	14235	35.6	6.29
TS Syngas	20492	15752	4740	76.8	6.29
TS Biomass	17951	9176	8775	51.1	6.28

5. Conclusions

This chapter presents a summary of the main conclusions of this work. In addition, future lines of research that were derived from this developed doctoral thesis are presented.

5.1. Main Conclusions

- The soluble coffee production process of the plant located in Guayaquil, Ecuador was evaluated through an exergoeconomic analysis. It was determined that the exergy efficiency of the global process was 46.3%, the exergy destruction rate was 12.5 MJ/s, the exergy destruction cost rate was $2609/h, and the investment cost rate was $605.9/h.
- The conventional steam generation and the solid-liquid extraction were identified as the stages with the highest exergy destruction rate, 5.0 MJ/s, and 1.8 MJ/s respectively. On the other hand, the stages that had the greatest impact on the operating costs were the solid-liquid extraction, the double effect evaporation, spray drying and the vapor-compression refrigeration system.
- The solid-liquid extraction represents the 32.5% of the overall exergy destruction cost rate. The double effect evaporator represents the 20.0% of it. The spray dryer represents the 15.4% of it and finally the vapor-compression refrigeration system represents the 20.0%.
- The simulation of the production process of biomass, syngas and biodiesel from spent coffee grounds was carried out to reduce the exergy destruction in the solid-liquid extraction stage, taking advantage of the waste generated. The model was validated with experimental data from previous studies, obtaining a maximum relative error of 6%.
- The proposed biomass, syngas, and biodiesel production process was evaluated through an exergoeconomic analysis and it was determined that the exergy destruction rate of this process was 14.1 MJ/s. As a result, the specific costs of biomass, syngas and biodiesel were $ 0.007/kg, $ 0.037/kg, and $ 0.71/kg, respectively.
- The biomass and the syngas could replace the use of fuel oil No.6 in the plant. While the biodiesel produced is not economically competitive to replace the diesel in the roasting process.
- A trigeneration system based on syngas and biomass was proposed in order to replace the conventional steam generation and refrigeration systems. It was simulated and

validated with experimental data from previous studies, obtaining a maximum relative error of 11.1%.

- The proposed system for the generation of steam, chilled water, and power allowed increasing the exergetic efficiency of the global system from 46.3% to 51.2% and reducing the exergy destruction rate by 3775 kW, when using biomass as biofuel instead of fuel oil No. 6.
- The use of syngas instead of biomass in the trigeneration system resulted in an increase in the overall exergetic efficiency to 76.8% and a reduction in the exergy destruction rate of 7811 kW.
- The cost of the steam produced in the proposed system compared to the conventional system decreased from $24.6/t to $13.9/t when biomass was used as fuel instead of Fuel oil. 6. While when syngas was used, this price was reduced to $23.5/t
- The cost of the chilled water produced in the absorption cycle, compared to the vapor compression system, decreased from $30.2/t to $1.4/t when using biomass and $1.5/Tn when using syngas.
- The trigeneration system based on fuel oil No 6. Reduced in 47.9% the cost of the overall product of the plant, but increased the exergy destruction rate.
- For the overall process, it is reduced the exergy destruction rate from 12550 kW to 8775 kW, when biomass is used as the fuel in a trigeneration system.
- The use of syngas in the trigeneration system reduced more the exergy destruction rate than using biomass (from 12550 kW to 4740 kW).

5.2 Future research lines

- Although the simulations were validated with data from previous experimental studies, there are limitations given that the spent coffee grounds of the plant come from a mixture of Arabica and Robusta coffee, and the biomass found in the literature from Arabica species. Therefore, a characterization of the spent coffee grounds of the plant is required, which allows to define the characteristics and develop a closer simulation.
- An experimental study of spent coffee grounds drying kinetics as well as a trigeneration system based on this biomass is recommended to be carried out on a pilot scale. These data will be useful for a closer simulation of the production process of biofuels.

- It is recommended to perform an advanced exergoeconomic analysis of the whole production system to quantify the avoidable and unavoidable exergy destruction cost rates, and thus, to identify the opportunities to reduce the costs.
- The development of an exergoeconomic optimization of the entire process is another topic of interest since it would allow to further reduce the operating costs and maximize the exergetic efficiency, modifying the established operating conditions.
- A life cycle assessment to the overall process is also recommended, taking into account also the production of coffee beans and the packing, transportation and consumption of coffee powder.

6. References

[1] S. Mayson, I.D. Williams, Applying a circular economy approach to valorize spent coffee grounds, Resour. Conserv. Recycl. 172 (2021) 105659. https://doi.org/10.1016/j.resconrec.2021.105659.
[2] H.A. Kibret, Y.-L. Kuo, T.-Y. Ke, Y.-H. Tseng, Gasification of spent coffee grounds in a semi-fluidized bed reactor using steam and CO 2 gasification medium, 000 (2021). https://doi.org/10.1016/j.jtice.2021.01.029.
[3] B. Killian, L. Rivera, M. Soto, D. Navichoc, Carbon Footprint across the Coffee Supply Chain: The Case of Costa Rican Coffee, Agric. Sci. Technol. 3 (2013).
[4] A. Bejan, G. Tsatsaronis, M. Moran, Thermal Design and Optimization, Wiley, New York, 1996.
[5] Coherent Market Insights, Instant Coffee Market Size Share Forecast Report 2026, (2019).
[6] M. Mojarab Soufiyan, A. Dadak, S.S. Hosseini, F. Nasiri, M. Dowlati, M. Tahmasebi, M. Aghbashlo, Comprehensive exergy analysis of a commercial tomato paste plant with a double-effect evaporator, Energy. (2016). https://doi.org/10.1016/j.energy.2016.06.030.
[7] F. Bühler, T. Van Nguyen, J.K. Jensen, F.M. Holm, B. Elmegaard, Energy, exergy and advanced exergy analysis of a milk processing factory, Energy. 162 (2018) 576–592. https://doi.org/10.1016/j.energy.2018.08.029.
[8] M. Mojarab Soufiyan, M. Aghbashlo, Application of exergy analysis to the dairy industry: A case study of yogurt drink production plant, Food Bioprod. Process. 101 (2017) 118–131.
[9] Z. Liu, Z. Liu, X. Cao, T. Luo, X. Yang, Advanced exergoeconomic evaluation on supercritical carbon dioxide recompression Brayton cycle, J. Clean. Prod. (2020). https://doi.org/10.1016/j.jclepro.2020.120537.
[10] Statista, Consumer Market Outlook for Instant Coffee. URL: https://www.statista.com/outlook/30010200/100/instant-coffee/worldwide. (Last accessed: 20.05. 2020), (2020).
[11] A. Svilaas, A.K. Sakhi, L.F. Andersen, T. Svilaas, E.C. Ström, D.R. Jacobs, L. Ose, R. Blomhoff, Intakes of Antioxidants in Coffee, Wine, and Vegetables Are Correlated with Plasma Carotenoids in Humans, J. Nutr. 134 (2004) 562–567. https://doi.org/10.1093/jn/134.3.562.
[12] J. Gebhardt, S., Lemar, L., Haytowitz, D., Pehrsson, P., Nickle, M., Showell, B., ... & Holden, USDA national nutrient database for standard reference, release 21. United States Department of AgricultureAgricultural Research Service., (2008).
[13] A. Lucas, M., Mirzaei, F., Pan, A., Okereke, O. I., Willett, W. C., O'Reilly, É. J., ... & Ascherio, Coffee, caffeine, and risk of depression among women. Archives of internal medicine, 171(17), 1571-1578., (2011).
[14] A. Market, Global Industry Analysis, Size, Share, Growth, Trends and Forecast 2019–2025. URL: https://www. transparencymarketresearch. com/logistics-market. html (Last accessed: 20.05. 2020)., (2019).
[15] M. Aghbashlo, H. Mobli, S. Rafiee, A. Madadlou, A review on exergy analysis of drying processes and systems, Renew. Sustain. Energy Rev. 22 (2013) 1–22. https://doi.org/10.1016/j.rser.2013.01.015.
[16] M.H.T. Mondal, M.A. Hossain, M.A.M. Sheikh, Md. Akhtaruzzaman, M.S.H. Sarker, Energetic and exergetic investigation of a mixed flow dryer: A case study of maize grain drying, Dry. Technol. 0 (2020) 1–15. https://doi.org/10.1080/07373937.2019.1709077.
[17] N. Yildirim, S. Genc, Energy and exergy analysis of a milk powder production system, Energy Convers. Manag. 149 (2017) 698–705.

https://doi.org/10.1016/j.enconman.2017.01.064.
[18] H. Sheikhshoaei, M. Dowlati, M. Aghbashlo, M.A. Rosen, Exergy analysis of a pistachio roasting system, Dry. Technol. 0 (2019) 1–19. https://doi.org/10.1080/07373937.2019.1649276.
[19] N. Colak, E. Kuzgunkaya, A. Hepbasli, Exergetic assessment of drying of mint leaves in a heat pump dryer, J. Food Process Eng. 31 (2008) 281–298. https://doi.org/10.1111/j.1745-4530.2007.00155.x.
[20] M. Aghbashlo, H. Mobli, A. Madadlou, S. Rafiee, Influence of spray dryer parameters on exergetic performance of microencapsulation processs, Int. J. Exergy. 10 (2012) 267–289. https://doi.org/10.1504/IJEX.2012.046812.
[21] G. Tsatsaronis, Thermoeconomic analysis and optimization of energy systems, Prog. Energy Combust. Sci. 19 (1993) 227–257. https://doi.org/10.1016/0360-1285(93)90016-8.
[22] L. Ozgener, Exergoeconomic analysis of small industrial pasta drying systems, Proc. Inst. Mech. Eng. Part A J. Power Energy. 221 (2007) 899–906. https://doi.org/10.1243/09576509JPE481.
[23] M. Ozturk, I. Dincer, Exergoeconomic analysis of a solar assisted tea drying system, Dry. Technol. 38 (2019) 655–662. https://doi.org/10.1080/07373937.2019.1669044.
[24] Z. Erbay, N. Koca, Exergoeconomic performance assessment of a pilot-scale spray dryer using the specific exergy costing method, Biosyst. Eng. 122 (2014) 127–138. https://doi.org/10.1016/j.biosystemseng.2014.04.006.
[25] T.G. Walmsley, M.R.W. Walmsley, M.J. Atkins, J.R. Neale, A.H. Tarighaleslami, Thermo-economic optimisation of industrial milk spray dryer exhaust to inlet air heat recovery, Energy. 90 (2015) 95–104. https://doi.org/10.1016/j.energy.2015.03.102.
[26] T.G. Walmsley, M.R.W. Walmsley, M.J. Atkins, J.R. Neale, Thermo-Economic assessment tool for industrial milk spray dryer exhaust heat recovery systems with particulate fouling, Chem. Eng. Trans. 39 (2014) 1459–1464. https://doi.org/10.3303/CET1439244.
[27] M.K. Yesilyurt, C. Cesur, V. Aslan, Z. Yilbasi, The production of biodiesel from safflower (Carthamus tinctorius L.) oil as a potential feedstock and its usage in compression ignition engine: A comprehensive review, Renew. Sustain. Energy Rev. 119 (2020) 109574. https://doi.org/10.1016/j.rser.2019.109574.
[28] F. Martins, C. Felgueiras, M. Smitkova, N. Caetano, Analysis of fossil fuel energy consumption and environmental impacts in european countries, Energies. 12 (2019) 1–11. https://doi.org/10.3390/en12060964.
[29] M.A. Mayorga, J.G. Cadavid Estrada, J.A. Bonilla Paez, C. Lopez, M. Lopez, se of Biofuels in the Aeronautical Industry. Case of the Colombian Air Force., Tecciencia. 14 (2019) 33–43. https://doi.org/10.18180/tecciencia.2019.26.7.
[30] D. Zhu, S.M. Mortazavi, A. Maleki, A. Aslani, H. Yousefi, Analysis of the robustness of energy supply in Japan: Role of renewable energy, Energy Reports. 6 (2020) 378–391. https://doi.org/10.1016/j.egyr.2020.01.011.
[31] C.H.W. Ruhe, Statistical Review, JAMA J. Am. Med. Assoc. 225 (2019) 299–306. https://doi.org/10.1001/jama.1973.03220300055017.
[32] S.S. Hassan, G.A. Williams, A.K. Jaiswal, Lignocellulosic Biorefineries in Europe: Current State and Prospects, Trends Biotechnol. 37 (2019) 231–234. https://doi.org/10.1016/j.tibtech.2018.07.002.
[33] S. Datta, Arup; Hossain, Aslam; Roy, An Overview on Biofuels and Their Advantages and Disadvantages, Asian J. Chem. 26 (2014) 70–73.
[34] A.B. Guerrero, E. Muñoz, Life cycle assessment of second generation ethanol derived from banana agricultural waste: Environmental impacts and energy balance, J. Clean.

Prod. 174 (2018) 710–717. https://doi.org/10.1016/j.jclepro.2017.10.298.
[35] M.A. Rajaeifar, A. Akram, B. Ghobadian, S. Rafiee, R. Heijungs, M. Tabatabaei, Environmental impact assessment of olive pomace oil biodiesel production and consumption: A comparative lifecycle assessment, Energy. 106 (2016) 87–102. https://doi.org/10.1016/j.energy.2016.03.010.
[36] J.H. Ebner, R.A. Labatut, J.S. Lodge, A.A. Williamson, T.A. Trabold, Anaerobic co-digestion of commercial food waste and dairy manure: Characterizing biochemical parameters and synergistic effects, Waste Manag. 52 (2016) 286–294. https://doi.org/10.1016/j.wasman.2016.03.046.
[37] D.Y.C. Leung, L.C. Yu, G.C.K. Lam, H.Y.H. Kwok, W.K. Cheng, Bioethanol: Is It a Suitable Biofuel for Hong Kong for Reducing Its Vehicular Emissions and Carbon Footprint?, Energy Procedia. 142 (2017) 2892–2897. https://doi.org/10.1016/j.egypro.2017.12.413.
[38] M. Mehrpooya, M. Khalili, M.M.M. Sharifzadeh, Model development and energy and exergy analysis of the biomass gasification process (Based on the various biomass sources), Renew. Sustain. Energy Rev. (2018). https://doi.org/10.1016/j.rser.2018.04.076.
[39] L. Pattanaik, F. Pattnaik, D.K. Saxena, S.N. Naik, Biofuels from agricultural wastes, Elsevier Inc., 2019. https://doi.org/10.1016/B978-0-12-815162-4.00005-7.
[40] K.K. Jaiswal, B. Jha, R.A. Prasath, Biodiesel production from discarded fish waste for sustainable clean energy development, J. Chem. Pharm. Sci. 2014-Decem (2014) 113–114.
[41] J.J. Milledge, The challenge of algal fuel : economic processing of the entire algal biomass, Condens. Matter -Materials Eng. Newsl. (2010) 1–5.
[42] R.W. Jenkins, N.E. Stageman, C.M. Fortune, C.J. Chuck, Effect of the type of bean, processing, and geographical location on the biodiesel produced from waste coffee grounds, Energy and Fuels. 28 (2014) 1166–1174. https://doi.org/10.1021/ef4022976.
[43] Y. Liu, Q. Tu, G. Knothe, M. Lu, Direct transesterification of spent coffee grounds for biodiesel production, Fuel. 199 (2017) 157–161. https://doi.org/10.1016/j.fuel.2017.02.094.
[44] M.J. Haas, K. Wagner, Simplifying biodiesel production: The direct or in situ transesterification of algal biomass, Eur. J. Lipid Sci. Technol. 113 (2011) 1219–1229. https://doi.org/10.1002/ejlt.201100106.
[45] J. Park, B. Kim, J.W. Lee, In-situ transesterification of wet spent coffee grounds for sustainable biodiesel production, Bioresour. Technol. 221 (2016) 55–60. https://doi.org/10.1016/j.biortech.2016.09.001.
[46] T.R. Pacioni, D. Soares, M. Di Domenico, M.F. Rosa, R. de F.P.M. Moreira, H.J. José, Bio-syngas production from agro-industrial biomass residues by steam gasification, Waste Manag. 58 (2016) 221–229. https://doi.org/10.1016/j.wasman.2016.08.021.
[47] Z.A. Antonova, V.S. Krouk, Y.E. Pilyuk, Y. V. Maksimuk, L.S. Karpushenkava, M.G. Krivova, Exergy analysis of canola-based biodiesel production in Belarus, Fuel Process. Technol. 138 (2015) 397–403. https://doi.org/10.1016/j.fuproc.2015.05.005.
[48] A. Amelio, T. Van De Voorde, C. Creemers, J. Degrève, S. Darvishmanesh, P. Luis, B. Van Der Bruggen, Comparison between exergy and energy analysis for biodiesel production, Energy. 98 (2016) 135–145. https://doi.org/10.1016/j.energy.2016.01.018.
[49] R.A.M. Boloy, M.E. Silva, A.E. Valle, J.L. Silveira, C.E. Tuna, Thermoeconomic analysis of hydrogen incorporation in a biodiesel plant, Appl. Therm. Eng. 113 (2017) 519–528. https://doi.org/10.1016/j.applthermaleng.2016.10.171.
[50] E. Shayan, V. Zare, I. Mirzaee, On the use of different gasification agents in a biomass fueled SOFC by integrated gasifier: A comparative exergo-economic evaluation and

optimization, Energy. 171 (2019) 1126–1138. https://doi.org/10.1016/j.energy.2019.01.095.
[51] Y. Wu, W. Yang, W. Blasiak, Energy and exergy analysis of high temperature agent gasification of biomass, Energies. 7 (2014) 2107–2122. https://doi.org/10.3390/en7042107.
[52] H. Ansarinasab, M. Mehrpooya, M. Sadeghzadeh, Life-cycle assessment (LCA) and techno-economic analysis of a biomass-based biorefinery, J. Therm. Anal. Calorim. (2020). https://doi.org/10.1007/s10973-020-10324-7.
[53] T. Nakyai, Y. Patcharavorachot, A. Arpornwichanop, D. Saebea, Comparative exergoeconomic analysis of indirect and direct bio-dimethyl ether syntheses based on air-steam biomass gasification with CO2 utilization, Energy. 209 (2020) 118332. https://doi.org/10.1016/j.energy.2020.118332.
[54] M. Aghbashlo, M. Tabatabaei, S. Soltanian, H. Ghanavati, A. Dadak, Comprehensive exergoeconomic analysis of a municipal solid waste digestion plant equipped with a biogas genset, Waste Manag. 87 (2019) 485–498. https://doi.org/10.1016/j.wasman.2019.02.029.
[55] C. Xiao, Q. Liao, Q. Fu, Y. Huang, A. Xia, W. Shen, H. Chen, X. Zhu, Exergy analyses of biogas production from microalgae biomass via anaerobic digestion, Bioresour. Technol. 289 (2019) 121709. https://doi.org/10.1016/j.biortech.2019.121709.
[56] I. Polygeneration, P. Plant, B.S.S. Firing, M. Alghassab, O.D. Samuel, Z.A. Khan, M. Imran, M. Farooq, Exergoeconomic and Environmental Modeling of, (2020).
[57] J. Jiang, W. Gao, Y. Gao, X. Wei, S. Kuroki, Performance Analysis of CCHP System for University Campus in North China, Procedia - Soc. Behav. Sci. 216 (2016) 361–372. https://doi.org/10.1016/j.sbspro.2015.12.049.
[58] A.E. Atabani, S.M. Mercimek, S. Arvindnarayan, S. Shobana, G. Kumar, M. Cadir, A.H. Al-Muhatseb, Valorization of spent coffee grounds recycling as a potential alternative fuel resource in Turkey: An experimental study, J. Air Waste Manag. Assoc. 68 (2018) 196–214. https://doi.org/10.1080/10962247.2017.1367738.
[59] M. Prakash, A. Sarkar, J. Sarkar, J.P. Chakraborty, S.S. Mondal, R.R. Sahoo, Performance assessment of novel biomass gasification based CCHP systems integrated with syngas production, Energy. 167 (2019) 379–390. https://doi.org/10.1016/j.energy.2018.10.172.
[60] K. Yang, N. Zhu, Y. Ding, C. Chang, D. Wang, T. Yuan, Exergy and exergoeconomic analyses of a combined cooling, heating, and power (CCHP) system based on dual-fuel of biomass and natural gas, J. Clean. Prod. 206 (2019) 893–906. https://doi.org/10.1016/j.jclepro.2018.09.251.
[61] X. Zhang, R. Zeng, K. Mu, X. Liu, X. Sun, H. Li, Exergetic and exergoeconomic evaluation of co-firing biomass gas with natural gas in CCHP system integrated with ground source heat pump, Energy Convers. Manag. 180 (2019) 622–640. https://doi.org/10.1016/j.enconman.2018.11.009.
[62] M. Miar Naeimi, M. Eftekhari Yazdi, G. Reza Salehi, Energy, exergy, exergoeconomic and exergoenvironmental analysis and optimization of a solar hybrid CCHP system, Energy Sources, Part A Recover. Util. Environ. Eff. 00 (2019) 1–21. https://doi.org/10.1080/15567036.2019.1702122.
[63] H. Ghaebi, T. Parikhani, H. Rostamzadeh, A novel trigeneration system using geothermal heat source and lique fi ed natural gas cold energy recovery : Energy , exergy and exergoeconomic analysis, Renew. Energy. 119 (2018) 513–527. https://doi.org/10.1016/j.renene.2017.11.082.
[64] A. da S. Marques, M. Carvalho, A.B. Lourenço, C.A.C. dos Santos, Energy, exergy,

and exergoeconomic evaluations of a micro-trigeneration system, J. Brazilian Soc. Mech. Sci. Eng. 42 (2020). https://doi.org/10.1007/s40430-020-02399-y.
[65] H. Ding, J. Li, D. Heydarian, Energy, exergy, exergoeconomic, and environmental analysis of a new biomass-driven cogeneration system, Sustain. Energy Technol. Assessments. 45 (2021) 101044. https://doi.org/10.1016/j.seta.2021.101044.
[66] J. Wu, J. Wang, J. Wu, C. Ma, Exergy and exergoeconomic analysis of a combined cooling, heating, and power system based on solar thermal biomass gasification, Energies. 12 (2019). https://doi.org/10.3390/en12122418.
[67] T. Gholizadeh, M. Vajdi, H. Rostamzadeh, Exergoeconomic optimization of a new trigeneration system driven by biogas for power, cooling, and freshwater production, Energy Convers. Manag. 205 (2020) 112417. https://doi.org/10.1016/j.enconman.2019.112417.
[68] H. Li, X. Zhang, L. Liu, R. Zeng, G. Zhang, Exergy and environmental assessments of a novel trigeneration system taking biomass and solar energy as co-feeds, Appl. Therm. Eng. 104 (2016) 697–706. https://doi.org/10.1016/j.applthermaleng.2016.05.081.
[69] R. Dorfner, T. Ferge, C. Yeretzian, A. Kettrup, R. Zimmermann, Laser Mass Spectrometry as On-Line Sensor for Industrial Process Analysis: Process Control of Coffee Roasting, Anal. Chem. 76 (2004) 1386–1402. https://doi.org/10.1021/ac034758n.
[70] C. Yeretzian, A. Jordan, R. Badoud, W. Lindinger, From the green bean to the cup of coffee: Investigating coffee roasting by on-line monitoring of volatiles, Eur. Food Res. Technol. 214 (2002) 92–104. https://doi.org/10.1007/s00217-001-0424-7.
[71] T. Murakami, G. Xu, T. Suda, Y. Matsuzawa, H. Tani, T. Fujimori, Some process fundamentals of biomass gasification in dual fluidized bed, Fuel. 86 (2007) 244–255. https://doi.org/10.1016/j.fuel.2006.05.025.
[72] D.R. Vardon, B.R. Moser, W. Zheng, K. Witkin, R.L. Evangelista, T.J. Strathmann, K. Rajagopalan, B.K. Sharma, Complete utilization of spent coffee grounds to produce biodiesel, bio-oil, and biochar, ACS Sustain. Chem. Eng. 1 (2013) 1286–1294. https://doi.org/10.1021/sc400145w.
[73] C.H. Dang, T.D. Nguyen, Physicochemical Characterization of Robusta Spent Coffee Ground Oil for Biodiesel Manufacturing, Waste and Biomass Valorization. 10 (2019) 2703–2712. https://doi.org/10.1007/s12649-018-0287-9.
[74] J.L. Diaz de Tuesta, A. Quintanilla, D. Moreno, V.R. Ferro, J.A. Casas, Simulation and optimization of the CWPO process by combination of aspen plus and 6-factor doehlert matrix: Towards autothermal operation, Catalysts. 10 (2020). https://doi.org/10.3390/catal10050548.
[75] F.J. Gómez-de la Cruz, J.M. Palomar-Carnicero, Q. Hernández-Escobedo, F. Cruz-Peragón, Experimental studies on mass transfer during convective drying of spent coffee grounds generated in the soluble coffee industry, J. Therm. Anal. Calorim. (2020).
[76] E.C. Carlson, Don't Gamble With Physical Properties for Simulations - Aspen Technology, Inc., Chem. Eng. Prog. (1996) 35–46.
[77] J. Han, Y. Liang, J. Hu, L. Qin, J. Street, Y. Lu, F. Yu, Modeling downdraft biomass gasification process by restricting chemical reaction equilibrium with Aspen Plus, Energy Convers. Manag. 153 (2017) 641–648. https://doi.org/10.1016/j.enconman.2017.10.030.
[78] L.P.R. Pala, Q. Wang, G. Kolb, V. Hessel, Steam gasification of biomass with subsequent syngas adjustment using shift reaction for syngas production: An Aspen Plus model, Renew. Energy. 101 (2017) 484–492.

https://doi.org/10.1016/j.renene.2016.08.069.
[79] D. Han, X. Yang, R. Li, Y. Wu, Environmental impact comparison of typical and resource-efficient biomass fast pyrolysis systems based on LCA and Aspen Plus simulation, J. Clean. Prod. 231 (2019) 254–267. https://doi.org/10.1016/j.jclepro.2019.05.094.
[80] M. Haile, Integrated volarization of spent coffee grounds to biofuels, Biofuel Res. J. 1 (2014) 65–69. https://doi.org/10.18331/BRJ2015.1.2.6.
[81] M.M.R. De Melo, H.M.A. Barbosa, C.P. Passos, C.M. Silva, Supercritical fluid extraction of spent coffee grounds: Measurement of extraction curves, oil characterization and economic analysis, J. Supercrit. Fluids. 86 (2014) 150–159. https://doi.org/10.1016/j.supflu.2013.12.016.
[82] M. Prakash, A. Sarkar, J. Sarkar, S.S. Mondal, J.P. Chakraborty, Proposal and design of a new biomass based syngas production system integrated with combined heat and power generation, Energy. 133 (2017) 986–997. https://doi.org/10.1016/j.energy.2017.05.161.
[83] H.Y. Park, K. Han, H.H. Kim, S. Park, J. Jang, G.S. Yu, J.H. Ko, Comparisons of combustion characteristics between bioliquid and heavy fuel oil combustion in a 0.7 MWth pilot furnace and a 75 MWe utility boiler, Energy. 192 (2020). https://doi.org/10.1016/j.energy.2019.116557.
[84] C. Somers, A. Mortazavi, Y. Hwang, R. Radermacher, P. Rodgers, S. Al-Hashimi, Modeling water/lithium bromide absorption chillers in ASPEN Plus, Appl. Energy. 88 (2011) 4197–4205. https://doi.org/10.1016/j.apenergy.2011.05.018.
[85] S. Garcia-Freites, A. Welfle, A. Lea-Langton, P. Gilbert, P. Thornley, The potential of coffee stems gasification to provide bioenergy for coffee farms: a case study in the Colombian coffee sector, Biomass Convers. Biorefinery. 10 (2020) 1137–1152. https://doi.org/10.1007/s13399-019-00480-8.
[86] Z. Hajabdollahi, P.F. Fu, Multi-objective based configuration optimization of SOFC-GT cogeneration plant, Appl. Therm. Eng. 112 (2017) 549–559. https://doi.org/10.1016/j.applthermaleng.2016.10.103.
[87] S.B. Kang, H.Y. Oh, J.J. Kim, K.S. Choi, Characteristics of spent coffee ground as a fuel and combustion test in a small boiler (6.5 kW), Renew. Energy. 113 (2017) 1208–1214. https://doi.org/10.1016/j.renene.2017.06.092.
[88] M. Terhan, K. Comakli, Energy and exergy analyses of natural gas-fired boilers in a district heating system, Appl. Therm. Eng. 121 (2017) 380–387. https://doi.org/10.1016/j.applthermaleng.2017.04.091.
[89] A.A.V. Ochoa, J.C.C. Dutra, J.R.G. Henríquez, C.A.C. Dos Santos, Dynamic study of a single effect absorption chiller using the pair LiBr/H2O, Energy Convers. Manag. 108 (2016) 30–42. https://doi.org/10.1016/j.enconman.2015.11.009.
[90] K. Burmester, H. Fehr, R. Eggers, A comprehensive study on thermophysical material properties for an innovative coffee drying process, Dry. Technol. 29 (2011) 1562–1570. https://doi.org/10.1080/07373937.2011.582595.
[91] D.R. Morris, J. Szargut, Standard chemical exergy of some elements and compounds on the planet earth, Energy. 11 (1986) 733–755. https://doi.org/10.1016/0360-5442(86)90013-7.
[92] G. Tsatsaronis, M.H. Park, On avoidable and unavoidable exergy destructions and investment costs in thermal systems, in: Energy Convers. Manag., 2002. https://doi.org/10.1016/S0196-8904(02)00012-2.
[93] A. Bejan, G. Tsatsaronis, M. Michael, Thermal design and optimization, New York, 1996. https://doi.org/10.1016/s0360-5442(96)90000-6.
[94] A. Lazzaretto, G. Tsatsaronis, SPECO: A systematic and general methodology for

calculating efficiencies and costs in thermal systems, Energy. 31 (2006) 1257–1289. https://doi.org/10.1016/j.energy.2005.03.011.
[95] E. Hidalgo, Estimación de emisiones gaseosas de Fuentes fijas en el sector industrial del Cantón Rumiñahui, Universidad Central del Ecuador, 2014.
[96] D.B. Cardoso, E.T. de Andrade, R.A.A. Calderón, M.H.S. Rabelo, C. de Almeida Dias, I.Á. Lemos, Determination of thermal properties of coffee beans at different degrees of roasting, Coffee Sci. 13 (2018) 498–509. https://doi.org/10.25186/cs.v13i4.1491.
[97] H.G. Schwartzberg, Modeling bean heating during batch roasting of coffee beans, Eng. Food 21st Century. (2002) 871–890. https://doi.org/10.1201/9781420010169-67.
[98] J. Telis-Romero, A.L. Gabas, M.A. Polizelli, V.R.N. Telis, Temperature and water content influence on thermophysical properties of coffee extract, Int. J. Food Prop. 3 (2000) 375–384. https://doi.org/10.1080/10942910009524642.
[99] M. Özilgen, Nutrition and production related energies and exergies of foods, Renew. Sustain. Energy Rev. 96 (2018) 275–295. https://doi.org/10.1016/j.rser.2018.07.055.
[100] F. Wei, M. Tanokura, Chemical Changes in the Components of Coffee Beans during Roasting, Elsevier Inc., 2015. https://doi.org/10.1016/B978-0-12-409517-5.00010-3.
[101] G. Song, L. Shen, J. Xiao, Estimating specific chemical exergy of biomass from basic analysis data, Ind. Eng. Chem. Res. 50 (2011) 9758–9766. https://doi.org/10.1021/ie200534n.
[102] PetroEcuador E.P, Precios de venta a nivel de terminal para las comercializadoras calificadas y autorizadas a nivel nacional, (2021) 1.
[103] Tarifa eléctrica para las industrias se reduce, El Telégrafo. (2021) 1.
[104] M. Puertas, Con multas y todo, el agua es un gran negocio en Guayaquil, La Hist. (2020).
[105] T. Morosuk, G. Tsatsaronis, Advanced exergy-based methods used to understand and improve energy-conversion systems, Energy. 169 (2019) 238–246. https://doi.org/10.1016/j.energy.2018.11.123.
[106] F. Petrakopoulou, G. Tsatsaronis, T. Morosuk, A. Carassai, Advanced exergoeconomic analysis applied to a complex energy conversion system, J. Eng. Gas Turbines Power. 134 (2012) 1–7. https://doi.org/10.1115/1.4005115.
[107] D.L. Tinoco-Caicedo, A. Lozano-Medina, A.M. Blanco-Marigorta, Conventional and Advanced Exergy and A Case Study of an Instant Co ff ee Factory in Ecuador, Energies. 13 (21) (2020) 5622.
[108] A. Gungor, G. Tsatsaronis, H. Gunerhan, A. Hepbasli, Advanced exergoeconomic analysis of a gas engine heat pump (GEHP) for food drying processes, Energy Convers. Manag. 91 (2015) 132–139. https://doi.org/10.1016/j.enconman.2014.11.044.
[109] Y.B. Yao Clément, Y.N. Benjamin, K.B. Roger, A. Djédjro Clément, T. Kablan, Moisture Adsorption Isotherms Characteristic of Coffee (Arabusta) Powder at Various Fitting Models, Int. J. Curr. Res. Biosci. Plant Biol. 5 (2018) 26–35. https://doi.org/10.20546/ijcrbp.2018.502.004.
[110] W.J. Wepfer, R.A. Gaggioli, E.F. Obert, Proper evaluation of available energy for HVAC, ASHRAE Transcactions. 85(1) (1979) 214–230.
[111] G.D. Vučković, M.M. Stojiljković, M. V. Vukić, G.M. Stefanović, E.M. Dedeić, Advanced exergy analysis and exergoeconomic performance evaluation of thermal processes in an existing industrial plant, Energy Convers. Manag. 85 (2014) 655–662. https://doi.org/10.1016/j.enconman.2014.03.049.
[112] F. Cziesla, G. Tsatsaronis, Z. Gao, Avoidable thermodynamic inefficiencies and costs in an externally fired combined cycle power plant, Energy. 31 (2006) 1472–1489. https://doi.org/10.1016/j.energy.2005.08.001.

[113] F. Bühler, T. Van Nguyen, J.K. Jensen, F.M. Holm, B. Elmegaard, Energy, exergy and advanced exergy analysis of a milk processing factory, Energy. (2018). https://doi.org/10.1016/j.energy.2018.08.029.
[114] G. de comercialización nacional EP PETROECUADOR, Precios de venta a nivel de Terminal para las comercializadoras calificadas y autorizadas a nivel nacional, (2019). https://www.eppetroecuador.ec/wp-content/uploads/downloads/2019/03/PRECIOS-MARZO-2019-MENSUAL-SNI-DEL-07-AL-13-DE-MARZO-2019.pdf.
[115] Informe Anual 2018-2019 International Water Services (Guayaquil) Interagua C. Ltda., (n.d.).
[116] O.O.D. Afolabi, M. Sohail, Y.L. Cheng, Optimisation and characterisation of hydrochar production from spent coffee grounds by hydrothermal carbonisation, Renew. Energy. 147 (2020) 1380–1391. https://doi.org/10.1016/j.renene.2019.09.098.
[117] A.B.A. de Azevedo, T.G. Kieckbush, A.K. Tashima, R.S. Mohamed, P. Mazzafera, S.A.B.V. de Melo, Extraction of green coffee oil using supercritical carbon dioxide, J. Supercrit. Fluids. 44 (2008) 186–192. https://doi.org/10.1016/j.supflu.2007.11.004.
[118] B. Leśniak, łukasz Słupik, G. Jakubina, The determination of the specific heat capacity of coal based on literature data, Chemik. 67 (2013) 560–571.
[119] C. Dupont, R. Chiriac, G. Gauthier, F. Toche, Heat capacity measurements of various biomass types and pyrolysis residues, Fuel. 115 (2014) 644–651. https://doi.org/10.1016/j.fuel.2013.07.086.
[120] D.A. Jahn, F.O. Akinkunmi, N. Giovambattista, Effects of temperature on the properties of glycerol: A computer simulation study of five different force fields, J. Phys. Chem. B. 118 (2014) 11284–11294. https://doi.org/10.1021/jp5059098.
[121] A. Bejan, G. Tsatsaronis, M. Moran, Thermal Design & Optimization, John Wiley & Sons, Inc., Canada, 1996.
[122] G. Song, L. Shen, J. Xiao, L. Chen, Estimation of specific enthalpy and exergy of biomass and coal ash, Energy Sources, Part A Recover. Util. Environ. Eff. 35 (2013) 809–816. https://doi.org/10.1080/15567036.2011.586983.
[123] S. V. Vassilev, D. Baxter, L.K. Andersen, C.G. Vassileva, An overview of the chemical composition of biomass, Fuel. 89 (2010) 913–933. https://doi.org/10.1016/j.fuel.2009.10.022.
[124] ASTM International, Standard Test Method for Heat of Combustion of Liquid Hydrocarbon Fuels by Bomb Calorimeter (reapproved 2007), ASTM Stand. D240-02. i (2009) 1–9.
[125] D.L. Tinoco-Caicedo, A. Lozano-Medina, A.M. Blanco-Marigorta, Conventional and advanced exergy and exergoeconomic analysis of a spray drying system: a case study of an instant coffee factory in ecuador, Energies. 13 (2020). https://doi.org/10.3390/en13215622.
[126] Interagua, Informe Anual 2018-2019, Guayaquil, 2019.
[127] E.O. Odebumni, E. a. Ogunsakin, And, P.E.P. Ilukor, Characterization of crude oil and petroleum products, Bull. Chem. Soci. Ethiop. 16 (2002) 115–132.
[128] C. Giller, B. Malkani, J. Parasar, Coffee to Biofuels Coffee to Biofuels, Http://Repository.Upenn.Edu/Cbe_Sdr/94. (2017) 1–129.
[129] C.S.C. and B. of S. USA, Thermal Properties of Petroleum Products: November 9, 1929 - Carl Susan Cragoe - Google Libros, (1933).
[130] G. Xu, T. Murakami, T. Suda, Y. Matsuzawa, H. Tani, Gasification of coffee grounds in dual fluidized bed: Performance evaluation and parametric investigation, Energy and Fuels. 20 (2006) 2695–2704. https://doi.org/10.1021/ef060120d.
[131] J. Baratto, J. Gallego, Análisis Exergético De Un Sistema De Refrigeración Por Absorción De Doble Efecto Con Eyecto-Compresión, Repos. Univ. Tecnol. Pereira. 53

(2014) 123.
[132] E. B. R. Bakshi, T. G. Gutowski, and D. P. Sekulić, Thermodynamics and the Destruction of Resources - Google Libros, (2011).
[133] Staffell Iain, The Energy and Fuel Data Sheet, (2011).
[134] A. International, ASTM D240-09 - International Standards, (2004).
[135] G. of Canada, Stack Losses for Heavy No. 6 Fuel Oil, Can. Ind. Progr. Energy Conserv. (2018).
[136] H.A. Kibret, Y.L. Kuo, T.Y. Ke, Y.H. Tseng, Gasification of spent coffee grounds in a semi-fluidized bed reactor using steam and CO2 gasification medium, J. Taiwan Inst. Chem. Eng. 119 (2021) 115–127. https://doi.org/10.1016/j.jtice.2021.01.029.
[137] A.K. Eswara, S.C. Misra, U.S. Ramesh, Introduction to natural gas: A comparative study of its storage, fuel costs and emissions for a harbor tug, in: Annu. Meet. Soc. Nav. Archit. Mar. Eng., Washington, 2013: pp. 1–21.
[138] F.A. Torres, O. Doustdar, J.M. Herreros, R. Li, R. Poku, A. Tsolakis, J. Martins, S.A.B.V. de Melo, Fischer-tropsch diesel and biofuels exergy and energy analysis for low emissions vehicles, Appl. Sci. 11 (2021). https://doi.org/10.3390/app11135958.
[139] Apak, Energy exergy analyses, Turkey (Supervisor: Prof. Dr. Ramazan K€OSE), in: A Ceramic Factory, Mechanical Engineering Branche; Engineering Faculty, Dumlupınar University, Kütahya, 2007, p. 110. pages (in Turkish)., (n.d.).
[140] Z. Utlu, A. Hepbaşli, Exergoeconomic analysis of energy utilization of drying process in a ceramic production, Appl. Therm. Eng. 70 (2014) 748–762. https://doi.org/10.1016/j.applthermaleng.2014.05.070.
[141] G. Saygi, Z. Erbay, N. Koca, F. Pazir, Energy and exergy analyses of spray drying of a fruit puree (cornelian cherry puree), Int. J. Exergy. 16 (2015) 315–336. https://doi.org/10.1504/IJEX.2015.068229.
[142] A. Cay, E.P. Akcakoca Kumbasar, S. Morsunbul, Exergy analysis of encapsulation of photochromic dye by spray drying, IOP Conf. Ser. Mater. Sci. Eng. 254 (2017). https://doi.org/10.1088/1757-899X/254/2/022003.
[143] Z. Erbay, N. Koca, Energetic, Exergetic, and Exergoeconomic Analyses of Spray-Drying Process during White Cheese Powder Production, Dry. Technol. 30 (2012) 435–444. https://doi.org/10.1080/07373937.2011.647183.
[144] L.E. Kurozawa, K.J. Park, M.D. Hubinger, Spray drying of chicken meat protein hydrolysate: Influence of process conditions on powder property and dryer performance, Dry. Technol. 29 (2011) 163–173. https://doi.org/10.1080/07373937.2010.482711.
[145] A. Mohammadi, M.H. Ahmadi, M. Bidi, F. Joda, A. Valero, S. Uson, Exergy analysis of a Combined Cooling, Heating and Power system integrated with wind turbine and compressed air energy storage system, Energy Convers. Manag. 131 (2017) 69–78. https://doi.org/10.1016/j.enconman.2016.11.003.
[146] M.J. Jokandan, M. Aghbashlo, S.S. Mohtasebi, Comprehensive exergy analysis of an industrial-scale yogurt production plant, Energy. 93 (2015) 1832–1851. https://doi.org/10.1016/j.energy.2015.10.003.
[147] G. Singh, P.J. Singh, V. V. Tyagi, P. Barnwal, A.K. Pandey, Exergy and thermo-economic analysis of ghee production plant in dairy industry, Energy. 167 (2019) 602–618. https://doi.org/10.1016/j.energy.2018.10.138.
[148] M. Camci, Thermodynamic analysis of a novel integration of a spray dryer and solar collectors: A case study of a milk powder drying system, Dry. Technol. 38 (2020) 350–360. https://doi.org/10.1080/07373937.2019.1570935.
[149] B. Li, C. Li, J. Huang, C. Li, Exergoeconomic Analysis of Corn Drying in a Novel Industrial Drying System, Entropy. 22 (2020) 689. https://doi.org/10.3390/e22060689.

[150] A. Gungor, Z. Erbay, A. Hepbasli, Exergoeconomic (Thermoeconomic) Analysis and Performance Assessment of a Gas Engine–Driven Heat Pump Drying System Based on Experimental Data, Dry. Technol. 30 (2012) 52–62. https://doi.org/10.1080/07373937.2011.618897.
[151] Z. Erbay, A. Hepbasli, Exergoeconomic evaluation of a ground-source heat pump food dryer at varying dead state temperatures, J. Clean. Prod. 142 (2017) 1425–1435. https://doi.org/10.1016/j.jclepro.2016.11.164.
[152] Z. Erbay, A. Hepbasli, Advanced exergoeconomic evaluation of a heat pump food dryer, Biosyst. Eng. 124 (2014) 29–39. https://doi.org/10.1016/j.biosystemseng.2014.06.008.
[153] A. Gungor, G. Tsatsaronis, H. Gunerhan, A. Hepbasli, Advanced exergoeconomic analysis of a gas engine heat pump (GEHP) for food drying processes, Energy Convers. Manag. 91 (2015) 132–139. https://doi.org/10.1016/j.enconman.2014.11.044.
[154] L. Wang, P. Fu, Z. Yang, T.E. Lin, Y. Yang, G. Tsatsaronis, Advanced Exergoeconomic Evaluation of Large-Scale Coal-Fired Power Plant, J. Energy Eng. 146 (2020). https://doi.org/10.1061/(ASCE)EY.1943-7897.0000633.
[155] Z. Erbay, A. Hepbasli, Assessment of cost sources and improvement potentials of a ground-source heat pump food drying system through advanced exergoeconomic analysis method, Energy. 127 (2017) 502–515. https://doi.org/10.1016/j.energy.2017.03.148.
[156] H. Sheikhshoaei, M. Dowlati, M. Aghbashlo, M.A. Rosen, Exergy analysis of a pistachio roasting system, Dry. Technol. 38 (2020) 1565–1583. https://doi.org/10.1080/07373937.2019.1649276.
[157] A. Singh, J. Sarkar, R.R. Sahoo, Experimental energy, exergy, economic and exergoeconomic analyses of batch-type solar-assisted heat pump dryer, Renew. Energy. 156 (2020) 1107–1116. https://doi.org/10.1016/j.renene.2020.04.100.
[158] M. Beigi, M. Tohidi, M. Torki-Harchegani, Exergetic analysis of deep-bed drying of rough rice in a convective dryer, (2017). https://doi.org/10.1016/j.energy.2017.08.100.
[159] C. Ofori-Boateng, T.L. Keat, L. Jitkang, Feasibility study of microalgal and jatropha biodiesel production plants: Exergy analysis approach, Appl. Therm. Eng. 36 (2012) 141–151. https://doi.org/10.1016/j.applthermaleng.2011.12.010.
[160] G. Khoobbakht, K. Kheiralipour, H. Rasouli, M. Rafiee, M. Hadipour, M. Karimi, Experimental exergy analysis of transesterification in biodiesel production, Energy. 196 (2020). https://doi.org/10.1016/j.energy.2020.117092.
[161] Y. Ji-chao, B. Sobhani, Integration of biomass gasification with a supercritical CO2 and Kalina cycles in a combined heating and power system: A thermodynamic and exergoeconomic analysis, Energy. 222 (2021) 119980. https://doi.org/10.1016/j.energy.2021.119980.
[162] M. Hosseini, I. Dincer, M.A. Rosen, Steam and air fed biomass gasification: Comparisons based on energy and exergy, Int. J. Hydrogen Energy. 37 (2012) 16446–16452. https://doi.org/10.1016/j.ijhydene.2012.02.115.
[163] D. Tapasvi, R.S. Kempegowda, K.Q. Tran, Ø. Skreiberg, M. Grønli, A simulation study on the torrefied biomass gasification, Energy Convers. Manag. 90 (2015) 446–457. https://doi.org/10.1016/j.enconman.2014.11.027.
[164] L. Jin, H. Zhang, Z. Ma, Study on capacity of coffee grounds to be extracted oil, produce biodiesel and combust, Energy Procedia. 152 (2018) 1296–1301. https://doi.org/10.1016/j.egypro.2018.09.185.
[165] H. Atalay, Comparative assessment of solar and heat pump dryers with regards to exergy and exergoeconomic performance, (2019). https://doi.org/10.1016/j.energy.2019.116180.

[166] R.B. Keey, Introduction to Industrial Drying Operation, Pergamon Press. New York. (1978).
[167] S. Zohrabi, S.S. Seiiedlou, M. Aghbashlo, H. Scaar, J. Mellmann, Enhancing the exergetic performance of a pilot-scale convective dryer by exhaust air recirculation, Dry. Technol. 38 (2020) 518–533. https://doi.org/10.1080/07373937.2019.1587617.
[168] B. Fakhimghanbarzadeh, B. Farhanieh, H. Marzi, A. Javadzadegan, Evolutionary algorithm for multi-objective exergoeconomic optimization of biomass waste gasification combined heat and power system, IEEE Int. Conf. Ind. Informatics. (2009) 361–366. https://doi.org/10.1109/INDIN.2009.5195831.
[169] M. Fani, B. Farhanieh, A.A. Mozafari, Exergoeconomic optimization of black liquor gasification combined cycle using evolutionary and conventional iterative method, Int. J. Chem. React. Eng. 8 (2010). https://doi.org/10.2202/1542-6580.1894.
[170] A. Abuadala, I. Dincer, Exergoeconomic Analysis of a Hybrid Steam Biomass Gasification-Based Tri-Generation System, Prog. Exergy, Energy, Environ. (2014) 51–67. https://doi.org/10.1007/978-3-319-04681-5.
[171] Y. Kalinci, A. Hepbasli, I. Dincer, Exergoeconomic analysis and performance assessment of hydrogen and power production using different gasification systems, Fuel. 102 (2012) 187–198. https://doi.org/10.1016/j.fuel.2012.06.040.
[172] E.J.C. Cavalcanti, M. Carvalho, D.R.S. da Silva, Energy, exergy and exergoenvironmental analyses of a sugarcane bagasse power cogeneration system, Energy Convers. Manag. 222 (2020) 113232. https://doi.org/10.1016/j.enconman.2020.113232.
[173] J. Jia, G. Zang, M.C. Paul, Energy, exergy, and economic (3E) evaluation of a CCHP system with biomass gasifier, solid oxide fuel cells, micro-gas turbine, and absorption chiller, Int. J. Energy Res. 45 (2021) 15182–15199. https://doi.org/10.1002/er.6794.
[174] J. Wang, Y. Chen, N. Lior, Exergo-economic analysis method and optimization of a novel photovoltaic/thermal solar-assisted hybrid combined cooling, heating and power system, Energy Convers. Manag. 199 (2019) 111945. https://doi.org/10.1016/j.enconman.2019.111945.
[175] E.J.C. Cavalcanti, Energy, exergy and exergoenvironmental analyses on gas-diesel fuel marine engine used for trigeneration system, Appl. Therm. Eng. 184 (2021) 116211. https://doi.org/10.1016/j.applthermaleng.2020.116211.
[176] D.L. Tinoco-caicedo, M. Mero-benavides, M. Santos-torres, A. Lozano-medina, A.M. Blanco-marigorta, Case Studies in Thermal Engineering Simulation and exergoeconomic analysis of the syngas and biodiesel production process from spent coffee grounds, Case Stud. Therm. Eng. 28 (2021) 101556. https://doi.org/10.1016/j.csite.2021.101556.
[177] E.J.C. Cavalcanti, J.V.M. Ferreira, M. Carvalho, Exergy assessment of a solar-assisted combined cooling, heat and power system, Sustain. Energy Technol. Assessments. 47 (2021). https://doi.org/10.1016/j.seta.2021.101361.
[178] O. Balli, Performance Evaluation of a Trigeneration System with Micro Gas Turbine Engine (MICTRIGEN) based on Exergy Analysis, Type Double Blind Peer Rev. Int. Res. J. Publ. Glob. Journals Inc. 17 (2017).

7. Annexes

energies

MDPI

Article

Conventional and Advanced Exergy and Exergoeconomic Analysis of a Spray Drying System: A Case Study of an Instant Coffee Factory in Ecuador

Diana L. Tinoco-Caicedo [1,2,*], Alexis Lozano-Medina [2] and Ana M. Blanco-Marigorta [2]

[1] Facultad de Ciencias Naturales y Matemáticas, Escuela Superior Politécnica del Litoral, 090903 Guayaquil, Ecuador

[2] Department of Process Engineering, Universidad de las Palmas de Gran Canaria, 35017 Las Palmas de Gran Canaria, Spain; alexis.lozano@ulpgc.es (A.L.-M.); anamaria.blanco@ulpgc.es (A.M.B.-M.)

* Correspondence: dtinoco@espol.edu.ec

Received: 14 September 2020; Accepted: 23 October 2020; Published: 27 October 2020

Abstract: Instant coffee is produced worldwide by spray drying coffee extract on an industrial scale. This production process is energy intensive, 70% of the operational costs are due to energy requirements. This study aims to identify the potential for energy and cost improvements by performing a conventional and advanced exergy and exergoeconomic analysis to an industrial-scale spray drying process for the production of instant coffee, using actual operational data. The study analyzed the steam generation unit, the air and coffee extract preheater, the drying section, and the final post treatment process. The performance parameters such as exergetic efficiency, exergoeconomic factor, and avoidable investment cost rate for each individual component were determined. The overall energy and exergy efficiencies of the spray drying system are 67.6% and 30.6%, respectively. The highest rate of exergy destruction is located in the boiler, which amounts to 543 kW. However, the advanced exergoeconomic analysis shows that the highest exergy destruction cost rates are located in the spray dryer and the air heat exchanger (106.9 $/h and 60.5 $/h, respectively), of which 47.7% and 3.8%, respectively, are avoidable. Accordingly, any process improvement should focus on the exergoeconomic optimization of the spray dryer.

Keywords: advanced exergoeconomic analysis; spray dryer; exergy destruction cost rate

1. Introduction

Instant coffee is one of the most commonly consumed drinks worldwide; around 118 billion dollars of it were sold in the global market in 2019. The worldwide market for instant coffee has high growth expectations: projected to grow by 11.6% in the next 5 years [1]. Coffee has a high concentration of antioxidants [2], vitamins B, and minerals [3]. It benefits physical performance and stimulates the central nervous system [4]. Coffee is sold as whole bean, ground coffee, instant coffee, coffee pods, and capsules. Among these, instant coffee is quickly becoming popular all over the world because of cheaper transportation and convenience in preparation, which increases its demand among urban consumers [5]. Many industrial-scale plants have been established around the word to produce this kind of coffee.

The production process of instant coffee powder begins with roasting the coffee beans and grinding them. Later, they pass through a liquid solid extraction. The extracted liquid is then concentrated and, finally, it is spray dried. The drying process reduces the amount of water in the coffee and allows its shelf-life to be increased. This operation requires the most energy resources [6], and is also considered highly exergy-destructive [7]. Spray dryers are considered to be limiting units within a productive

process, and one of the operations with the highest exergy improvement potential [8]. A previous study has demonstrated that the exergy efficiency of spray dryers is lower than that of other drying technologies such as tray dryers, continuous dryers, heat pump assisted dryers, fluidized bed dryers, solar dryers, freeze dryers, vacuum dryers, and flash dryers [7].

Exergy analysis has become an important tool for the assessment of different energy-intensive industrial processes, such as spray drying [9]. These analyses have allowed for the identification of the components with the highest exergy losses, the avoidable exergy losses, and the operational conditions, which most affect the irreversibility of the systems. Erbay et al. [10] used a pilot-scale spray dryer on white cheese slurry to demonstrate experimentally that parameters like atomization pressure and drying air temperature can affect the exergetic efficiency of the spray dryer. Another study of the same scale for the drying of cherry puree showed that drying agents could reduce the exergy destruction rate of the process [11]. Some studies were done at a laboratory scale. One lab-scale study, evaluated the exergetic efficiency of spray drying of photochromic dyes and obtained efficiency below 4% [12]. Further, Aghbashlo et al. [13] studied the influence of parameters such as air and feed flow rate in the exergy destruction rate of the spray drying of microencapsulation of fish oil. Only two studies have been done on industrial-scale spray dryers, and both took place in a powdered milk factory. The first analyzed each step of the production process and concluded that the spray dryer was one of the most exergy destructive components (2196 kW) [14]. In the second study, Camci et al. [15] analyzed a spray drying system with solar collectors for preheating the drying air in a closed loop, resulting in an increase of the exergetic efficiency to 22.6%.

However, although the exergetic analysis identifies the location and magnitude of the thermal energy losses, it has limitations given that it can not quantify the cost of those losses. Furthermore, an exergy analysis is not conclusive about which components should have investment priority in order to reduce the exergy losses [16]. In order to complete an exergy analysis, an exergoeconomic analysis can be applied, which combines exergy and economic principles at the component level to identify the real cost sources in a thermal system [17]. Since the thermodynamic considerations of exergoeconomics are based on the exergy concept, the term exergoeconomics can also be used to describe the combination of exergy analysis and economics [18]. Exergoeconomic analysis has been applied in different industrial processes in order to minimize the economic losses due to irreversibility, and, consequently, provide the added benefit of reducing production costs of the entire complex energy system. Few conventional exergoeconomic analyses of different drying technologies on both the pilot and industrial scale have been found in the literature; they focused on the production of pasta [19], tea leaves [20], powdered cheese [21], and powdered milk [22,23]. Of these, only the last two refer to spray drying technology at an industrial scale. These exergoeconomic analysis performed were useful for the evaluation of the economic viability of the proposed improvements to the spray dryer in a powdered milk factory. Erbay et al. [21] also performed an exergoeconomic analysis on a pilot-scale spray dryer for cheese powder and concluded that some investments should be made in order to reduce the operational cost rates by increasing exergetic efficiency of the process.

Although the exergy and exergoeconomic analyses allow for the quantification of the exergetic and cost losses, they do not provide sufficient information about which losses are avoidable; this information is essential for industrial plants to make decisions about improvement potential. Advanced exergoeconomic analysis is a proposed tool that has been applied to different industrial processes in order to quantify the avoidable and unavoidable economic losses and determine the potential for improvement [24]. However, there have not been any studies that apply an advanced exergoeconomic analysis in spray-drying technology in order to quantify this kind of exergy destruction.

The aim of the present work is to carry out a conventional and advanced exergy and exergoeconomic analysis on the spray drying process of instant coffee at a factory in Guayaquil, Ecuador in order to quantify total operating cost rates at a component level and split into avoidable and unavoidable parts. There are two main novelties in this study: first, real data from an instant coffee plant in operation have been used; second, an advanced exergoeconomic analysis on the spray-drying system of an instant

coffee plant has been applied for the first time. This analysis will be a valuable decision-making tool for the factory for future improvements focused on operational cost reduction, and sustainability increase.

2. Materials and Methods

2.1. System Description

The instant coffee was dried in an industrial scale spray drying system. Figure 1 illustrates a schematic diagram of the process. The coffee extract (44% m/m of soluble coffee) comes from a storage tank that had a temperature of 12 °C. A flow rate of 528 kg/h of coffee extract (stream 2) was pumped by a low-pressure pump (LP) and mixed with 7.4 kg/h of carbon dioxide (stream 1). Then it was pumped by a high-pressure pump (HP) into a heat exchanger unit (HXE) where steam increased its temperature to 32 °C. The coffee extract (stream 6) was sprayed by a nozzle into the drying unit (SD), which is at vacuum pressure. A flow rate of 9922 kg/h of ambient air (stream 7) was heated by the main heat exchanger (MHX) using steam until it reached the temperature of 180 °C. A flow rate of 4002 kg/h of ambient air (stream 10) with an absolute humidity of 0.02 kg water/kg dry air was dehumidified to 8×10^{-3} kg water/kg dry air by a cooler (CHX) and then a fraction of it (stream 11) was heated and distributed in order to maintain a fluidized bed in the bottom of the spray dryer. The dried instant coffee produced with a humidity of about 3% m/m (stream 23) was then collected on a belt (BT), where two streams of dehumidified air at 85 °C (stream 16) and 27 °C (stream 20) were used to gradually cool the coffee and prevent it from agglomerating. Then the instant coffee (stream 25) was passed through vibratory screen (S) in order to obtain the required particle size. The fraction of instant coffee with the smallest particle size (stream 28) was recirculated to the process using dried air at 27 °C (stream 22) while the biggest particle size of instant coffee (stream 27) was considered waste. The humidified air (stream 29) that exits the spray dryer was passed through a cyclone separator (FF) to remove solid coffee particles. These solid particles (stream 32) were recirculated into the process and the humidified air (stream 31) was released to the environment.

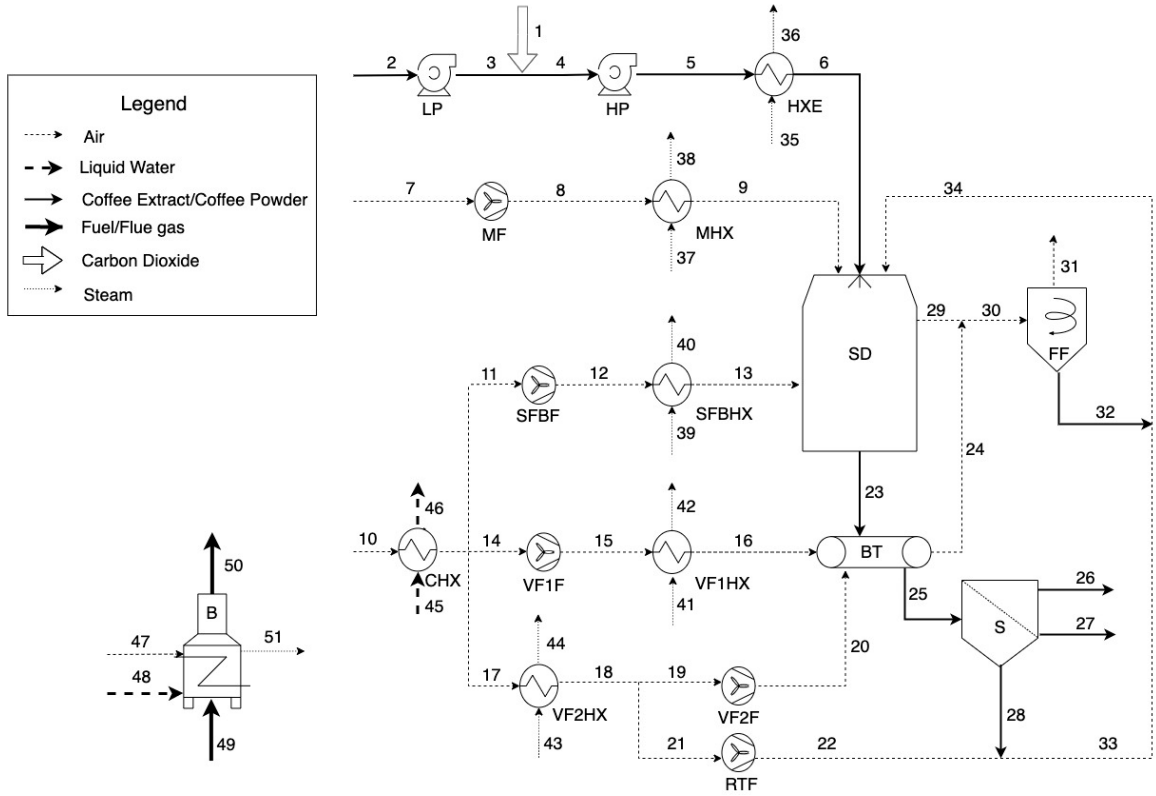

Figure 1. Process flow diagram of the spray dryer system.

To develop the process modeling, the following assumptions were made:

- The process was at a steady state condition.
- The coffee extract was modeled as a solution with a constant concentration of soluble solids from *Coffea arabica* beans.
- The heat losses from the components were neglected.
- The pressure losses in the pipes, heat exchangers, bag filter, and spray dryer were neglected.
- The properties of the incoming air were considered as constants.

2.2. Exergy Analysis

The analysis of the spray drying system was performed by using the engineering equation solver (EES) software for the formulation of mass, energy, and exergy balances for each component. In their general form, they are, respectively:

$$\sum_{in} \dot{m}_{in} - \sum_{out} \dot{m}_{out} = 0 \tag{1}$$

$$\sum_{in} h_{in}\dot{m}_{in} - \sum_{out} h_{out}\dot{m}_{out} + \dot{W}_k + \dot{Q}_k = 0 \tag{2}$$

$$\sum_{k} \dot{E}_{q,k} + \dot{W}_k + \sum_{in} \dot{E}_{in} - \sum_{out} \dot{E}_{out} - \dot{E}_{D,k} = 0 \tag{3}$$

The exergy rate, specific exergy, physical exergy, kinetics exergy, and potential exergy were calculated using Equations (4)–(8). Table 1 shows the expressions of both fuel and product exergy of each component.

$$\dot{E} = \dot{m} * e \tag{4}$$

$$e = e^{PH} + e^{CH} + e^{KN} + e^{PT} \tag{5}$$

$$e^{PH} = (h - h_0) - T_0(s - s_0) \tag{6}$$

$$e^{PT} = gz \tag{7}$$

$$e^{KN} = \frac{v^2}{2} \tag{8}$$

Table 1. Composition of the different states.

State	Description	Soluble Solids (kg/kg)	Water (kg/kg)	Dried Air (kg/kg)
2	Coffee extract	0.440	0.560	-
23	Soluble Coffee powder	0.970	0.030	-
24	Mixture BT	0.001	0.009	0.990
29	Mixture SD	0.004	0.040	0.955
33	Mixture S	0.038	0.008	0.954
34	Mixture FF	0.117	0.001	0.882

The velocities of different streams were estimated by the Bernoulli relationship, Equation (9), where γ is the specific heat ratio and ρ is the density of the stream.

$$\frac{\Delta v^2}{2} + \left(\frac{\gamma}{\gamma - 1}\right) * \frac{P}{\rho} = \left(\frac{\gamma}{\gamma - 1}\right) * \frac{P_0}{\rho_0} \tag{9}$$

For the streams that had soluble coffee solids as part of their compositions, Equations (10) and (11) were used to determine the thermodynamic properties such as entropy and enthalpy. The c_p value was

obtained from Burmester et al. [25]. The dead state conditions have been taken as T_0 = 27.5 °C and P_0 = 101.13 kPa.

$$h - h_0 = c_p(T - T_0) \tag{10}$$

$$s - s_0 = c_p \ln\left(\frac{T}{T_0}\right) - Rln\left(\frac{P}{P_0}\right) \tag{11}$$

The composition for the different states of the system is shown in Table 1. This information was used to calculate the different thermodynamic properties.

For the calculation of chemical exergy of each state point that has soluble coffee solids and water, Equation (12) [17] was used. The concentration of water and coffee in equilibrium with the environment (x_i^e) was chosen as the dead state of reference. Those values were obtained from previous studies on Arabica coffee by Yao et al. [26]. For the calculation of the chemical exergy of each state point that has soluble coffee solids, water, and air, Equation (13) [17] was used, where x_i is the mole fraction of the different substances.

$$e_{CE}^{CH} = -RT_0 \sum x_i \ln\left(\frac{x_i^e}{x_i}\right) \tag{12}$$

$$e_{mix}^{CH} = \sum x_i e_i^{ch} + RT_0 \sum x_i \ln(x_i) \tag{13}$$

The chemical exergy of air for the different moisture content in air was calculated using an expression from Wepfer et al. [27], according to Equation (14), where w_o and w are mole fraction of water vapor at environmental conditions and operational conditions, respectively.

$$e_{air}^{CH} = 0.2857 c_{p,air} T_o ln\left[\left[\frac{1 + 1.6078 w_o}{1 + 1.6078 w}\right]^{(1+1.6078w)} \left[\frac{w}{w_o}\right]^{1.6078w}\right] \tag{14}$$

The exergy balance can also be formulated as Equation (15).

$$\dot{E}_{F,k} - \dot{E}_{P,k} = \dot{E}_{D,k} - \dot{E}_{L,k} \tag{15}$$

where $\dot{E}_{F,k}$ corresponds to the fuel exergy, $\dot{E}_{P,k}$ is the product exergy, $\dot{E}_{D,k}$ is the destroyed, exergy and $\dot{E}_{L,k}$ is the exergy loss. The exergy of the fuel and the exergy of the product for each single component were formulated following Lazzareto and Tsatsaronis rules [28] and they are shown in Table 2.

For the total system the exergetic efficiency was calculated as the sum of the product exergy rates divided by the sum of the fuel exergy rates.

Other interesting parameters involved in an exergy analysis were the relative exergy destruction ($y_{D,k}^*$), which represents the relationship between the destroyed exergy of a component and the total destroyed exergy of the system, as shown in Equation (16) [17]. The exergy destruction ratio ($y_{D,k}$), which relates the destroyed exergy of a component with the total fuel exergy of the system, is shown in Equation (17). The exergetic efficiency ($n_{ex,k}$), which represents the amount of exergy that is useful in relation to the fuel exergy in the component, is shown in Equation (18).

$$y_{D,k}^* = \frac{\dot{E}_{D,k}}{\dot{E}_{D,tot}} \tag{16}$$

$$y_{D,k} = \frac{\dot{E}_{D,k}}{\dot{E}_{F,tot}} \tag{17}$$

$$n_{ex,k} = \frac{\dot{E}_{P,k}}{\dot{E}_{F,k}} \tag{18}$$

Table 2. Definitions of fuel and product exergy for each component.

Component	$\dot{E}_{P,k}$	$\dot{E}_{F,k}$
LP	$\dot{E}_3 - \dot{E}_2$	$\dot{W}_{LP}$
HP	$\dot{E}_5 - \dot{E}_4$	$\dot{W}_{HP}$
HXE	$\dot{E}_6 - \dot{E}_5$	$\dot{E}_{35} - \dot{E}_{36}$
MHX	$\dot{E}_9 - \dot{E}_8$	$\dot{E}_{37} - \dot{E}_{38}$
SFBHX	$\dot{E}_{13} - \dot{E}_{12}$	$\dot{E}_{39} - \dot{E}_{40}$
VF1HX	$\dot{E}_{16} - \dot{E}_{15}$	$\dot{E}_{41} - \dot{E}_{42}$
VF2HX	$\dot{E}_{18} - \dot{E}_{17}$	$\dot{E}_{43} - \dot{E}_{44}$
MF	$\dot{E}_8 - \dot{E}_7$	$\dot{W}_{MF}$
SFBF	$\dot{E}_{12} - \dot{E}_{11}$	$\dot{W}_{SFBF}$
VF1F	$\dot{E}_{15} - \dot{E}_{14}$	$\dot{W}_{VF1F}$
VF2F	$\dot{E}_{20} - \dot{E}_{19}$	$\dot{W}_{VF2F}$
RFF	$\dot{E}_{22} - \dot{E}_{21}$	$\dot{W}_{RFF}$
FF	$\dot{E}_{32} + \dot{E}_{31} - \dot{E}_{30}$	$\dot{W}_{FF}$
SD	$\dot{E}_{23} - \dot{E}_6 - \dot{E}_{34}$	$\dot{E}_{13} + \dot{E}_9 - \dot{E}_{29}$
BT	$\dot{E}_{25} - \dot{E}_{23}$	$\dot{E}_{20} + \dot{E}_{16} - \dot{E}_{24}$
S	$\dot{E}_{26} + \dot{E}_{28} - \dot{E}_{25}$	$\dot{E}_{27} + \dot{W}_S$
B	$\dot{E}_{51} - \dot{E}_{48}$	$\left(\dot{E}_{49} + \dot{E}_{47}\right) - \dot{E}_{50}$
CHX	$\dot{E}_{14} + \dot{E}_{17} + \dot{E}_{11} - \dot{E}_{10}$	$\dot{E}_{45} - \dot{E}_{46}$

2.3. Advanced Exergy Analysis

In order to obtain the real potential of improvement of each component, the avoidable and unavoidable parts of the exergy destruction were calculated. The unavoidable part of the exergy destruction ($\dot{E}_{D,k}^{UN}$) would be the exergy that will inevitably be destroyed, due to technological limitations, no matter how much capital is invested, and can be calculated by using Equation (19) [29], where $(\dot{E}_D/\dot{E}_P)_k^{UN}$ is the relationship between the exergy destruction and exergy product rates estimated using the unavoidable conditions for each component.

$$\dot{E}_{D,k}^{UN} = \dot{E}_{P,k}\left(\frac{\dot{E}_D}{\dot{E}_P}\right)_k^{UN} \tag{19}$$

Values of the unavoidable and real operation conditions of the components are summarized in Table 3, and were assumed according to previous studies [14,30]. For the spray dryer, the minimum air flow required to supply the energy for water evaporation was calculated as an avoidable condition [31].

Table 3. Assumptions that are considered for real conditions (RC), unavoidable thermodynamic inefficiency conditions (RTI), and unavoidable investment cost conditions (UIC).

Component	RC	RTI	UIC
Heat Exchangers	$\Delta T_{min,\,HXE} = 51$ $\Delta T_{min,\,MHX} = 12$ $\Delta T_{min,\,SFBHX} = 69$ $\Delta T_{min,\,VF1HX} = 80$ $\Delta T_{min,\,VF2HX} = 139$ $\Delta T_{min,\,CHX} = 9$	$\Delta T_{min,\,HXE} = 30$ $\Delta T_{min,\,MHX} = 10$ $\Delta T_{min,\,SFBHX,\,VFIHX} = 20$ $\Delta T_{min,\,VF2HX} = 80$ $\Delta T_{min,\,CHX} = 4$	$\Delta T_{min,\,HXE} = 60$ $\Delta T_{min,\,MHX} = 20$ $\Delta T_{min,\,SFBHX} = 80$ $\Delta T_{min,\,VF1HX} = 90$ $\Delta T_{min,\,VF2HX} = 145$ $\Delta T_{min,\,CHX} = 15$
Pumps	$\eta_{is} = 60\%$	$\eta_{is} = 86\%$	$\eta_{is} = 65\%$
F	$\eta_{is} = 60\%$	$\eta_{is} = 90\%$	$0.85\ \dot{Z}_k^{real}$
S	$\eta_{elec} = 78\%$	$\eta_{elec} = 90\%$	$\eta_{elec} = 78\%$
BT	$\eta_{elec} = 60\%$	$\eta_{elec} = 85\%$	$\eta_{elec} = 60\%$
B	$\eta_{con} = 90\%$	$\eta_{con} = 95\%$	$0.66\ \dot{Z}_k^{real}$
SD	AP-Ratio = 18.8	AP-Ratio = 8.6	$0.90\ \dot{Z}_k^{real}$

2.4. Exergoeconomic Analysis

The exergoeconomic analysis consists of the formulation of a cost balance and its auxiliary equations at a component level, for each component of the process. The general cost balance [17] is shown in Equation (20) where c_{out} and c_{in} represent the costs of the outflows and inflows respectively, $c_{w,k}$ represents the cost rate related with the work and $\dot{Z}_k$ represents the investment cost of each component. Table 2 shows the cost balance of each component present in the system.

$$\sum_k c_{q,k}\dot{E}_{q,k} + c_{w,k}\dot{W}_k + \sum_{in} c_{in}\dot{E}_{in} - \sum_{out} c_{out}\dot{E}_{out} - c_{D,k}\dot{E}_{D,k} + \dot{Z}_k = 0 \quad (20)$$

The cost balance can be written in terms of the fuel and product formulation [28] as is shown in Equations (21) and (22).

$$\dot{C}_{P,k} = \dot{C}_{F,k} + \dot{Z}_k - \dot{C}_{D,k} \quad (21)$$

$$c_{P,k}\dot{E}_{P,k} = c_{F,k}\dot{E}_{F,k} + \dot{Z}_k - \dot{C}_{D,k} \quad (22)$$

where $\dot{C}_{P,k}$ is the product cost rate, $\dot{C}_{F,k}$ is the fuel cost rate, and $\dot{C}_{D,k}$ is the cost rate associated with the destroyed exergy for each component.

The exergy destroyed in the k-th component has an associated cost rate $\dot{C}_{D,k}$ that can be calculated in terms of the cost of the additional fuel ($c_{F,k}$) that needs to be supplied to this component to cover the exergy destruction and to generate the same exergy flow rate of the product, when $\dot{E}_{P,k}$ stay constant (Equation (23)) [17]. Table 4 shows the cost balance of each component present in the system.

$$\dot{C}_{D,k} = c_{F,k}\dot{E}_{D,k} \quad (23)$$

Table 4. Cost balance equations and auxiliary equations for exergy costs of the system.

Component	Fuel Cost Expression	Product Cost Expression	Auxiliary Equations
LP	$\dot{C}_3 + \dot{W}_{LP}$	$\dot{C}_2 + \dot{Z}_{LP}$	-
HP	$\dot{C}_5 + \dot{W}_{HP}$	$\dot{C}_4 + \dot{Z}_{HP}$	$c_4 = c_3 + c_1$
HXE	$\dot{C}_6 + \dot{C}_{36}$	$\dot{C}_5 + \dot{C}_{35}$	$c_{36} = c_{35} = c_{51}$
MHX	$\dot{C}_9 + \dot{C}_{38}$	$\dot{C}_8 + \dot{C}_{37}$	$c_{38} = c_{37} = c_{51}$
SFBHX	$\dot{C}_{13} + \dot{C}_{40}$	$\dot{C}_{12} + \dot{C}_{39}$	$c_{40} = c_{39} = c_{51}$
VF1HX	$\dot{C}_{16} + \dot{C}_{42}$	$\dot{C}_{15} + \dot{C}_{41}$	$c_{42} = c_{41} = c_{51}$
VF2HX	$\dot{C}_{18} + \dot{C}_{44}$	$\dot{C}_{17} + \dot{C}_{43}$	$c_{44} = c_{43} = c_{51}$
MF	$\dot{C}_8 + \dot{W}_{MF}$	$\dot{C}_7$	$c_7 = 0$
SFBF	$\dot{C}_{12} + \dot{W}_{SFBF}$	$\dot{C}_{11}$	-
VF1F	$\dot{C}_{15} + \dot{W}_{VF1F}$	$\dot{C}_{14}$	-
VF2F	$\dot{C}_{20} + \dot{W}_{VF2F}$	$\dot{C}_{19}$	$c_{19} = c_{18}$
RFF	$\dot{C}_{22} + \dot{W}_{RFF}$	$\dot{C}_{21}$	$c_{21} = c_{18}$
FF	$\dot{C}_{31} + \dot{C}_{32} + \dot{W}_{FF}$	$\dot{C}_{30}$	$c_{31} = c_{32}$
SD	$\dot{C}_{29} + \dot{C}_{23}$	$\dot{C}_6 + \dot{C}_9 + \dot{C}_{13} + \dot{C}_{34}$	$c_{29} = c_9$
BT	$\dot{C}_{24} + \dot{C}_{25}$	$\dot{C}_{16} + \dot{C}_{23}$	$c_{24} = c_{16}$
S	$\dot{W}_S$	$\dot{C}_{26} + \dot{C}_{27} - \dot{C}_{25} - \dot{C}_{28}$	$c_{28} = c_{30}; c_{29} = c_{31}$
B	$\dot{C}_{50} + \dot{C}_{51}$	$\dot{C}_{47} + \dot{C}_{48} + \dot{C}_{49}$	$c_{47} = 0; c_{49} = c_{50}$
CHX	$\dot{C}_{11} + \dot{C}_{14} + \dot{C}_{17} + \dot{C}_{46}$	$\dot{C}_{10} + \dot{C}_{45}$	$c_{10} = 0; c_{45} = c_{46}$ $c_{11} = c_{14} = c_{17}$

There are some non-energetic costs used in the calculations of the cost balance of each component. In the boiler, the fuel used to generate vapor was fuel oil 6. The price of the liquid fuel (stream 49) was

$1.07 per gallon [32]. The potable water (stream 48) had a cost of $0.53 per cubic meter [33]. The price of carbon dioxide (stream 1) injected into the coffee extract was $24.22 per kg.

The variable $\dot{Z}_k$ was calculated as the sum of capital investment ($\dot{Z}_k^{CI}$) and operation and maintenance costs ($\dot{Z}_k^{OM}$) for each component, as is shown in Equation (24) [17].

$$\dot{Z}_k = \dot{Z}_k^{OM} + \dot{Z}_k^{CI} \tag{24}$$

The capital investment for each component can be calculated by using Equation (25) [17]:

$$\dot{Z}_k^{CI} = \frac{PEC_k * CRF}{\tau} \tag{25}$$

where PEC_k is the purchase price of the kth component and τ is the number of annual operating hours (24 h per day, 365 days per year). It was assumed that the ordinary annuities transaction occurs at the end of each time interval, thus the *CRF* (capital recovery factor) could be obtained using Equation (26) [17], where i_{eff} is the interest rate (10%), and n is the lifetime of the system (20 years).

$$CRF = \frac{i_{eff} * \left(1 + i_{eff}\right)^{\mathrm{n}}}{\left(1 + i_{eff}\right)^{\mathrm{n}} - 1} \tag{26}$$

The rate of operation and maintenance costs ($\dot{Z}_k^{OM}$) can be calculated by using Equation (27). The operation and maintenance cost ($\mathrm{OMC_k}$) of each component is determined by using Equation (28), which is a close approximation used by Bejan et al [17]. The constant-escalation levelization factor (CELF) was determined by using Equation (29), which depends on the factor k_{OMC} defined by Equation (30) [17]. For the nominal escalation rate (r_{OM}), it was assumed that all costs except fuel costs and the values of by-products change annually with the constant average inflation rate of 4% [17].

$$\dot{Z}_k^{OM} = \frac{OMC_k * CELF_{OM}}{\tau} \tag{27}$$

$$OMC_k = 0.2 * PEC_k \tag{28}$$

$$CELF_{OM} = \frac{k_{OMC} * (1 - {k_{OMC}}^n) * CRF}{(1 - k_{OMC})} \tag{29}$$

$$k_{OMC} = \frac{1 + r_{OM}}{1 + i_{eff}} \tag{30}$$

For a better interpretation of the results, the exergoeconomic factor (f_k) and relative cost difference (r_k) were determined. The first factor represents the relationship between the investment cost and the total operating cost rate, while the r_k represents the increase of the specific exergy cost in a component divided by the specific exergy cost of the fuel.

$$f_k = \frac{\dot{Z}_k}{\dot{Z}_k + \dot{C}_{D,k}} \tag{31}$$

$$r_k = \frac{c_{P,k} - c_{F,k}}{c_{F,k}} \tag{32}$$

2.5. Advanced Exergoeconomic Analysis

The unavoidable ($\dot{C}_{D,k}^{UN}$) and avoidable cost ($\dot{C}_{D,k}^{AV}$) associated with exergy destruction were calculated using Equations (33) and (34). The unavoidable ($\dot{Z}_k^{UN}$) and avoidable investment cost rates

($\dot{Z}_k^{AV}$) were calculated by using Equations (35) and (36). The relation between the investment cost rate and the exergy product rate $(\dot{Z}_k/\dot{E}_P)_k^{UN}$ was estimated by using the unavoidable cost conditions presented in Table 4. For the heat exchangers, a Pro/II ®simulator was used to estimate the new heat transfer area based on the minimum temperature difference.

$$\dot{C}_{D,k}^{UN} = c_{F,k}\dot{E}_{D,k}^{UN} \tag{33}$$

$$\dot{C}_{D,k}^{AV} = \dot{C}_{D,k} - \dot{C}_{D,k}^{AV} \tag{34}$$

$$\dot{Z}_k^{UN} = \dot{E}_{P,k}\left(\frac{\dot{Z}_k}{\dot{E}_P}\right)_k^{UN} \tag{35}$$

$$\dot{Z}_k^{AV} = \dot{Z}_k - \dot{Z}_k^{UN} \tag{36}$$

3. Results and Discussions

3.1. Conventional Exergy Analysis

The parameters of the exergetic analysis were calculated for each state throughout the entire studied system. Table 5 shows the flow rate ($\dot{m}$), temperature (T), pressure (P), specific chemical exergy (e^{CH}), specific physical exergy (e^{PH}), specific kinetic exergy (e^{KN}), and exergy rate ($\dot{E}$) of each stream.

Table 5. Thermodynamic values of the streams.

State	$\dot{m}$ (kg/h)	T (°C)	P (kPa)	e^{CH} (kJ/kg)	e^{PH} (kJ/kg)	e^{KN} (kJ/kg)	$\dot{E}$ (kJ/h)
1	7.4	12	101	322	0.22	0.0	2383
2	528	14	101	2.25	10.8	0.0	6891
3	528	15	750	2.25	9.70	0.5	6593
4	528	16	750	1.56	8.84	0.5	5776
5	528	18	5400	1.56	4.73	4.0	5470
6	528	39	5400	1.56	13.4	4.0	10,045
7	9922	28	101	0.00	0.00	0.0	0
8	9922	28	105	0.01	0.00	1.0	10,286
9	9922	178	105	0.01	29.9	1.0	307,205
10	4002	28	101	0.00	0.00	0.0	0
11	1626	15	101	0.002	0.27	0.0	436
12	1626	15	105	0.012	0.27	1.0	2126
13	1626	96	105	0.012	6.97	1.0	13,031
14	1100	15	101	0.002	0.27	0.0	295
15	1100	15	105	0.012	0.27	1.0	1438
16	1100	85	105	0.012	5.02	1.0	6665
17	1276	15	101	0.002	0.27	0.0	342
18	1276	26	101	0.002	0.00	0.0	6
19	1101	26	101	0.002	0.00	0.0	6
20	1101	27	105	0.012	0.00	1.0	1146
21	175	26	101	0.002	0.00	0.0	1
22	175	27	105	0.012	0.00	1.0	182
23	209	80	101	5.80	8.24	6.0	4202
24	2203	58	101	0.002	1.49	0.0	3298
25	207	35	101	5.80	0.18	1.0	1450
27	0.04	30	101	4.18	0.07	0.0	0.04
26	200	30	101	5.80	0.02	0.0	1163
28	6.96	30	101	5.80	0.02	0.0	40
29	12,065	96	100	0.001	7.45	2.1	114,790
30	14,268	94	100	0.003	6.94	0.0	99,094

Table 5. *Cont.*

State	$\dot{m}$ (kg/h)	T (°C)	P (kPa)	e^{CH} (kJ/kg)	e^{PH} (kJ/kg)	e^{KN} (kJ/kg)	$\dot{E}$ (kJ/h)
31	14,252	94	105	0.003	6.94	0.9	111,685
32	16	94	100	1647	11.2	0.0	26,942
33	182	30	101	1647	0.01	0.0	26,763
34	198	40	101	1647	0.26	0.9	27,009
35	20	90	70	480	418	0.0	18,231
36	20	90	70	2.50	23.9	0.0	537
37	806	190	1250	480	499	0.0	789,231
38	806	190	1250	2.50	29.0	0.0	25,387
39	80	165	700	480	753	0.0	98,620
40	80	165	700	2.50	104	0.0	8507
41	43	165	700	480	753	0.0	53,008
42	43	165	700	2.50	104	0.0	4581
43	10	165	700	480	753	0.0	12,328
44	10	165	700	2.50	104	0.0	1063
45	25,438	2	500	2.50	5.13	0.0	194,111
46	25,438	6	500	2.50	3.71	0.0	157,878
47	959	190	1250	480	499	0.0	938,861
48	959	104	1250	2.50	39.3	0.0	40,075
49	2217	28	101	0.00	0.00	0.0	0
50	77	28	101	43,293	0.00	0.0	3,332,277
51	2294	650	101	26.0	331	0.0	817,815

The exergy rate of the fuel ($\dot{E}_F$) and the product ($\dot{E}_P$), the exergetic (n_{ex}) and energetic (n_{en}) efficiencies, and the exergy destruction ratios ($y^*_{D,k}$ and $y_{D,k}$) were calculated for each component in the system. The results are summarized in Table 6. The components with the highest exergy fuel rates were the B, the MHX, and the SD. The MHX is the component with the highest exergetic efficiency (38.9%), followed by the boiler (37%). There is a big difference between the exergetic and the energetic efficiencies of the majority of the components, and consequently the overall system also exhibited the same behavior. Therefore, despite the energy efficiency of the system (the conservation of the quantity of energy) being 67.8%, the overall exergy efficiency (the quality of that energy) was only 33.3%. Similar results were obtained in a study on the spray drying process in an industrial scale ceramic factory, in which the energetic efficiency was found to be between 43% and 87% [34], and the exergetic efficiency was between 12% and 64% [35]. However, in a pilot-scale study of spray drying of cherry puree the energetic and exergetic efficiencies were only 3.2% and 0.7%, respectively [11]. This, along with laboratory-scale studies [10,12,36], demonstrates that pilot-scale and laboratory-scale studies do not accurately represent the energetic and exergetic performances of the industrial-scale spray drying process.

Figure 2 shows the fuel and product exergy rate of the overall system, and the destroyed exergy rate of each component. The results show that the components that had electric energy as the main fuel exergy source such as the vibrating screen, belt, and fans had the lowest impact on the exergetic destruction. This occurs because the electric energy was used for mechanical operations, instead of being used as a heat source. The exergy destruction ratio (y_D) was lower than 5% for these components. These results were similar to other studies that determined an exergy destruction ratio lower than 2% for the compressors and pumps in a CCHP system [37]. Furthermore, in a yogurt plant the devices that required electric energy accounted for less than 5% of the total exergy destruction [38].

Table 6. Results of the exergy analysis of all the components of the spray drying system.

Component	$\dot{E}_F$ (kJ/h)	$\dot{E}_P$ (kJ/h)	n_{ex} (%)	n_{en} (%)	$y^*_{D,k}$	$y_{D,k}$
SD	205,446	32,852	16.0	93.9	0.058	0.040
LP	7920	298	3.8	27.2	0.003	0.002
HP	19,800	307	1.5	34.2	0.007	0.005
HXE	17,694	4576	25.9	76.4	0.005	0.003
MHX	763,844	296,918	38.9	79.4	0.174	0.116
SFBHX	90,114	10,906	12.1	81.4	0.030	0.020
VF1HX	48,427	5227	10.8	88.6	0.016	0.011
VF2HX	11,264	336	3.0	69.2	0.004	0.003
MF	66,600	10,286	15.4	46.3	0.021	0.014
SFBF	19,800	1690	8.5	24.0	0.007	0.005
VF1F	14,400	1143	7.9	22.4	0.005	0.003
VF2F	14,400	1140	7.9	23.3	0.005	0.003
RFF	1980	181	9.2	29.4	0.001	0.001
FF	108,000	39,534	36.6	51.5	0.026	0.017
CHX	36,233	1072	3.0	27.8	0.013	0.009
B	2,514,427	898,786	35.7	73.3	0.611	0.374
BT	7920	546	6.9	69.9	0.003	0.002
S	3600	247	6.9	n/a	0.001	0.001

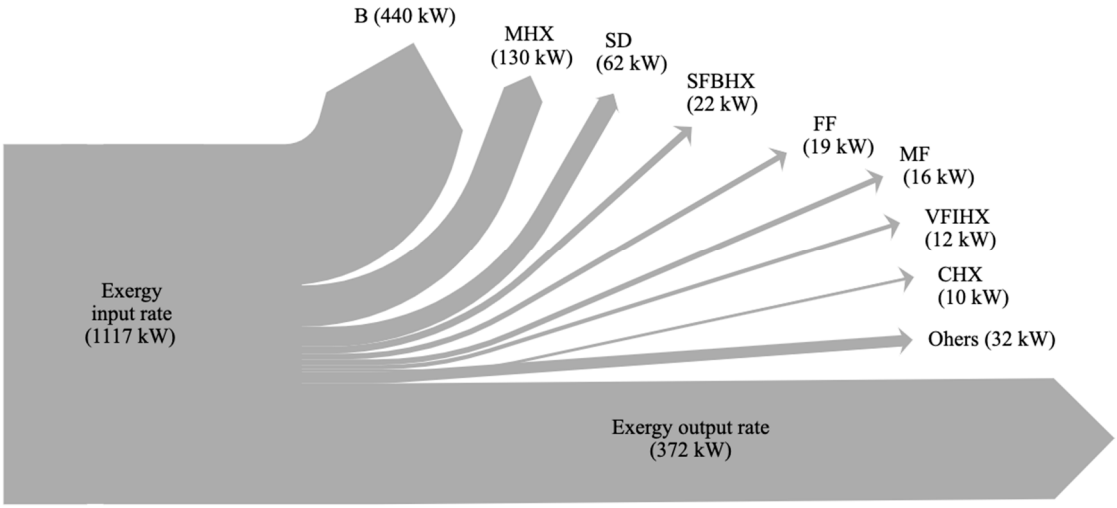

Figure 2. Grassmann's diagram of the spray drying process.

Conversely, the boiler destroyed 39.4% of the overall fuel exergy rate. This percentage was similar to other plants where the boiler was used as an auxiliary supply of steam. For instance, in a factory, which produces ghee, the boiler has the highest exergy destruction ratio 39% [39]. This is because the main purpose of this component is to convert a high-quality energy (chemical energy of fuel oil) to a low-quality energy (heat).

The MHX also has a high exergy destruction rate, despite having one of the highest exergetic efficiencies. The air heater used in this process was a steam-heated type, which is one of the most used in food industry, it had an exergy efficiency of 38.9% and a high specific exergy destruction of 287 kJ per kg of heated air, with a minimum temperature difference of 12 °C. There are other types of air heaters that could reduce the exergy destruction rate and the minimum temperature difference such as a system with a heat exchanger that uses geothermic fluid. A previous study showed that this kind of heat exchanger has an exergy efficiency of 42% and specific destruction exergy of 57.5 kJ per kilogram of heated air with a minimum temperature difference of 5 °C [40]. Another type of air heater was one that uses electric energy as the source of heat. A previous study on the spray drying of

photochromic dyes determined that the exergy efficiency of this kind of heater was 16.4% [12], this has the lowest exergy efficiency because it is transforming high quality energy (electric energy) to low quality energy (heat).

The SD also affects the performance of the overall system, since it has one of the highest rates of exergy destruction at 595 kJ/kg of evaporated water. Previous studies by Bühler et al. [31] found that the spray dryer is a highly exergy-destructive component in a powdered milk factory. Similarly in a large dairy factory producing primarily milk powder, they obtained an exergy destruction rate of 1345 kJ/kg of evaporated water [14]. In a ceramic plant, the exergy destruction rate was 1111.4 kJ/kg of evaporated water [35].

3.2. Advanced Exergy Analysis

In order to determine the avoidable and unavoidable fractions of the exergy destruction rate, it was split at a component level by considering the unavoidable thermodynamic inefficiency conditions listed in Table 3. Figure 3 shows that the components with the highest avoidable exergy destruction rates. Even though the MHX had one of the highest exergy destruction rates, more than 96% of the MHX destroyed exergy was unavoidable, this is because the real operational conditions were close to the unavoidable ones.

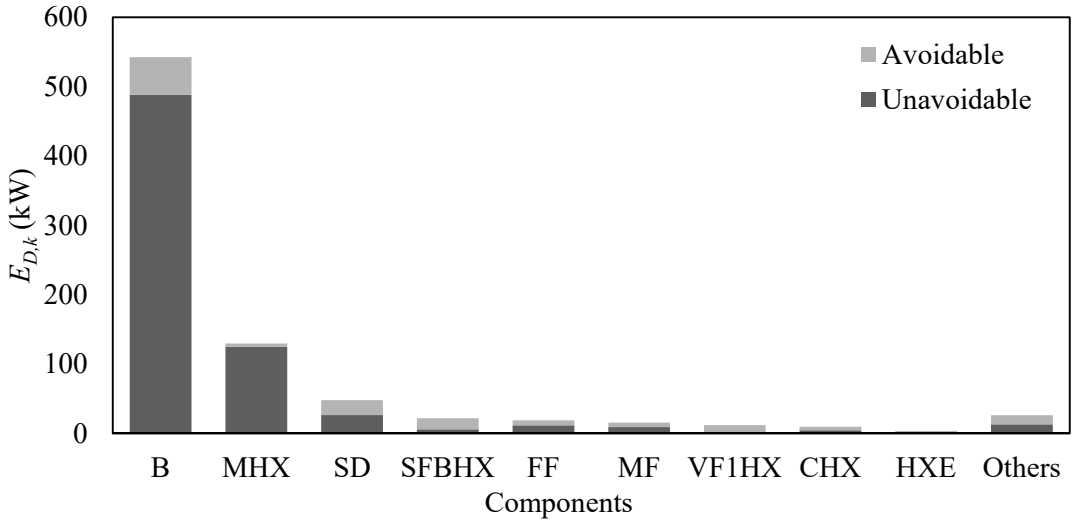

Figure 3. Irreversibility rate distribution of the main components of the system.

Conversely, the B and the SD were responsible for 38% (54 kW) and 15% (21 kW) of the total avoidable exergy destruction rate, respectively. Vuckovic et al. [30] and Bühler [14] found similar results for the boiler in an industrial energy supply plant (16.4%) and the spray dryer for a milk processing factory (16.5%), respectively.

Structural changes in spray drying systems have been studied as an alternative to reduce avoidable exergy destruction rates. Walmsley et al. [22] concluded that a closed drying air loop for the recovery of heat waste in a spray drying system for the production of powdered milk could achieve a reduction of 14.4% of steam used. This reduction would consequently reduce the avoidable exergy destruction rate for the system. In addition, Camci et al. [15] determined that the exergy destruction rate could decrease by 11% when solar collectors for preheating the drying air were used.

3.3. Conventional Exergoeconomic Analysis

The conventional exergoeconomic analysis was carried out at a level component and it is presented in Table 7 different indicators such as the specific fuel cost (c_F), the destruction exergy cost rate ($\dot{C}_D$), the exergoeconomic factor (f_k), the relative cost difference (r_k), and the total operating cost rate ($\dot{C}_D + \dot{Z}_k$) in descending order.

Table 7. Results of the thermoeconomic analysis.

Component	c_F (\$/kJ)	$\dot{C}_D$ (\$/h)	$\dot{Z}_k$+$\dot{C}_D$ (\$/h)	r_k	f_k (%)
SD	6.2×10^{-4}	106.8	109.6	0.02	2.50
MHX	1.3×10^{-4}	60.5	61.6	0.01	1.73
B	6.7×10^{-6}	13.1	14.4	0.07	9.03
SFBHX	1.0×10^{-4}	8.2	8.3	0.02	2.06
VF1HX	1.0×10^{-4}	4.4	4.6	0.02	2.61
BT	5.7×10^{-4}	4.2	4.5	0.06	5.71
CHX	7.0×10^{-5}	2.4	3.0	0.20	17.43
HXE	1.4×10^{-4}	1.9	1.9	0.01	1.37
VF2HX	1.0×10^{-4}	1.1	1.2	0.03	3.17
FF	2.6×10^{-5}	1.8	1.9	0.05	7.83
MF	2.6×10^{-5}	1.5	1.6	0.08	9.00
HP	2.6×10^{-5}	0.5	1.1	1.14	53.73
RTF	2.6×10^{-5}	0.05	0.2	3.30	78.42
SFBF	2.6×10^{-5}	0.5	0.6	0.33	26.52
VF2F	2.6×10^{-5}	0.3	0.5	0.45	33.02
VF1F	2.6×10^{-5}	0.3	0.5	0.45	33.03
LP	2.6×10^{-5}	0.2	0.4	1.21	55.73
S	2.6×10^{-5}	0.1	0.4	8.16	78.49

The results show that the two highest total operating cost rates ($\dot{Z}_k + \dot{C}_D$) were from the SD followed by the MHX, meaning that the influence of these components on the total costs associated with the overall system was significant. Interesting results are presented, because although the B had a higher avoidable exergy destruction rate than the SD and MHX, the specific cost rate was higher in the SD than in the B, thus making the SD the component that had the greatest influence on the total operating cost rate. In contrast, the fans, the pumps, and the vibrating stream were the three components that contributed least to the total operating cost rate. Similar results were obtained by an exergoeconomic analysis in a corn dryer, where the drying chamber represented more than 98% of the total operational costs [41].

Furthermore, although the percentage relative cost differences for components such as the B (7%), SD (2%), and MHX (1%) were found to be low, their exergy destruction cost rates were high. The MHX and the SD had exergoeconomic factors of 1.6% and 3.3%, respectively, which means that the exergetic efficiency of these components must increase in order to reduce the overall system cost. Similar results were found in other drying technologies such as gas engine-driven heat pump dryer and a ground-source heat pump food dryer, which had exergoeconomic factors of 25% [42] and 14.6% [43], respectively. Another previous study on a pilot-scale spray dryer for the production of cheese powder, concluded similarly that in order to reduce the operational cost in spray drying systems, the exergy efficiency in the drying chamber should be increased even though this would require an increment in the capital investment [21].

3.4. Advanced Exergoeconomic Analysis

In order to determine the system's potential of improvement for the reduction of the overall operational cost, an advanced exergoeconomic analysis was performed. In Figure 4, the avoidable ($\dot{C}_{D,k}^{AV}$) and unavoidable ($\dot{C}_{D,k}^{UN}$) cost of exergy destruction, and the avoidable ($\dot{Z}_k^{AV}$) and unavoidable ($\dot{Z}_k^{UN}$) investment cost rates of the different components of the system are presented.

As it is shown in Figure 4 the combined avoidable investment cost rates of the B, the SD and the MHX, represents only 10.2% of the overall investment cost rate and less than 1% of the overall operational cost rate. These results show that the improvement potential for the investment cost rate of the SD and the MHX was low.

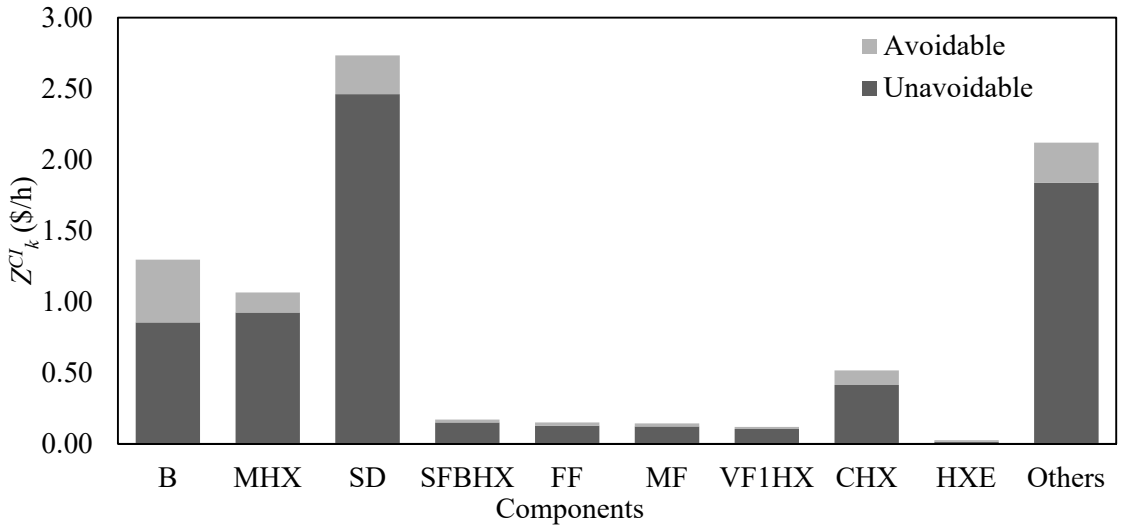

Figure 4. Avoidable and unavoidable investment cost rate of the components of the system.

On the other hand, the avoidable exergy destruction cost rate for the overall system represents 30% of the operational cost and 31% of the overall destruction cost. Only three advanced exergoeconomic analyses have been done in drying systems, but all of them were performed on heat pump dryers [44,45]. These previous studies reported that 46% and 74% of the overall destruction cost were avoidable. This indicates that spray drying process could have lower improvement potential than the heat pump drying process.

In Figure 5, the avoidable and unavoidable exergy destruction cost rates are presented at a component level. It is shown that the B and MHX had high unavoidable exergy destruction cost rate, combined they represented 49% of the total unavoidable exergy destruction. A previous advanced exergoeconomic analysis in a power plant showed similar results for the boiler: around 90% of the destruction cost rate was unavoidable [46].

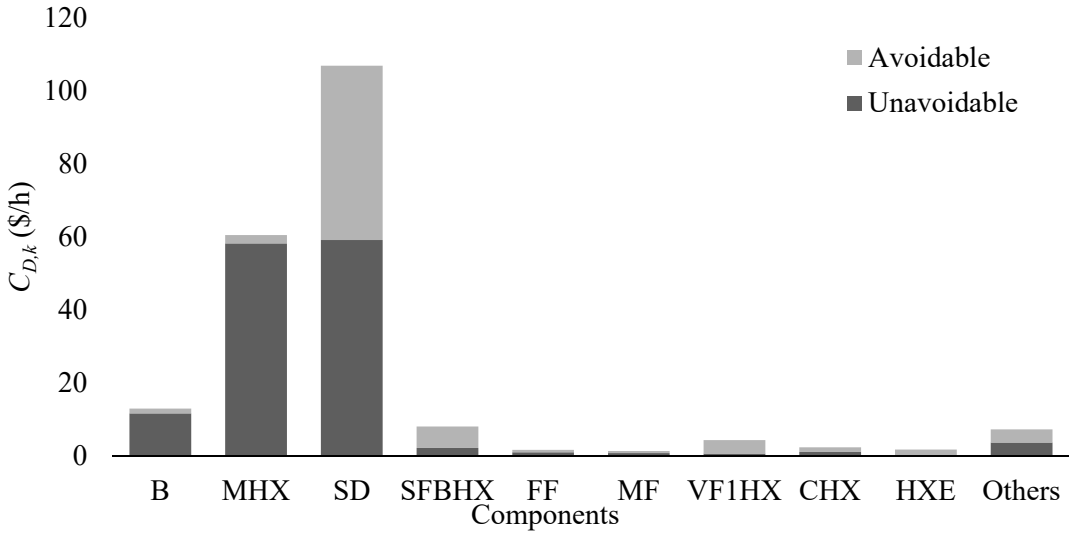

Figure 5. Avoidable and unavoidable exergy destruction cost rate of the components of the system.

Other components such as fans, pumps, and the vibrating screen had also low avoidable cost rates associated with exergy destruction (accounting for less than 1% of the total avoidable cost), which means that any improvement in these components will not significantly reduce the total operating cost. This result is also shown in other food drying systems where the components that require electric energy have avoidable costs that represent less than 1% of the total cost [45].

Conversely, although the B has the highest avoidable exergy destruction rate, the spray dryer has the highest avoidable exergy destruction cost rate ($47.7/h), which represents 73% of the overall avoidable destruction cost rate of the process. A previous study on a pump food dryer similarly concluded that 68.6% of the destruction cost rates were avoidable in the drying chamber [47]. These results imply that the SD had the highest level of improvement potential. A reduction of the exergy destruction rate in the spray dryer could reduce the total cost of the overall system by 22%.

4. Conclusions

According to the aim of this study, we developed conventional and advanced exergy and exergoeconomic analyses of a spray drying system of instant coffee for the first time, using real operational data. The components of the system where analyzed individually. The advanced analysis was found to be useful for quantifying the flow costs in the process and also for identifying which components have the greatest potential for improvement in order to make the overall system more cost effective.

According to the analysis and discussion, the following conclusions were obtained:

- The overall energy and exergy efficiencies of the spray drying system were calculated as 71% and 33% respectively, where the B had the highest exergy destruction rate, but most of it (90%) was unavoidable exergy destruction.
- The conventional exergoeconomic analysis allows for the quantification of the overall operational cost rate ($207.9/h); more than 70% of that cost rate was due to the SD and the MHX.
- The exergoeconomic factor allowed for the identification of the SD and MHX as the sources with the highest cost rate. More than 97% of the operating cost rate of the SD and the MHX were due to a high exergy destruction rate; of all the components in the studied system, these components were the most exergy destructive. The cost rates of the exergy destruction for the SD and the MHX were 106.9 $/h and 60.5$/h, respectively.
- The advanced exergoeconomic analysis revealed that 33% of the exergy destruction cost rate of the overall system was avoidable. Additionally, it established that 70% of the avoidable exergy destruction cost rate was located in the SD, demonstrating that this was the component with the highest improvement potential.

Finally, based on the results obtained in this analysis, the following recommendations were made for the plant: It would be useful to reduce the exergetic destruction cost rate of the SD and the MHX, by performing a parametric study and implementing structural changes within an exergoeconomic optimization in order to obtain f_k values as close to 50% as possible [48]. Further studies are necessary to analyze the interdependence of the SD and the rest of the system's components, in order to determine the percentage of avoidable costs that can be attributed to the irreversibilities of each component's operation.

Author Contributions: Conceptualization, investigation and data curation, D.L.T.-C.; methodology, A.M.B.-M.; software and validation, formal analysis, D.L.T.-C. and A.M.B.-M.; writing—original draft preparation, D.L.T.-C.; writing—review and editing, A.M.B.-M.; supervision and project administration, A.L.-M. and A.M.B.-M. All authors have read and agreed to the published version of the manuscript.

Funding: This research received no external funding.

Conflicts of Interest: The authors declare no conflict of interest.

Nomenclature

$\dot{C}$	cost rate associated with an exergy stream ($/h)
y	destruction rate
$\dot{E}$	exergy rate (kJ/h)
f	exergy rate (kJ/h)
i	interest rate
c_p	heat capacity (kJ/K*kg)
$\dot{Q}$	heat flow rate (kJ/h)
R	ideal gas constant (kJ/kmol*K)
$\dot{Z}$	investment cost rate ($/h)
$\dot{m}$	mass flow rate (kg/h)
n	life time of the system
P	pressure (kPa)
r	relative cost difference
y*	relative irreversibility
h	specific enthalpy (kJ/kg)
s	specific entropy (kJ/kg)
e	specific exergy rate (kJ/kg)
T	temperature (°C)
c	unit exergy cost ($/kJ)
w	mole fraction of water vapor
$\dot{W}$	power (kJ/h)
x	mole fraction
Greek letters	
Δ	difference
γ	specific heat ratio
η	efficiency
ρ	air density (kg/m^3)
τ	annual operating hours (h)
Abbreviations	
B	boiler
BT	belt
CHX	cooler heat exchanger
HXE	extract heat exchanger
RFF	fine returns fan
SFBF	fluidized bed fan
SFBHX	fluidized bed heat exchanger
HP	high pressure pump
LP	low pressure pump
MF	main fan
MHX	main heat exchanger
N	nozzle
PEC	purchased equipment cost
SD	spray dryer
FF	vacuum pump
VF1F	vf1 fan
VF1HX	vf1 heat exchanger
VF2F	vf2 fan
VF2HX	vf2 heat exchanger
S	vibrating screen

Subscripts	
con	conversion
D	exergy destruction
elec	electric
en	energy
ex	exergy
F	fuel exergy
in	inflow
is	isentropic
k	kth component
mech	mechanical
min	minimum
mix	mixture
out	outflow
P	product exergy
L	loss
tot	overall system
o	thermodynamic environment
Superscripts	
AV	avoidable
CH	chemical
CI	capital investment
KN	kinetic
OM	operating and maintenance
PH	physical
PT	potential
UN	unavoidable

References

1. Statista Consumer Market Outlook for Instant Coffee. 2020. Available online: https://www.statista.com/outlook/30010200/100/instant-coffee/worldwide (accessed on 20 May 2020).
2. Svilaas, A.; Sakhi, A.K.; Andersen, L.F.; Svilaas, T.; Ström, E.C.; Jacobs, D.R.; Ose, L.; Blomhoff, R. Intakes of Antioxidants in Coffee, Wine, and Vegetables Are Correlated with Plasma Carotenoids in Humans. *J. Nutr.* **2004**, *134*, 562–567. [CrossRef]
3. Gebhardt, S.; Lemar, L.; Haytowitz, D.; Pehrsson, P.; Nickle, M.; Showell, B.; Holden, J. *USDA National Nutrient Database for Standard Reference, Release 21*; United States Department of Agriculture Agricultural Research Service: Washington, DC, USA, 2008.
4. Lucas, M.; Mirzaei, F.; Pan, A.; Okereke, O.I.; Willett, W.C.; O'Reilly, É.J.; Koenen, K.; Ascherio, A. Coffee, Caffeine, and Risk of Depression Among Women. *Arch. Intern. Med.* **2011**, *171*, 1571–1578. [CrossRef]
5. Market, A. Global Industry Analysis, Size, Share, Growth, Trends and Forecast 2019–2025. 2019. Available online: https://www.transparencymarketresearch.com/logistics-market.html (accessed on 20 May 2020).
6. Bhandari, B. *Handbook of Industrial Drying*; Mujumdar, A.S., Ed.; CRC Press: Boca Raton, FL, USA, 2015; ISBN 978-1-4665-9665-8.
7. Aghbashlo, M.; Mobli, H.; Rafiee, S.; Madadlou, A. A review on exergy analysis of drying processes and systems. *Renew. Sustain. Energy Rev.* **2013**, *22*, 1–22. [CrossRef]
8. Johnson, W.P.; Langrish, A.T. Interpreting exergy analysis as applied to spray drying systems. *Int. J. Exergy* **2020**, *31*, 120–149. [CrossRef]
9. Johnson, P.W.; Langrish, T.A.G. Exergy analysis of a spray dryer: Methods and interpretations. *Dry. Technol.* **2017**, *36*, 578–596. [CrossRef]
10. Erbay, Z.; Koca, N. Energetic, Exergetic, and Exergoeconomic Analyses of Spray-Drying Process during White Cheese Powder Production. *Dry. Technol.* **2012**, *30*, 435–444. [CrossRef]
11. Saygı, G.; Erbay, Z.; Koca, N.; Pazir, F. Energy and exergy analyses of spray drying of a fruit puree (cornelian cherry puree). *Int. J. Exergy* **2015**, *16*, 315. [CrossRef]

12. Çay, A.; Kumbasar, E.P.A.; Morsunbul, S. Exergy analysis of encapsulation of photochromic dye by spray drying. *IOP Conf. Ser. Mater. Sci. Eng.* **2017**, *254*, 22003. [CrossRef]
13. Aghbashlo, M.; Mobli, H.; Madadlou, A.; Rafiee, S. Influence of spray dryer parameters on exergetic performance of microencapsulation processs. *Int. J. Exergy* **2012**, *10*, 267. [CrossRef]
14. Bühler, F.; Nguyen, T.-V.; Jensen, J.K.; Holm, F.M.; Elmegaard, B. Energy, exergy and advanced exergy analysis of a milk processing factory. *Energy* **2018**, *162*, 576–592. [CrossRef]
15. Camci, M. Thermodynamic analysis of a novel integration of a spray dryer and solar collectors: A case study of a milk powder drying system. *Dry. Technol.* **2019**, *38*, 350–360. [CrossRef]
16. Tsatsaronis, G. Definitions and nomenclature in exergy analysis and exergoeconomics. *Energy* **2007**, *32*, 249–253. [CrossRef]
17. Bejan, A.; Tsatsaronis, G.; Michael, M. *Thermal Design and Optimization*; John Wiley & Sons: New York, NY, USA, 1996; Volume 21, ISBN 0471584673.
18. Tsatsaronis, G. Thermoeconomic analysis and optimization of energy systems. *Prog. Energy Combust. Sci.* **1993**, *19*, 227–257. [CrossRef]
19. Ozgener, L. Exergoeconomic analysis of small industrial pasta drying systems. *Proc. Inst. Mech. Eng. Part A J. Power Energy* **2007**, *221*, 899–906. [CrossRef]
20. Ozturk, M.; Dincer, I. Exergoeconomic analysis of a solar assisted tea drying system. *Dry. Technol.* **2019**, *38*, 655–662. [CrossRef]
21. Erbay, Z.; Koca, N. Exergoeconomic performance assessment of a pilot-scale spray dryer using the specific exergy costing method. *Biosyst. Eng.* **2014**, *122*, 127–138. [CrossRef]
22. Walmsley, T.G.; Walmsley, M.R.; Atkins, M.J.; Neale, J.R.; Tarighaleslami, A.H. Thermo-economic optimisation of industrial milk spray dryer exhaust to inlet air heat recovery. *Energy* **2015**, *90*, 95–104. [CrossRef]
23. Walmsley, T.G.; Walmsley, M.R.W.; Atkins, M.J.; Neale, J.R. Thermo-Economic assessment tool for industrial milk spray dryer exhaust heat recovery systems with particulate fouling. *Chem. Eng. Trans.* **2014**, *39*, 1459–1464. [CrossRef]
24. Petrakopoulou, F.; Tsatsaronis, G.; Morosuk, T.; Carassai, A. Advanced Exergoeconomic Analysis Applied to a Complex Energy Conversion System. *J. Eng. Gas Turbines Power* **2011**, *134*, 031801. [CrossRef]
25. Burmester, K.; Fehr, H.; Eggers, R. A Comprehensive Study on Thermophysical Material Properties for an Innovative Coffee Drying Process. *Dry. Technol.* **2011**, *29*, 1562–1570. [CrossRef]
26. Clément, Y.B.Y.; Benjamin, Y.N.; Roger, K.B.; Clement, A.D.; Kablan, T. Moisture Adsorption Isotherms Characteristic of Coffee (Arabusta) Powder at Various Fitting Models. *Int. J. Curr. Res. Biosci. Plant Biol.* **2018**, *5*, 26–35. [CrossRef]
27. Wepfer, W.J.; Gaggioli, R.A.; Obert, E.F. Proper evaluation of available energy for HVAC. *ASHRAE Trans.* **1979**, *85*, 214–230.
28. Lazzaretto, A.; Tsatsaronis, G. SPECO: A systematic and general methodology for calculating efficiencies and costs in thermal systems. *Energy* **2006**, *31*, 1257–1289. [CrossRef]
29. Tsatsaronis, G.; Park, M.-H. On avoidable and unavoidable exergy destructions and investment costs in thermal systems. *Energy Convers. Manag.* **2002**, *43*, 1259–1270. [CrossRef]
30. Vučković, G.D.; Stojiljković, M.M.; Vukić, M.V.; Stefanović, G.M.; Dedeić, E.M. Advanced exergy analysis and exergoeconomic performance evaluation of thermal processes in an existing industrial plant. *Energy Convers. Manag.* **2014**, *85*, 655–662. [CrossRef]
31. Cziesla, F.; Tsatsaronis, G.; Gao, Z. Avoidable thermodynamic inefficiencies and costs in an externally fired combined cycle power plant. *Energy* **2006**, *31*, 1472–1489. [CrossRef]
32. Petroecuador, E.P. Precios de Venta a Nivel de Terminal para las Comercializadoras Calificadas y Autorizadas a Nivel Nacional. Ep Petroecuador Gerencia de Comericalización Nacional. 2019. Available online: http://bit.ly/2XeM8Zq (accessed on 20 March 2020).
33. Interagua. *Informe Anual 2018–2019*; International Water Services (Guayaquil) Interagua C. Ltda: Guayaquil, Ecuador, 2019.
34. Apak. Energy exergy analyses, Turkey (Supervisor: Prof. Dr. Ramazan K€OSE). In *A Ceramic Factory, Mechanical Engineering Branche*; Engineering Faculty, Dumlupınar University: Kütahya, Turkey, 2007; p. 110. (In Turkish)
35. Utlu, Z.; Hepbasli, A.; Hepbaşlı, A. Exergoeconomic analysis of energy utilization of drying process in a ceramic production. *Appl. Therm. Eng.* **2014**, *70*, 748–762. [CrossRef]

36. Kurozawa, L.E.; Park, K.J.; Hubinger, M.D. Spray Drying of Chicken Meat Protein Hydrolysate: Influence of Process Conditions on Powder Property and Dryer Performance. *Dry. Technol.* **2011**, *29*, 163–173. [CrossRef]
37. Mohammadi, A.; Ahmadi, M.H.; Bidi, M.; Joda, F.; Valero, A.; Uson, S. Exergy analysis of a Combined Cooling, Heating and Power system integrated with wind turbine and compressed air energy storage system. *Energy Convers. Manag.* **2017**, *131*, 69–78. [CrossRef]
38. Jokandan, M.J.; Aghbashlo, M.; Mohtasebi, S.S. Comprehensive exergy analysis of an industrial-scale yogurt production plant. *Energy* **2015**, *93*, 1832–1851. [CrossRef]
39. Singh, G.; Singh, P.; Tyagi, V.; Barnwal, P.; Pandey, A. Exergy and thermo-economic analysis of ghee production plant in dairy industry. *Energy* **2019**, *167*, 602–618. [CrossRef]
40. Yildirim, N.; Genc, S. Energy and exergy analysis of a milk powder production system. *Energy Convers. Manag.* **2017**, *149*, 698–705. [CrossRef]
41. Li, B.; Li, C.; Huang, J.; Li, C. Exergoeconomic Analysis of Corn Drying in a Novel Industrial Drying System. *Entropy* **2020**, *22*, 689. [CrossRef]
42. Gungor, A.; Erbay, Z.; Hepbasli, A. Exergoeconomic (Thermoeconomic) Analysis and Performance Assessment of a Gas Engine–Driven Heat Pump Drying System Based on Experimental Data. *Dry. Technol.* **2012**, *30*, 52–62. [CrossRef]
43. Erbay, Z.; Hepbasli, A. Exergoeconomic evaluation of a ground-source heat pump food dryer at varying dead state temperatures. *J. Clean. Prod.* **2017**, *142*, 1425–1435. [CrossRef]
44. Erbay, Z.; Hepbasli, A. Advanced exergoeconomic evaluation of a heat pump food dryer. *Biosyst. Eng.* **2014**, *124*, 29–39. [CrossRef]
45. Gungor, A.; Tsatsaronis, G.; Gunerhan, H.; Hepbasli, A. Advanced exergoeconomic analysis of a gas engine heat pump (GEHP) for food drying processes. *Energy Convers. Manag.* **2015**, *91*, 132–139. [CrossRef]
46. Wang, L.; Fu, P.; Yang, Z.; Lin, T.-E.; Yang, Y.; Tsatsaronis, G. Advanced Exergoeconomic Evaluation of Large-Scale Coal-Fired Power Plant. *J. Energy Eng.* **2020**, *146*, 04019032. [CrossRef]
47. Erbay, Z.; Hepbasli, A. Assessment of cost sources and improvement potentials of a ground-source heat pump food drying system through advanced exergoeconomic analysis method. *Energy* **2017**, *127*, 502–515. [CrossRef]
48. Hamdy, S.; Morosuk, T.; Tsatsaronis, G. Exergoeconomic optimization of an adiabatic cryogenics-based energy storage system. *Energy* **2019**, *183*, 812–824. [CrossRef]

PROCEEDINGS OF THE 31st European Symposium on Computer Aided Process Engineering (ESCAPE31), June 6-9, 2021, İstanbul, Turkey
M. Türkay, R. Gani (Editors).
http://dx.doi.org/10.1016/B978-0-323-88506-5.50056-5

Advanced exergoeconomic analysis of a double effect evaporation process in an instant coffee plant

Tinoco-Caicedo D.L.,[a,b,*] Feijoó-Villa E.,[a] Calle-Murillo J.,[a] Lozano-Medina A.,[b] and Blanco-Marigorta A.M.[b]

[a] *Facultad de Ciencias Naturales y Matemáticas, Escuela Superior Politécnica del Litoral, 090903 Guayaquil, Ecuador*
[b] *Department of Process Engineering, Universidad de las Palmas de Gran Canaria, 35017 Gran Canaria, Spain*
**dtinoco@espol.edu.ec*

Abstract

The advanced exergoeconomic analysis performed on different industrial processes is used to determine the avoidable exergy destruction and inversion cost rates in order to increase the rentability and sustainability of a factory. This study focuses on the performance of an advanced exergoeconomic analysis of a double effect evaporation process (DEEP) of coffee extract in a factory located in Ecuador. The avoidable and unavoidable exergy destruction cost rate and the avoidable investment cost rate were determined for each component by exergoeconomic balances using the results from the process simulation with the best operational conditions and with the worst operational conditions. The avoidable exergy destruction cost rate represents 18.3% of the overall exergy destruction cost rate. It was estimated that around 70.3 $/h of the overall operational costs could be saved if the exergetic efficiency of the first double effect evaporator (D-101) and the steam condenser (E-103) increased from 46.3% to 60.7% and 52.3% to 61.6%, respectively. Additionally, an increment of the initial concentration of soluble solids in the extract can reduce the avoidable operational costs by 15%.

Keywords: Advanced exergoeconomic analysis, Process simulation, Double effect evaporation, Avoidable cost rate

1. Introduction

Instant coffee is a widely consumed product worldwide, its market is projected to grow in the next seven years (Coherent Market Insights, 2019). One of the steps in industrial-scale instant coffee production is the evaporation of water from the extract in order to increase the concentration of soluble solids in preparation for the drying process. This evaporation process is energy-intensive, and consumes large amounts of fossil fuels since water has a high latent heat. Additionally, previous studies show that this process has low energetic and exergetic efficiencies (Mojarab Soufiyan et al., 2016), which lead to a high level of energy waste, and consequently raise production costs. In order to address these inefficiencies, it is not only necessary to identify and quantify the losses, but also to determine the fraction of avoidable losses. The advanced exergoeconomic analysis developed with computational tools allows for the determination of the exergy destruction rate and the avoidable and unavoidable costs of each component of the system. This analysis therefore becomes an important decision-making tool in production industries to reduce operational costs and increase the sustainability of the processes.

Some conventional exergy analyses have been done in food industries that have evaporation as part of their process, such as the production of tomato paste (Mojarab Soufiyan et al., 2016), powdered milk (Bühler et al., 2018), and yogurt (Mojarab Soufiyan and Aghbashlo, 2017). However there are no advanced exergoeconomic analyses performed in food industries; these studies would allow for the determination of the real potential for improvement of each component of the process (Liu et al., 2020).
In this context, this work presents an advanced exergoeconomic analysis of the double effect evaporation process of coffee extract, by using real operational data from a factory located in Ecuador. The aims of this study are to identify the main sources of exergy destruction that significantly affect the operational cost, and to quantify the avoidable cost that could be reduced. Additionally, a parametric study is performed to analyze the effect the initial concentration of soluble solids has on the operational cost indicators.

2. Methodology

2.1. Process Description

Figure 1 describes the double effect evaporation process of coffee extract in a factory located in Ecuador. Coffee extract (stream 1) is an aqueous solution with an initial concentration of soluble solids of 18 w/w%, from *Robusta* and *Arabica* beans. This extract is pumped to a heat exchanger (E-102) for pre-heating it up to 50ºC by using steam. The steam is generated in the boiler (B-201) by using fuel oil Nº6. Meanwhile, an already concentrated extract (stream 7) leaves the second effect (D-102); part of it is mixed with the heated extract and recirculated to D-102.The other part is sent to the first effect (D-101). The evaporated water (stream 11) in D-102 enters the condenser (E-101), where the temperature is reduced from 50°C to 32°C. The condensate water (stream 15) is mixed with condensate from de D-102 (stream 16) and then it is discarded. The concentrated coffee (stream 8) that leaves the D-101 reaches a concentration of 50 w/w% and then it is cooled from 66°C to 11°C in a heat exchanger of multiple flow (E-103), where cooling-tower water (C1) and chilled water (W3) are used.

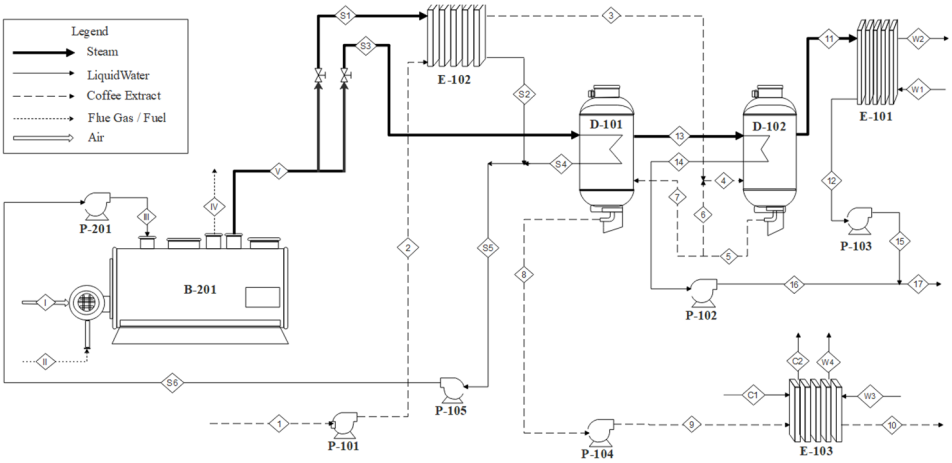

Figure 1. Process flow diagram of the double effect evaporation of coffee extract and the steam generation unit.

The process simulation was developed taking into account the following assumptions:

- The system was at steady state and the elevation in the coffee extract boiling point, due to concentration of solution, was assumed to be negligible.
- The heat loss rate and the pressure lost in all the components were negligible.
- A complete combustion was assumed in the combustion chamber.
- The steam and gases were considered as ideal gases when the pressure was below 1000 kPa. For higher pressures, the SRK-Equation was used as the equation of state.
- The coffee extract and liquid water were considered as ideal solutions.

2.2. Advanced Exergoeconomic Analysis

The advanced exergoeconomic analysis of the double effect evaporation process of coffee extract was performed with the aim to determine the avoidable (AV) and unavoidable (UN) exergy destruction cost rates and investment cost rates at a component level. This analysis was done with the real operational data (ROD) from the plant. The dead state in the system was considered at 298 K and 1 atm. For each component the best operational conditions (BOC) and the worst operational conditions (WOC) were established based on a previous study (Morosuk and Tsatsaronis, 2019) as shown in Table 1. The BOC were used for the process simulation in Pro/II ®. The values of each state and the results from the kth component were used to perform the exergetic analysis (to calculate $\dot{E}_{D,k}^{UN}$), the economic analysis (to calculate $c_{F,k}$) and the exergoeconomic analysis at a component level (to calculate $\dot{C}_{D,k}^{UN}$). The thermodynamic model formulation was performed in Engineering Equation Solver (ESS), software.

Table 1. Values of Parameters for Different Operation Conditions.

Component	Parameter	ROD	BOC	WOC
D-101	ΔT_{min} [°C]	35.0	9.5	50.2
D-102	ΔT_{min} [°C]	15.1	5.0	20.0
P-101	η_{is} [−]	0.80	0.95	0.70
P-102	η_{is} [−]	0.80	0.95	0.70
P-103	η_{is} [−]	0.80	0.95	0.70
P-104	η_{is} [−]	0.80	0.95	0.70
P-105	η_{is} [−]	0.80	0.95	0.70
E-101	ΔT_{min} [°C]	4.0	2.0	23.0
E-102	ΔT_{min} [°C]	77.0	10.0	85.0
E-103	ΔT_{min-cw} [°C]	10.0	2.0	20.0
E-103	ΔT_{min-rw} [°C]	6.0	2.0	20.0
B-201	λ [−]	1.24	1.00	1.93
P-201	η_{is} [−]	0.80	0.95	0.70

The equations used for the exergetic analysis, the economic analysis (TRR methodology) (Bejan et al., 1996) and the advanced exergoeconomic analysis (Petrakopoulou et al., 2012) are presented in Table 2. The auxiliary equations and specific costs for were obtained from a previous study (Tinoco-Caicedo et al., 2020).

Table 2. Equations used for Exergy, Economic and Advanced Exergeconomic Analyses.

Exergetic/Economic Analyses		Advanced Exergy/Exergoeconomic Analyses	
Parameters	Equations	Parameters	Equations
Exergy Balance	$E = E^{PH} + E^{CH}$	Exergoeconomic Balance	$\dot{C}_{P,k} = \dot{C}_{F,k} + \dot{Z}_k - \dot{C}_{D,k}$
Exergy destruction rate	$\dot{E}_{D,k} = \dot{E}_{F,k} - \dot{E}_{P,k}$	Exergy destruction cost rate ($\dot{C}_{D,k}$)	$\dot{C}_{D,k} = c_{F,k}\dot{E}_{D,k}$
Levelized Total Revenue	$TRR_L = CRF \sum_{1}^{n} \frac{TRR_j}{(1+i_{eff})^j}$	Relative cost difference (r_k)	$r_k = \frac{c_{P,k} - c_{F,k}}{c_{F,k}}$

Exergetic/Economic Analyses		Advanced Exergy/Exergoeconomic Analyses	
Parameters	Equations	Parameters	Equations
Requirement levelized carrying charges	$CC_L = TRR_L - FC_L - OMC_L$	Exergoeconomic Factor (f_k)	$f_k = \frac{\dot{Z}_k}{\dot{Z}_k + \dot{C}_{D,k}}$
Annual carrying charges ($Z_k^{\dot{CI}}$)	$Z_k^{\dot{CI}} = \frac{CC_L}{\tau} * \frac{PEC_k}{\sum_k PEC_k}$	Unavoidable Exergy destruciton rate ($\dot{Ex}_{D,k}^{UN}$)	$\dot{Ex}_{D,k}^{UN} = \dot{Ex}_{P,k}\left(\frac{\dot{Ex}_{D,k}}{\dot{Ex}_{P,k}}\right)^{UN}$
Annual operating and maintenance costs ($Z_k^{\dot{OM}}$)	$Z_k^{\dot{OM}} = \frac{OMC_L}{\tau} * \frac{PEC_k}{\sum_k PEC_k}$	Unavoidable Exergy destruction cost rate ($\dot{C}_{D,k}^{UN}$)	$\dot{C}_{D,k}^{UN} = c_{F,k}\dot{Ex}_{D,k}^{UN}$ $\dot{C}_{D,k}^{AV} = \dot{C}_{D,k} - \dot{C}_{D,k}^{UN}$
Annual total costs ($\dot{Z}_k$)	$\dot{Z}_k = Z_k^{\dot{CI}} + Z_k^{\dot{OM}}$	Unvoidable investment cost rate ($\dot{Z}_k^{UN}$)	$\dot{Z}_k^{UN} = \dot{Ex}_{P,k}\left(\frac{\dot{Z}_k}{\dot{Ex}_{P,k}}\right)^{UN}$ $\dot{Z}_k^{AV} = \dot{Z}_k - \dot{Z}_k^{UN}$

Furthermore, the unavoidable investment cost for the kth component was determined following the same methodology (simulation, exergetic analysis, economic analysis and exergoeconomic analysis), using the worst operational conditions (WOC) which implies the lowest possible component purchase costs (Gungor et al., 2015).

3. Results and Discussion

The results from the advanced exergoeconomic analysis are shown in Table 3. The components that have the highest avoidable exergy destruction rate ($\dot{E}_{D,k}^{AV}$) are (in descending order): B-201, D-101 and D-102. However, the components that have the highest avoidable exergy destruction cost rate are (in descending order): D-102, E-103 and D-101. These results are interesting because although B-201 is responsible for 71.7% of the overall avoidable exergy destruction rate, it only represents the 4.6% of the overall avoidable operating costs ($\dot{C}_{D,k}^{AV} + \dot{Z}_k^{AV}$). On the other hand, despite having a low $\dot{E}_{D,k}^{AV}$, the E-103 is responsible for 15.9% of the overall avoidable exergy destruction cost rate. This is due to this component having the highest specific cost of the system ($2x10^{-3}$ \$/kJ) because it uses tower water and chilled water for cooling the concentrated extract.

Table 3. Results of the Advanced Exergoeconomic Analysis

Comp.	$f_k(\%)$	r_k	$\dot{E}_{D,k}^{AV}(kW)$	$\dot{E}_{D,k}^{UN}(kW)$	$\dot{C}_{D,k}^{AV}\left(\frac{\$}{h}\right)$	$\dot{C}_{D,k}^{UN}\left(\frac{\$}{h}\right)$	$\dot{Z}_k^{AV}\left(\frac{\$}{h}\right)$	$\dot{Z}_k^{UN}\left(\frac{\$}{h}\right)$
E-101	2.0	4.5	0.4	51.0	2.4	300.1	0.7	5.4
D-102	55.0	1.5	27.9	12.7	57.2	26.2	7.8	93.5
D-101	86	6.4	27.7	60.6	4.3	9.3	4.1	78.1
E-103	8	$8x10^{-4}$	1.6	2.0	13.1	16.5	$8x10^{-3}$	2.7
B-201	8	2.5	168.5	596.9	4.2	15.0	0.2	1.3
E-102	23	7.4	6.8	13.3	1.1	2.2	$4x10^{-2}$	0.9
P-101	89	2.8	0.6	0.3	$3x10^{-2}$	0.1	$1x10^{-2}$	0.7
P-102	90	2.7	0.6	0.2	0.1	$2x10^{-2}$	$4x10^{-2}$	0.7
P-104	91	2.9	0.2	0.2	$2x10^{-2}$	$2x10^{-2}$	$2x10^{-2}$	0.4
P-103	91	2.6	0.6	0.2	0.1	$2x10^{-2}$	$3x10^{-2}$	0.7
P-105	93	3.0	0.1	0.1	$1x10^{-2}$	$1x10^{-2}$	$3x10^{-3}$	0.3
P-201	93	3.8	$1x10^{-2}$	0.1	$1x10^{-3}$	$1x10^{-2}$	$1x10^{-3}$	0.2

Additionally, component D-102 was found to have the greatest improvement potential, given that 68.6% of its exergy destruction costs are avoidable. In contrast, the pumps don't have improvement potential, as they account for less than 1% of the overall avoidable operating costs.

The required modifications should be focused to reduce the exergy destruction cost rate (even if this results in a higher investment cost), because the components that have the highest operating cost, also have the lowest exergoeconomic factor (less than 10%). These modifications could be done through changes to the operating conditions or through structural changes in the three components with the highest avoidable cost (D-102, E-103 and D-101) in order to increase their exergetic efficiency.

Figure 2 shows that an increase in the initial concentration of soluble solids in the extract from 18 w/w% to 26 w/w% causes a reduction of the avoidable exergy destruction cost rates of the D-101 and D-102, from 5.5 \$/h to 3.3 \$/h and 71.5 \$/h to 46.8 \$/h, respectively. Additionally, the avoidable investment cost in D-101 and D-102 are reduced from 4.5 \$/h to 3.7 \$/h and 8.6 \$/h to 7.1 \$/h, respectively.

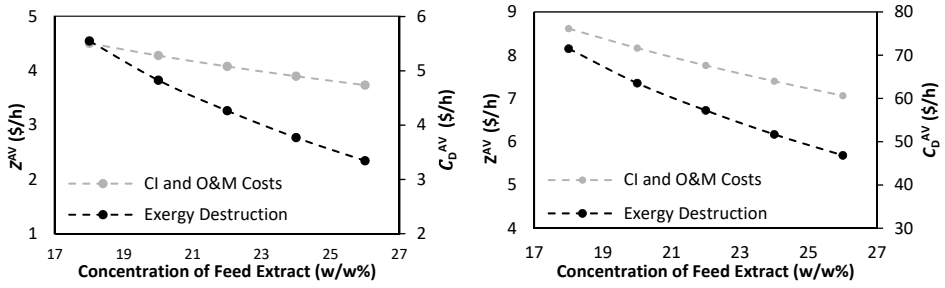

Figure 2. Effect of the initial concentration of soluble solids in coffee extract on the $\dot{C}_{D,k}^{AV}$ and $\dot{Z}_k^{AV}$ of the components (a) D-101 and (b) D-102.

Figure 3 shows that an increment of the initial concentration of soluble solids increases the r_k value in both evaporators (D-101 y D-102), causing a reduction of the final product cost from 22931 \$/T to 21875 \$/T. Furthermore, f_k presents an increment in evaporators D-101 and D-102 of 3.9% and 5.6%, respectively. This means that an increment in the initial concentration of coffee extract could also improve the balances between the investment rate and exergy destruction cost rate.

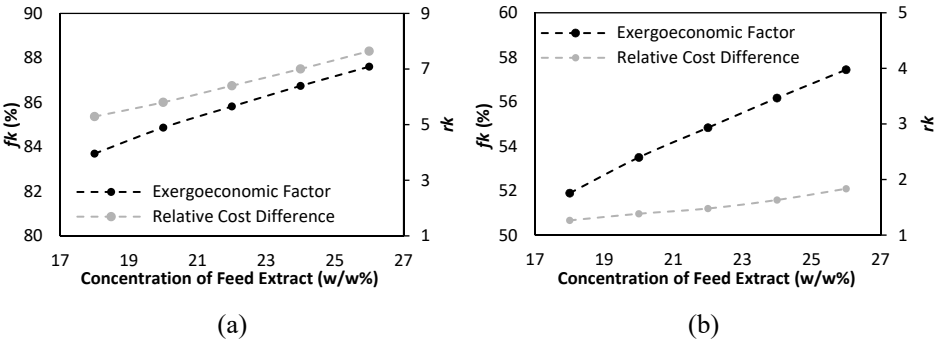

Figure 3. Effect of the initial concentration of soluble solids in the coffee extract on the r_k and f_k of the components (a) D-101 and (b) D-102.

4. Conclusions

The purpose of this study was to perform an advanced exergoeconomic analysis of the double effect evaporation process of coffee extract. The results of this research show that although B-201 is the component with the highest avoidable exergy destruction rate, it does not have a high avoidable cost rate. The components that have the highest potential for improvement are D-101, D-102 and E-103 because they have the highest avoidable exergy cost rate. Additionally, the initial concentration of soluble solids proved to be a significant parameter for the process, given that an 8 w/w% increase of the initial concentration of soluble solids reduced the avoidable exergy destruction cost by 15%.
These results suggest that a reduction of the avoidable exergy destruction rate in these components can be achieved and it is possible to have annual savings of $\$8.37x10^5$ in the overall operating costs.
Further research is needed to optimize the solid-liquid extraction of coffee, in order to achieve a higher initial concentration of soluble solids in the coffee extract. Also extended parametric and structural change studies are recommended in the double effect evaporation process in order to maximize the exergetic efficiency and minimize the operational costs.

References

Bejan, A., Tsatsaronis, G., Moran, M., 1996. Thermal Design and Optimization. Wiley, New York.

Bühler, F., Nguyen, T. Van, Jensen, J.K., Holm, F.M., Elmegaard, B., 2018. Energy, exergy and advanced exergy analysis of a milk processing factory. Energy 162, 576–592.

Coherent Market Insights, 2019. Instant Coffee Market Size Share Forecast Report 2026. URL https://www.coherentmarketinsights.com/market-insight/instant-coffee-market-1458 (accessed 7.9.20).

Gungor, A., Tsatsaronis, G., Gunerhan, H., Hepbasli, A., 2015. Advanced exergoeconomic analysis of a gas engine heat pump (GEHP) for food drying processes. Energy Convers. Manag. 91, 132–139.

Liu, Z., Liu, Z., Cao, X., Luo, T., Yang, X., 2020. Advanced exergoeconomic evaluation on supercritical carbon dioxide recompression Brayton cycle. J. Clean. Prod. 256, 120537.

Mojarab Soufiyan, M., Aghbashlo, M., 2017. Application of exergy analysis to the dairy industry: A case study of yogurt drink production plant. Food Bioprod. Process. 101, 118–131.

Mojarab Soufiyan, M., Dadak, A., Hosseini, S.S., Nasiri, F., Dowlati, M., Tahmasebi, M., Aghbashlo, M., 2016. Comprehensive exergy analysis of a commercial tomato paste plant with a double-effect evaporator. Energy 111, 910–922.

Morosuk, T., Tsatsaronis, G., 2019. Advanced exergy-based methods used to understand and improve energy-conversion systems. Energy 169, 238–246.

Petrakopoulou, F., Tsatsaronis, G., Morosuk, T., Carassai, A., 2012. Advanced exergoeconomic analysis applied to a complex energy conversion system. J. Eng. Gas Turbines Power 134, 3.

Tinoco-Caicedo, D.L., Lozano-Medina, A., Blanco-Marigorta, A.M., 2020. Conventional and Advanced Exergy and A Case Study of an Instant Coffee Factory in Ecuador. Energies 13, 21, 5622.

Case Studies in Thermal Engineering 28 (2021) 101556

Contents lists available at ScienceDirect

Case Studies in Thermal Engineering

journal homepage: www.elsevier.com/locate/csite

Simulation and exergoeconomic analysis of the syngas and biodiesel production process from spent coffee grounds

Diana L. Tinoco-Caicedo [a,b,c,*], Medelyne Mero-Benavides [a], Myrian Santos-Torres [a], Alexis Lozano-Medina [c], Ana M. Blanco-Marigorta [c]

[a] Facultad de Ciencias Naturales y Matemáticas (FCNM), Escuela Superior Politécnica del Litoral Ecuador, 090903, Guayaquil, Ecuador
[b] Centro de Energías Renovables y Alternativas (CERA), Escuela Superior Politécnica del Litoral Ecuador, 090903, Guayaquil, Ecuador
[c] Department of Process Engineering, Universidad de Las Palmas de Gran Canaria, 35017, Las Palmas de Gran Canaria, Canary Islands, Spain

ARTICLE INFO

Keywords:
Syngas
Biodiesel
Exergy destruction cost
Investment cost rate
Exergetic efficiency

ABSTRACT

The integrated production of biofuels from agro-industrial wastes is increasing around the world. The thermodynamic performance and economic analysis of these processes have become topics of interest given the need to reduce the cost of biofuels and their impact on the environment. This study develops a simulation of the production process of syngas and biodiesel from spent coffee grounds, and an exergoeconomic analysis that mainly determines the exergy destruction rate, the investment and operational cost rate, and the exergy destruction cost rate at component level and for the overall system. The total investment cost for the integrated process resulted in 13.2 million dollars. The specific cost of syngas and biodiesel from spent coffee grounds were estimated in $0.36/kg and $0.71/kg, respectively. The results show that the drying process including the air heating for the pretreatment of the biomass had an exergy destruction rate of 11,463 kW and was responsible of the 92% of the overall exergy destruction cost rate. An increment of the dead state temperature reduced the specific cost of syngas and biodiesel in 17% and 8%, respectively. Future studies should focus on the exergoeconomic optimization of the drying process of biomass in order to minimize the operational costs.

1. Introduction

Currently, fossil fuels are the primary source of energy. Approximately, 80% of the word's energy demand is supplied by them [1]. However, it's estimated that oil reserves would not be sufficient to meet the demand by 2050 [2]. To overcome this problem, it's important to look for renewable energy sources, especially in sectors that consume more energy: industries and transport [3]. Biofuels are one of the most common renewable energy sources and are considered the best option for industries especially when biofuel comes from an industrial waste [4]. During 2018, according to British Petroleum company, the United States became the first country with an annual production of 38.1 million tons of biofuel, followed by Brazil with a production of 21.4 million tons per year [5]. Nowadays there are 803 biorefineries in Europe where 45% of them produce biofuels [6]. The biofuels mostly produced are biodiesel, syngas and bioethanol [7]. In the last few years, different countries have produced biofuels from different sources, such as waste deriving from agriculture [8], agroindustry [9] and livestock [10]. These have gradually contributed to the reduction of 80% of the greenhouse

* Corresponding author. Facultad de Ciencias Naturales y Matemáticas (FCNM), Escuela Superior Politécnica del Litoral Ecuador, 090903, Guayaquil, Ecuador.
E-mail address: dtinoco@espol.edu.ec (D.L. Tinoco-Caicedo).

https://doi.org/10.1016/j.csite.2021.101556
Received 25 August 2021; Received in revised form 2 October 2021; Accepted 12 October 2021
Available online 13 October 2021

emissions from landfills [11].

The agricultural wastes that have been studied to be converted to biofuels included rice bran [12], oat straw [13], fish waste [14], alga [15] and spent coffee grounds (SCG) [16], where the last one has the highest calorific value (22 MJ/kg) and oil content (29%), becoming one of the best energetic potential resources for the production of liquid and solid biofuels. There are many experimental studies about the production of biofuels from SCG at laboratory scale. Liu et al. [17] studied the biodiesel production by applying in-situ transesterification method at 70 °C by 3 h, obtaining a yield of 98,61% greater than the 83% obtained by Haas et al. [18]. Meanwhile, Park et al. [19] applied indirect transesterification to the humidified SCG for the production of biodiesel and obtained a yield of 16.75%. Pacioni et al. [20] applied the gasification process with steam in a tubular reactor to produce syngas from SGC with a yield of 88.6%. Kibret et al. [21] applied the same process by using a semi-fluized bed and increased the yield to 95%.

In the last few years, many exergetic and exergoeconomic analyses of different biodiesel and syngas production processes have been developed in order to evaluate the sustainability of these processes. In the case of biodiesel, Antonova et al. [22] evaluated the production of biodiesel from the oil of canola seeds and found that the dryer and the transesterification reactor destroyed 7.8% and 25.2% of the fuel exergy rate, respectively. Amelio et al. [23] shows that an exergetic optimization in the biodiesel production from triolein oil achieves a higher reduction than energetic optimization, with a difference of 44.7 kW. Mancebo et al. [24] achieved an increase in the exergetic efficiency through an exergetic optimization from 10% to 22% and the reduction of exergy destruction cost rate from $0.13/h to $0.12/h. In the case of syngas, Shayan et al. [25] analyzed the gasification process of wood and determined the optimum temperature of gasification which allowed them to increase the exergetic efficiency by 24.9% and reduce the exergy destruction cost rates by 8.9%. Another similar study determined that the exergetic efficiency could be increased to 76.2% when the steam/biomass mass ratio is 1.83 [26]. Different exergetic analysis have been performed in processes that include a gasifier in combination with other treatments such as hydrotreatment, hydrocracking, steam reforming [27], direct and indirect synthesis of dimethyl ether [28], digestion plants [29] and integrated energy system [30]. In all these processes, the component with the highest exergy destruction rate was the gasifier.

As it is shown, although there are many experimental analysis on SCG that have demonstrated a high potential to be converted to biofuels, there are not exergetic and economic analyses focused on evaluating the sustainability of this process. The previous exergoeconomic analysis mentioned were only focused on evaluating specific steps such as transesterification or gasification of other types of biomass. Therefore, an exergetic and economic analyses of an integrated process for the production of biodiesel and syngas by indirect transesterification and gasification from SCG has never been reported.

In an effort to address the gap found in the literature, the aim of this study is to perform an exergetic and exergoeconomic analyses of an integrated production process of biodiesel and syngas from SCG. The process is simulated and validated with experimental data from previous studies. It includes drying of biomass, oil extraction, gasification of biomass, and indirect transesterification of the oil. The analyses allow us to identify the main components that have the highest exergy destruction rates and exergetic cost rates. The findings obtained herein can be useful for the design and optimization of biorefineries based on SCG.

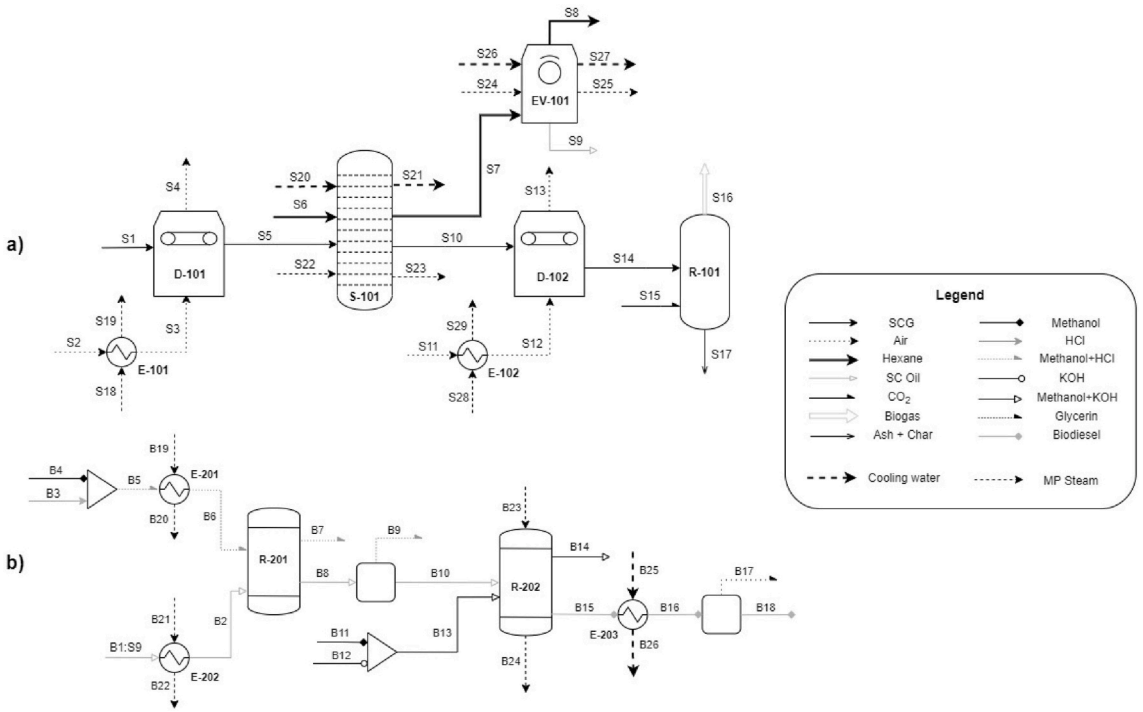

Fig. 1. Process flow diagram of the integrated process to produce a) syngas and b) biodiesel.

2. Materials and methods

2.1. System description

Fig. 1 shows the production of syngas and biodiesel from SCG with initial moisture of 61.1% w/w. Air (stream S3) is heated up to 150 ^{o}C (stream S4) in a heat exchanger (E−101), then it enters a dryer (D-101) to reduce the SCG's moisture to 12.4% w/w. The dried biomass (Stream S5) enters the soxhlet extractor (S-101), where it is in contact with hexane (stream S6) to extract 15% of the lipids from the SCG. The oil stream enters into a flash evaporator (EV-101) to recover the hexane (stream S8) and separate it from the lipids (stream S9). Traces of solvent in the spent biomass are evaporated in the dryer (D-102) with air preheated to 100 ^{o}C (stream S12). Then, the dried SCG enters a gasifier at 900 ^{o}C with carbon dioxide as the gasifying agent (stream S15) and produces syngas (stream 16), with a relative molar composition of 0.02, 0.43, 0.10, 0.37 for H_2, CH_4, CO, and CO_2, respectively [31]. In addition, the gasifier produces a solid stream with 95% char and 5% ash (stream 17). SCG oil (stream S9) is heated in a heat exchanger (E−202) with steam (stream B21) to 54 °C (stream B6). A mixture of methanol (stream B4) and hydrogen chloride (stream B3) is heated in a heat exchanger (E−201) with steam (stream B19) up to 54 °C. The heated mixture enters into a reactor (R-201) where the esterification reaction occurs to obtain methyl esters from free fatty acids. The methyl esters and the triglycerides of the oils leave the reactor (steam B8). Other products like excess reagent and produced water leave the reactor separately (stream B7). The product is decanted before going into the second reactor to eliminate the residues of methanol, water and HCl. In the second transesterification reactor (R-202), triglycerides from SCG oil (stream B10) react with methanol and KOH (stream B12) to produce water as a by-product (stream B14) and a mixture of glycerin and biodiesel as a product (stream B15). The product from the second reactor is cooled to room temperature (stream B16) and decanted to separate the glycerin (stream B17) from the biodiesel (stream B18).

2.2. Process simulation

The simulation of the process was performed in Aspen Plus V12.1. The SCG and the ash were simulated as unconventional components. Proximate and ultimate analyses were defined by applying the enthalpy and density model of the unconventional components (HCOALGEN and DCOALIGT) [32]. The oil chemical composition extracted from the SCG was obtained from a previous study [33], therefore the chemical compounds were simulated as conventional components using the NIST ThermoData Engine (TDE) database [34].

The conditions of the D-101 such as air/SCG mass ratio and initial and final humidity were established from experimental data in a convective dryer [35]. The EV-101 was simulated as a flash separator and a total solvent recovery was assumed. The ideal thermodynamic model was used for the gasification process because the pseudo-components were at a low pressure of 101.3 kPa [36]. The gasifier was simulated by the use of the RYIELD and the RGIBBS reactors [37]. Tar formation was not considered [38] and char was defined as pure coal, which was determined by the mass of fixed coal in the biomass.

For the esterification and transesterification processes, the UNIQUAC thermodynamic model was used, because the studied system has two liquid phases, some strong polar compounds and is at a low pressure of 101.3 kPa [39]. A yield of 100% and 85% were considered for the esterification and transesterification reactions occurring in R-201 and R-202, respectively, according to previous studies [40].

2.3. Model validation

The final moisture obtained in the dryers, the syngas composition obtained in the gasifier, the yield achieved in the oil extraction process, and the yield and composition of the biodiesel produced in the transesterification reactor were compared with the results obtained experimentally by previous studies using the same operational conditions, to ensure the validity of the modeled processes. For the esterification and the transesterification reactors, the operating conditions of Haile et al. [40] were used. The esterification reactor was operated at atmospheric pressure, with a methanol/FFA molar ratio of 20:1 and HCl at 10% w/w free fatty acids. The transesterification reactor had a methanol/oil molar ratio of 9:1 and KOH and 1% w/w of oil content. The D-101 was operated with the conditions presented in the experimental study of Gómez et al. [35].

The drying air temperature was 150 ^{o}C, and its relative humidity was 50%. The SCG initial moisture was 61.1% w/w. The inlet air flow was 524.8 kg wet air per kg of wet biomass.

For the soxhlet extraction the solvent/biomass mass ratio was 9.87 as used by De Melo et al. [41]. The gasifier was operated at 900 ^{o}C, with a CO_2/SCG molar ratio of 0.17 and with initial biomass moisture of 2.89% w/w, which are the conditions proposed by Kibret et al. [21].

2.4. Exergetic analysis

The exergetic analysis was conducted at the level of each system component. The Engineering Equations Solver (EES) software was used for the calculations. The enthalpy and entropy of most of the states were determined with the thermophysical properties library of EES, when possible. The specific heat capacity expressions for substances were not included in the EES database, such as SCG [42], lipids [43], ash [44], char [45] and glycerin [46], they were found in the literature.

The physical exergy and chemical exergy of the material streams were calculated using Eq. (1) and Eq. (2), respectively.

$$e_i^{PH} = h_i - h_o - T_o(s_i - s_o) \tag{1}$$

$$e_i^{CH} = \sum x_i e_i^{ch} + RT_o \sum x_i \ln(x_i) \tag{2}$$

where $T_0 = 27\ ^{o}C$ is the temperature of the dead state (with a dead state pressure of 1 atm), which is the annual average temperature in Guayaquil, Ecuador. x_i and e_i^{ch} are the molar composition and the standard chemical exergy, respectively of each compound presented in the stream *i*. The standard chemical exergies were obtained from the Model II [47].

The chemical exergy of moist air was calculated with Eq. (3) [48].

$$e_{air}^{ch} = 0.2857 c_{p,air} T_o ln\left[\left[\frac{1 + 1.6078 w_o}{1 + 1.6078 w}\right]^{(1+1.6078w)} \left[\frac{w}{w_o}\right]^{1.6078w}\right] \tag{3}$$

The exergy of wet biomass was calculated by using Eq. (4) [49] where x_{DB} is the composition of SCG in a dry free ash basis.

$$e_{WB}^{ch} = x_{DB} \cdot e_{DB}^{ch} + \sum x_i \cdot e_i^{ch} \tag{4}$$

The chemical exergy of the ashes was calculated by using the model proposed by Song et al. [50] which is based on a statistical study of ash in 86 varieties of biomass and depends on the total concentration of different minerals. For SCG, this total concentration was obtained from a study conducted on coffee waste [51]. The chemical exergies of SCG, defatted SCG, oil, char and the biodiesel were determined by using Eq. (5) applied to pure hydrocarbon fuels [49]. The molecular formula of each of these substances was estimated based on their respective ultimate analysis.

$$e_x^{ch} = \overline{HHV}(T_o,\ P_o) - T_o\left[\sum_R \nu_R \bar{s}_R - \sum_P \nu_P \bar{s}_P\right](T_o,\ P_o) - \left[\sum_P \nu_P \bar{e}_P^{ch} - \sum_R \nu_R \bar{e}_R^{ch}\right] \tag{5}$$

where $\overline{HHV}$ represents the higher heating value at the dead state conditions; $\nu$is the stochiometric coefficient of each combustion compound, and $\bar{s}$ the standard entropy of each compound. The higher heating values of SCG oil [40], biodiesel [52], SCG and defatted SCG [32], and char [20] were obtained from literature.

For the calculation of the chemical exergy of glycerin, a reaction involving reference substances has been considered:

$$C_3H_8O_3 + 5\ O_2 \rightarrow 3CO_2 + 4H_2O$$

Eq. (6) was used for the determination of the chemical exergy of glycerin [49]; where ΔG is the change in the Gibbs function at dead state conditions.

$$e_{gly}^{ch} = \Delta G - \left[\sum_P \nu_P \bar{e}_P^{ch} - \sum_r \nu_R \bar{e}_R^{ch}\right] \tag{6}$$

The exergy balance of each component of the process was performed according to Bejan et al. [49] using Eq. (7):

$$\dot{E}_{F,k} - \dot{E}_{P,k} = \dot{E}_{D,k} - \dot{E}_{L,k} \tag{7}$$

where $\dot{E}_{F,k}$corresponds to the fuel exergy, $\dot{E}_{P,k}$ is the product exergy, $\dot{E}_{D,k}$is the destroyed exergy and $\dot{E}_{L,k}$ is the exergy loss. Table 1

Table 1
Definitions of fuel and product exergy for each component.

Component	$\dot{E}_F$	$\dot{E}_p$
Heat exchanger (E−101)	$\dot{E}_{S18} - \dot{E}_{S19}$	$\dot{E}_{S3} - \dot{E}_{S2}$
Dryer (D-101)	$\dot{E}_{S1} + \dot{E}_{S3}$	$\dot{E}_{S5}$
Soxhlet extractor (S-101)	$(\dot{E}_{S22} - \dot{E}_{S23}) - (\dot{E}_{S21} - \dot{E}_{S20}) + (\dot{E}_{S5} - \dot{E}_{S10})$	$\dot{E}_{S7} - \dot{E}_{S6}$
Evaporator (EV-101)	$(\dot{E}_{S24} - \dot{E}_{S25}) + \dot{E}_{S7} - (\dot{E}_{S27} - \dot{E}_{S26})$	$\dot{E}_{S8} + \dot{E}_{S9}$
Heat exchanger (E−102)	$\dot{E}_{S28} - \dot{E}_{S29}$	$\dot{E}_{S12} - \dot{E}_{S11}$
Dryer (D-102)	$\dot{E}_{S10} + \dot{E}_{S12}$	$\dot{E}_{S14}$
Reactor (R-101)	$\dot{E}_{S14} + \dot{E}_{S15} - \dot{E}_{S17}$	$\dot{E}_{S16}$
Heat exchanger (E−201)	$\dot{E}_{B19} - \dot{E}_{B20}$	$\dot{E}_{B6} - \dot{E}_{B5}$
Heat exchanger (E−202)	$\dot{E}_{B21} - \dot{E}_{B22}$	$\dot{E}_{B2} - \dot{E}_{B1}$
Heat exchanger (E−203)	$\dot{E}_{B15} - \dot{E}_{B16}$	$\dot{E}_{B26} - \dot{E}_{B25}$
Reactor (R-201)	$\dot{E}_{B6} + \dot{E}_{B2} - \dot{E}_{B7} - \dot{E}_{B9}$	$\dot{E}_{B10}$
Reactor (R-202)	$(\dot{E}_{B13} - \dot{E}_{B14}) + (\dot{E}_{B23} - \dot{E}_{B24}) + \dot{E}_{B10}$	$\dot{E}_{B15}$
Overall system	$\dot{E}_{heating} - \dot{E}_{cooling} + \dot{E}_{S6} - \dot{E}_{S8} + \dot{E}_{S1} + \dot{E}_{S15} + \dot{E}_{B5} - (\dot{E}_{B7} - \dot{E}_{B9}) + \dot{E}_{B13} - \dot{E}_{B14}$	$\dot{E}_{B16} + \dot{E}_{S16}$

presents the definitions of the fuel and product exergy for each component of the process. For the overall system, the $\dot{E}_{heating}$ is the sum of the changes of exergy rates of the streams of steam used in the heating processes. $\dot{E}_{cooling}$ is the sum of the change of exergy rates of the streams of cooling water used in the cooling processes.

2.5. Economic analysis

The economic analysis was performed by following the Total Revenue Requirement methodology [49]. The purchase equipment cost (PEC) for each component of the process was obtained from vendors based on the required characteristics and are presented in the results section. The costs of steam and carbon dioxide were considered as \$0.03/kg and \$24.22/kg, respectively [53]. The cost of cooling water [54] is \$0.72/m^3. The cost of n-hexane, methanol, hydrogen chloride and sodium hydroxide were \$0.03/kg, \$1.15/kg, \$0.50/kg, \$0.04/kg, respectively, which were obtained from vendors.

The total cost rate for operation and investment ($\dot{Z}_k$) was determined as is shown in Eq. (8).

$$\dot{Z}_k = \dot{Z}_k^{O\&M} + \dot{Z}_k^{CI} \tag{8}$$

where $\dot{Z}_k^{CI}$ is the capital investment cost rate and $\dot{Z}_k^{O\&M}$ is the operation and maintenance cost rate of the kth component. These variables were calculated by using the economic indicators presented in Table 2, obtained from a previous study [49].

2.6. Exergoeconomic analysis

The exergoeconomic analysis was carried out by performing a cost balance in each component of the system following Eq. (9):

$$\dot{C}_{F,k} + \dot{Z}_k = \dot{C}_{P,k} \tag{9}$$

where $\dot{C}_{F,k}$ and $\dot{C}_{P,k}$ are the fuel and the product cost rate of the *k*-th component, respectively. These costs were determined following the expressions from Table 3. The exergoeconomic indicators such as the exergoeconomic factor (f_k), the relative cost difference (r_k), and the exergy destruction cost rate ($\dot{C}_D$) for each component of the system were calculated following the methodology reported by Bejan et al. [49].

3. Results and discussions

3.1. Model validation

In order to verify the validity of each component's calculation models, the values of the main operating parameters obtained in this work have been compared with those reported in experimental studies from other literature. On Table 4, the final moisture obtained in the dryer (D-101), the yield of the Soxhlet extractor (S-101), the syngas composition that is produced in the gasifier (R-101) and the yield and biodiesel composition produced in the reactor (R-202) were presented and compared. It can be observed that the results of the model are close to the results reported in the experimental studies, with a maximum absolute error of 5.3, which represents a 6% relative error. Therefore, it is concluded that the models can be used to represent the syngas and biodiesel production process from SCG oil under the established operating conditions.

3.2. Exergetic analysis

Table 5 shows the mass flow rate ($\dot{m}$), the temperature (T), the pressure (P), the specific enthalpy (h), the specific entropy (s), the physical exergy ($\dot{E}^{ph}$), the chemical exergy ($\dot{E}^{ch}$) and the total exergy ($\dot{E}$) of each material stream. It can be observed that the chemical exergy is higher than the physical exergy in most of the states, especially in the streams that have lipids, hexane, biomass, and its

Table 2
Economic parameters used for the economic analysis [49].

Parameter	Value
Average general inflation rate	0.05
Average nominal escalation of all costs	0.05
Average nominal escalation of fuel costs	0.05
Plant economic life in years (n)	20
Plant life for tax purposes in years	15
Average combined income tax rate	0.38
Average property tax rate (%PFI)	0.015
Average insurance rate (%PFI)	0.5
Average capacity factor	0.85
Labor positions for O&M	20
Average labor rate (\$/h)	18

Table 3
Cost balance equations and auxiliary equations for exergy costs of the system.

Component	Fuel Cost	Product Cost	Auxiliary Equations
E−101	$\dot{C}_{S18} - \dot{C}_{S19}$	$\dot{C}_{S3} - \dot{C}_{S2}$	$c_{S2} = 0$ $c_{S19} = c_{S18}$
D-101	$\dot{C}_{S1} + \dot{C}_{S3}$	$\dot{C}_{S5}$	$c_{S1} = 0$
S-101	$(\dot{C}_{S22} - \dot{C}_{S23}) - (\dot{C}_{S21} - \dot{C}_{S20}) + (C_{S5} - \dot{C}_{S10})$	$\dot{C}_{S7} - \dot{C}_{S6}$	$c_{S21} = c_{S20}$ $c_{S23} = c_{S22}$ $c_{S10} = c_{S7}$
EV-101	$(\dot{C}_{S24} - \dot{C}_{S25}) + \dot{C}_{S7} - (\dot{C}_{S27} - \dot{C}_{S26})$	$\dot{C}_{S8} + \dot{C}_{S9}$	$c_{S25} = c_{S24}$ $c_{S27} = c_{S26}$ $c_{S8} = c_{S9}$
E−102	$\dot{C}_{S28} - C_{S29}$	$\dot{C}_{S12} - \dot{C}_{S11}$	$c_{S11} = 0$ $c_{S29} = c_{S28}$
D-102	$\dot{C}_{S10} + \dot{C}_{S12}$	$\dot{C}_{S14}$	–
R-101	$\dot{C}_{S14} + \dot{C}_{S15} - \dot{C}_{S17}$	$\dot{C}_{S16}$	$c_{S17} = c_{S16}$
E−201	$\dot{C}_{B19} - \dot{C}_{B20}$	$\dot{C}_{B6} - \dot{C}_{B5}$	$c_{B19} = c_{B20}$
E−202	$\dot{C}_{B21} - \dot{C}_{B22}$	$\dot{C}_{B2} - \dot{C}_{B1}$	$c_{B21} = c_{B22}$
E−203	$\dot{C}_{B15} - \dot{C}_{B16}$	$\dot{C}_{B26} - \dot{C}_{B25}$	$c_{B26} = c_{B25}$ $c_{B17} = c_{B18}$
R-201	$\dot{C}_{B6} + \dot{C}_{B2} - \dot{C}_{B7} - \dot{C}_{B9}$	$\dot{C}_{B10}$	$c_{B7} = c_{B6}$ $c_{B9} = c_{B6}$
R-202	$(\dot{C}_{B13} - \dot{C}_{B14}) + (\dot{C}_{B23} - \dot{C}_{B24}) + \dot{C}_{B10}$	$\dot{C}_{B15}$	$c_{B23} = c_{B24}$ $c_{B14} = c_{B13}$
Overall System	$\dot{C}_{heating} - \dot{C}_{cooling} + \dot{C}_{S6} - \dot{C}_{S8} + \dot{C}_{S1} + \dot{C}_{S15} + \dot{C}_{B5} - (\dot{C}_{B7} - \dot{C}_{B9}) + \dot{C}_{B13} - \dot{C}_{B14}$	$\dot{C}_{B16} + \dot{C}_{S16}$	

Table 4
Validation of the models.

Component	Parameter	This work	Literature	Absolute Error
D-101	Final moisture (%, wb)	12.4	12.4 [35]	0
S-101	Yield (%, db)	15.0	15.0 [41]	0
R-101	CO_2	0.370	0.373 [21]	0.003
	CO	0.100	0.040 [21]	0.060
	CH_4	0.430	0.526 [21]	0.096
	H_2	0.020	0.061 [21]	0.041
R-202	Yield	82.0	87.3 [40]	5.3
	Linoleic Acid	0.37	0.41 [40]	0.04
	Palmitic Acid	0.36	0.36 [40]	0.00
	Oleic	0.14	0.14 [40]	0.00
	Stearic	0.08	0.08 [40]	0.00

derivatives. Therefore, this production process is focused on using the chemical exergy of biomass through chemical reactions, for the transformation into biofuels.

Table 6 shows the exergy of the fuel ($\dot{E}_F$), the exergy of the product ($\dot{E}_P$), the exergy destruction ($\dot{E}_D$) and the exergetic efficiency (η) for each component and for the overall system. The components E−201, E−202 and E−203 have an exergy destruction rate lower than 0.5 kW, therefore they were excluded from the table. It can be observed that the E−101 and D-101 are the main sources of irreversibility, they cause 53% and 28% of the overall exergy destruction rate, respectively. Similar results were found in a spray drying process of instant coffee [53] where the dryer was responsible for 23% of the exergy destruction. Similarly, Mehrpooya et al. [12] reported that air heat exchangers based on steam were the components with the lowest exergetic efficiency in the drying process of wood chips because a great amount of high quality energy was destroyed when the air was discharged.

Some studies show that the heat source in heat exchangers significantly affects the exergy destruction rate. When the heat source is flue gases, the exergy destruction rate is reduced [55]. Singh et al. [56] found that the use of solar energy for heating air increased the exergetic efficiency of the heat exchanger and the dryer from 15.3% to 24%. Another reason for a low exergetic efficiency is the high drying temperature. Beigi et al. [57] identified that an increase in the air temperature, increases the rate of heat and mass transfer and thus, increases the exergy of the exhaust air and the exergy losses.

Additionally, other components such as the R-202 and the R-101 destroy 5% of the overall destroyed exergy. Ofori-Boateng et al. [58] identified that transesterification reactors have a high exergy destruction rate because the reaction produces glycerin as a by-product and it has a high chemical exergy. Some factors that reduced the exergetic efficiency of these reactors were a high concentration of the catalyst, a high methanol/oil ratio and a high temperature of reaction [59]. Regarding the gasifier, Ji-chao et al. [60] found that unwanted products in the reaction such as char, increase the exergy destruction rate of this component, because it has a high

Table 5
Thermodynamic values of the streams.

State	$\dot{m}$(kg/h)	T (°C)	P (bar)	h (kJ/kg)	s (kJ/kg K)	$\dot{E}^{ph}$ (kW)	$\dot{E}^{ch}$(kW)	$\dot{E}$(kW)
S1	1071	30	1	197	0.5905	6.2	3630	3636
S2	562,075	25	1	0	0.0000	0.0	0	0
S3	562,075	150	1	151	0.4206	4010.0	0	4010
S4	562,670	80	1	57	0.1763	730.3	2	732
S5	476	80	1	159	0.4873	1.9	3622	3624
S6	4570	25	1	0	0.0000	0.0	60,608	60,608
S7	4586	68	1	71	0.2238	6.0	61,127	61,133
S8	4524	69	1	72	0.2264	6.1	60,001	60,008
S9	62.5	30	1	11	0.0350	0.0	1126	1126
S10	459	68	1	113	0.3517	1.0	3094	3095
S11	50,651	25	1	0	0.0000	0.0	0	0
S12	50,651	100	1	78	0.2330	118.0	0	118
S13	50,746	60	1	36	0.1156	27.4	578	605
S14	365	60	1	94	0.2967	0.6	2240	2240
S15	0.01	25	1	0	0.0000	0.0	0	0
S16	289	425	1	876	1.9150	24.5	1334	1358
S17	75.8	900	1	981	1.5350	11.4	596	608
S18	34,874	190	13	2681	6.1420	8234.0	5108	13,342
S19	34,874	190	13	702	1.8670	1408.0	484	1891
S20	7550	25	1	0	0.0000	0.0	105	105
S21	7550	68	1	179	0.5596	24.5	105	129
S22	976	190	13	2681	6.1420	230.5	143	374
S23	976	190	13	702	1.8670	39.4	14	53
S24	745	190	13	2681	6.1420	175.8	109	285
S25	745	190	13	702	1.8670	30.1	10	40
S26	7680	25	1	0	0.0000	0.0	107	107
S27	7680	69	1	184	0.5750	26.3	107	133
S28	1882	190	13	2681	6.1420	444.3	276	720
S29	1882	190	13	702	1.8670	76.0	26	102
B1	63	30	1	11	0.0350	0.0	1126	1126
B2	63	54	1	61	0.1959	0.1	1126	1126
B3	6	30	1	12	0.0391	0.0	2	1909
B4	6	30	1	13	0.0424	0.0	39	39
B5	12	25	1	0	0.0000	0.0	37	37
B6	12	54	1	72	0.2306	0.0	37	37
B7	1	54	1	61	0.1958	0.0	0	0
B8	71	54	1	64	0.2036	0.1	1125	1125
B9	11	54	1	93	0.2963	0.0	39	39
B10	63	53	1	57	0.1824	0.0	1095	1095
B11	26	30	1	13	0.0424	0.0	159	159
B12	1	30	1	17	0.0580	0.0	0	0
B13	26	30	1	13	0.0428	0.0	159	159
B14	0	54	1	77	0.2464	0.0	0	0
B15	89	54	1	46	0.1471	0.1	881	881
B16	89	30	1	7826	0.0260	0.0	881	881
B17	34	30	1	11	0.0352	0.0	343	343
B18	55	30	1	6607	0.0220	0.0	767	767
B19	0	190	13	2681	6.1420	0.1	0	0
B20	0	190	13	703	1.8690	0.0	0	0
B21	2	190	13	2681	6.1420	0.4	0	1
B22	2	190	13	703	1.8690	0.1	0	0
B23	0	190	13	2681	6.1420	0.0	0	0
B24	0	190	13	703	1.8690	0.0	0	0
B25	156	27	1	8366	0.0280	0.0	2	2
B26	156	40	1	63	0.2053	0.1	2	2

chemical exergy. Another study identified that parameters such as a high initial humidity of the biomass [61] and a low gasifying agent/biomass mass ratio [62] decreased the exergetic efficiency of the gasifier.

Furthermore, the components with the least impact on the overall exergy destruction rate are the E−201 and E−202, because they destroy less than 1%. Fig. 2 shows the exergy flows rates across the process. It can be observed that the S-101 and EV-101 have an input exergy rate higher than 60 MW. This occurs because the input solvent has the highest chemical exergy rate. That is why the recuperation of the solvent in the EV-101 is so important in order to reduce the exergy destruction rate and the operating costs. A previous experimental study showed that the use of a recycled solvent in the extraction process did not affect the extraction yield of SCG oil [63].

Table 6
Results of the exergetic analysis of all the main components of the process.

Component	$\dot{E}_F$ (kW)	$\dot{E}_P$ (kW)	$\dot{E}_D$ (kW)	η (%)	y^*_D	y_D
E−101	11,451	4010	7441	35	0.526	0.050
D-101	7646	3624	4022	47	0.285	0.027
S-101	61,433	61,133	300	99	0.021	0.002
EV-101	61,351	61,133	217	99	0.015	0.001
E−102	617	118	499	19	0.035	0.003
D-102	3213	2240	972	69	0.069	0.006
R-101	1633	1358	274	83	0.019	0.002
R-201	1125	1095	30	97	0.000	0.000
R-202	1254	877	376	70	0.000	0.000
Overall System	149,725	135,588	14,135	91	1.000	1.000

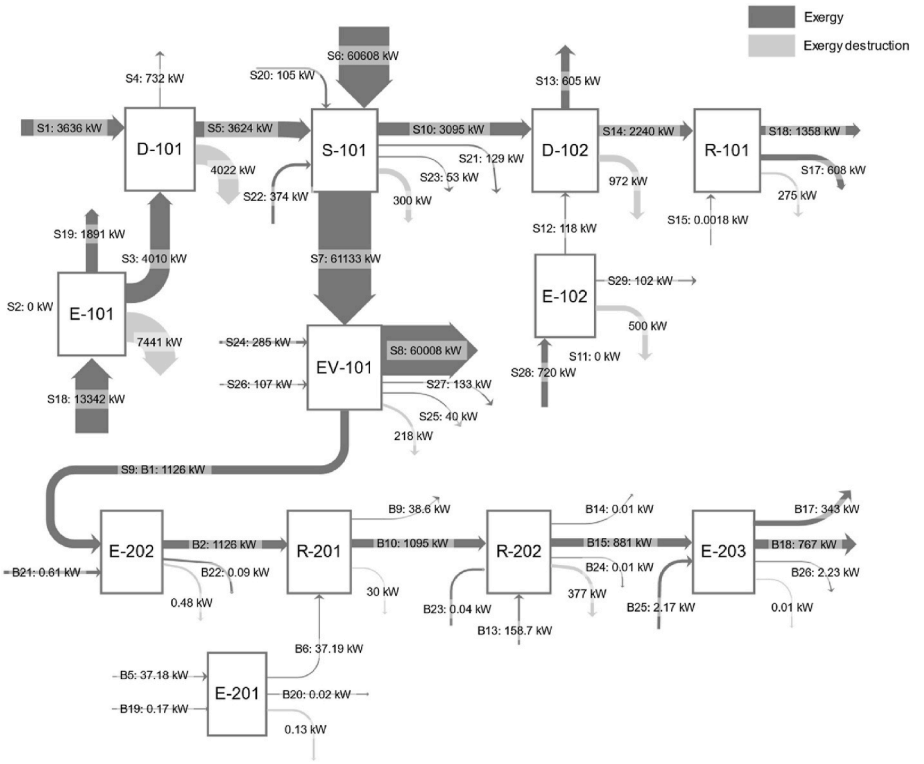

Fig. 2. Grassmann's diagram of the process.

Table 7
Results of exergoeconomic analysis.

Component	*PEC ($)*	c_f ($/MJ)	$\dot{Z}_k^{CI}$ ($/h)	$\dot{Z}_k^{O\&M}$ ($/h)	$\dot{Z}_k + \dot{C}_D$($/h)	$\dot{C}_D$ ($/h)	f_k	r_k
E−101	1415	0.028	0.44	0.25	759.20	758.50	0.09	1.86
D-101	6000	0.042	1.87	1.08	617.40	614.40	0.48	1.12
S-101	15,000	0.005	4.69	2.69	12.94	5.56	57.02	0.01
EV-101	5000	0.006	1.56	0.90	7.06	4.60	34.85	0.01
E−102	1415	0.028	0.44	0.25	51.65	50.96	1.35	4.29
D-102	6000	0.011	1.87	1.08	41.73	38.78	7.07	0.47
R-101	10,000	0.015	3.12	1.79	19.95	15.03	24.66	0.27
E−201	3000	0.028	0.82	0.42	1.25	0.01	98.93	1121.00
E−202	3000	0.028	0.82	0.42	1.29	0.05	96.22	269.00
R-201	25,000	0.001	6.80	3.49	10.44	0.14	98.67	2.10
R-202	20,000	0.003	5.44	2.79	12.90	4.66	63.87	1.20
E−203	4000	0.014	1.09	0.56	1.65	0.00	99.96	628.00

3.3. Exergoeconomic analysis

The total investment cost for the plant of syngas and biodiesel from SCG is estimated to be $13.2 million. The annual fuel cost and the operation and maintenance costs are $375,100 and $49,820 dollars, respectively, for a production of 289 kg/h of syngas and 55 kg/h of biodiesel, from processing a mass flow of 41,500 kg/h of SCG.

Table 7 shows the purchase equipment cost (*PEC*), the specific fuel costs (c_f), the capital investment cost rate ($\dot{Z}_k^{CI}$), the operational and maintenance cost rate ($\dot{Z}_k^{O\&M}$), the total operational cost rates ($\dot{Z}_k + \dot{C}_D$), the exergy destruction cost rate ($\dot{C}_D$), the exergoeconomic factor (f_k), and the relative difference (r_k) for each component. It can be observed that the components with the highest purchased costs such as R-201 and R-202 are not the components with the highest operational cost rates. Also there are other components with lower investment costs that have higher exergy destruction cost rates, such as the heat exchangers and the dryers.

Fig. 3 shows that the E−101 and the D-101 are the components with the highest operating costs rates ($Z_k + \dot{C}_D$), followed by the E−102 and the D-102. This means that the air heater and the dryer influence significantly the overall costs of the system. These components have an exergoeconomic factor (f_k) of less than 10%, which means that the predominant cost is related to the destruction of exergy. At the same time, these components have the highest exergy destruction rate. Similar results have been found in a study related to a food drying process [64], where the dryer and the air heat exchanger presented an exergoeconomic factor of less than 5%.

A previous study had demonstrated that the avoidable exergy destruction cost rate could be more than 50% in components such as dryers or heat exchangers. Therefore, if the exergy destruction cost rate is reduced by at least 50% in D-101 and E−101, the overall operational cost of the process can be reduced by 45% and the overall exergetic efficiency could increase from 90.6% to 94.4%.

In order to reduce costs, it is possible to optimize the operational conditions of the process and to analyze the different factors that significantly affect the exergy destruction cost rate. A previous study [65] proposed solar heat pump dryers, which allowed the reduction of the exergy destruction cost rate from $0.06/h to $0.0044/h and the increase in the f_k from 5% to 51%; so that a balance is reached between the investment cost and exergy destruction cost rate with this structural change. Another study identified that recycling the drying air in continuous dryers has an economic and exergetic benefit for the process [66]. S. Zohrabi et al. [67] studied the recirculation of air in a convective dryer and achieved an increase of the exergetic efficiency from 55% to 95%.

According to different studies, the gasifier is one of the components that has the highest exergy destruction cost rate. Fakhimghanbarzadeh et al. [68] determined that this component was responsible for 11% of the operational cost rate and that it could be reduced 10% by increasing the temperature of the reaction and reducing the biomass/gasifying agent mass ratio. Fani et al. [69] found that the decrease of pressure in the reactor also reduces the cost rate. In addition, there are other important factors that are more dependent on the fuel used to operate the plant's facilities [70]. In a previous study, the specific cost of the gasifying agent was found to be key in this cost rate [71].

The dead state temperature is also another important factor because it is determined by the initial condition of the air and the water used in the system and influences the exergy rates of each process stream. This variable changes over time, as it depends on climatic changes. Fig. 4 shows the effect of the dead state temperatures between 15 °C and 35 °C on the exergy destruction rate and the cost of exergy destruction rate. The results are favorable for high dead state temperatures, and a 10°C change reduces the process cost rate by $150/h.

Fig. 5 shows the components of the process that are most affected by the change of the dead state temperature; in this case, they are the components with the highest exergy destruction cost rate. This means that the overall operational cost rate could be reduced by $300/h when the temperature of the environment is increased. Erbay et al. [72] presented similar results when they analyzed the effect of the dead state temperature between 0 and 20 °C in the exergetic efficiency and total exergy costs of a ground-source heat pump food dryer. Other components such as the R-101 are not significantly affected by the change of the dead state temperature, because they do not have inputs from the environment. Dryers and heat exchangers require ambient air, which means that environmental conditions strongly affect the performance of these components.

4. Conclusions

The integrated production process of biodiesel and syngas from spent coffee grounds was simulated and evaluated by an exergoeconomic analysis. The model was validated with experimental data obtaining a maximum relative error of 6%. The exergetic and economic indicators were determined at a component level and an overall system level.

The economic analysis revealed that the first stage of the process, which includes the pretreatment of the biomass and the oil extraction, has a lower capital investment cost rate but a higher operating and maintenance cost rate than the stage of syngas and biodiesel production.

The overall exergetic efficiency of the process was 91% with an exergy destruction rate of 14,135 kJ/s. The overall exergy destruction cost rate ($1,493/h) represents 97% of the total cost rate of the plant. The main components that caused the highest exergy destruction rates and cost rates were the SGC dryers (D-101 and D-201) and the air heat exchangers (E−101 and E−201). These components are responsible for 92% of the overall exergy destruction cost rate.

An increase in the dead state temperature could reduce the exergy destruction cost rate of the process up to 9%. The biodiesel and syngas specific costs could be reduced by maximizing the exergetic efficiency and minimizing the exergy destruction cost rate in the dryers and the air heat exchangers.

An advanced exergoeconomic analysis should be performed in order to quantify the avoidable exergy destruction cost rate, mainly in the dryers and air heat exchangers.

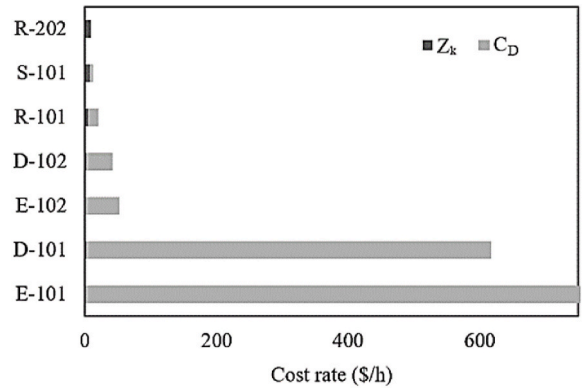

Fig. 3. Main operational cost rates.

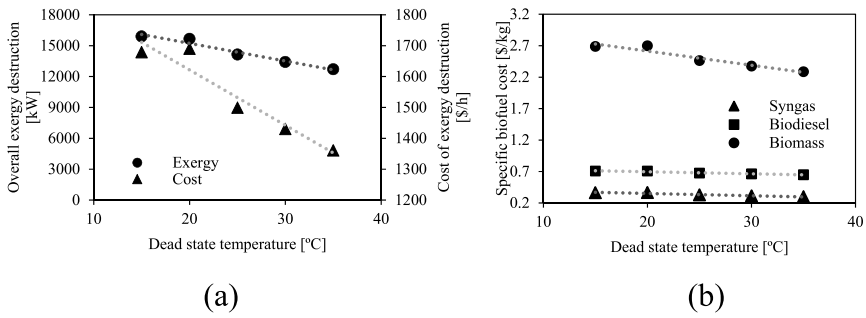

Fig. 4. Effect of dead state temperature on a) overall exergy destruction and cost of exergy destruction and b) specific biofuels cost.

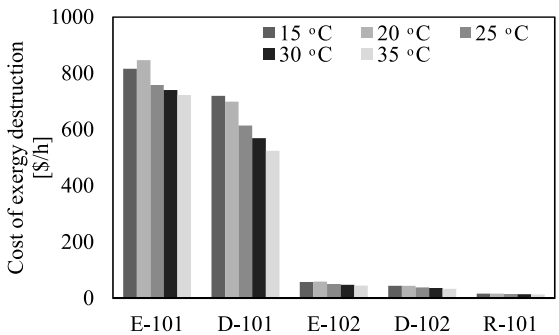

Fig. 5. Effect of the dead state temperature on the costs of exergy destruction of the main components.

Finally, it can be concluded that the exergetic and economic analyses reveal the components that are responsible for the highest exergy destruction rate and also the components that have a greater impact on the final product cost of the process. In order to increase the feasibility and sustainability of the process, future research should be focused on integrating different sources of energy, including renewable sources, for the air heating in order to minimize the exergy destruction rate in the drying process. Furthermore, experimental analysis are considered necessary to determine the impact of operational parameters and structural changes on the SCG drying process.

Informed consent

Informed consent has been obtained from all individuals included in this study.

CRediT authorship contribution statement

Diana L. Tinoco-Caicedo: Conceptualization, Investigation, Data curation, Writing – original draft. **Medelyne Mero-Benavides:** Software, Validation, Formal analysis, Writing – original draft. **Myrian Santos-Torres:** Software, Validation, Formal analysis, Writing – original draft. **Alexis Lozano-Medina:** Supervision, Project administration. **Ana M. Blanco-Marigorta:** Methodology, Writing – review & editing, Supervision, Project administration.

Declaration of Competing Interest

The authors declare that they have no known competing financial interests or personal relationships that could have appeared to influence the work reported in this paper.

Acknowledgements

This research received no external funding.

Nomenclature

c	unit exergy cost ($/MJ)
c_p	heat capacity (kJ/kg K)
$\dot{C}$	cost rate associated with an exergy stream ($/h)
e	specific exergy rate (kJ/kg)
$\dot{E}$	exergy rate (kJ/h)
f	exergoeconomic factor
h	specific enthalpy (kJ/kg)
$\overline{HHV}$	High heating value (MJ/kg)
$\dot{m}$	mass flow rate (kg/h)
n	lifetime of the system (years)
P	pressure (kPa)
r	relative cost difference
R	ideal gas constant (kJ/kmol K)
s	specific entropy (kJ/kg)
T	temperature (°C)
w	mole fraction of water vapor
x	mole fraction
y	destruction rate
y*	relative irreversibility
$\dot{Z}$	investment cost rate ($/h)

Greek letters

Δ	difference
η	exergetic efficiency (%)

Superscript

ch	chemical
ph	physical

Subscripts

B	biodiesel process
CI	cost investment
D	destruction
DB	dry biomass
F	fuel
gly	glycerin compound
i	ith compound
k	kth component
L	loss
o	thermodynamic environment
O&M	operation and maintenance
P	product

R	Reagents
S	oil extraction and syngas process
x	hydrocarbon fuels
WB	wet biomass

Abbreviations

D	dryer
E	heat exchanger
EV	evaporator
FFA	free fatty acids
NIST	National Institute of Standards and Technology
O&M	operation and maintenance
PEC	purchased equipment cost
PFI	Plant-facilities investment
R	Reactor
S	soxhlet
SC	spent coffee
SCG	spent coffee ground
TDE	ThermoData Engine
UNIQUAC	Universal quasichemical

References

[1] M.K. Yesilyurt, C. Cesur, V. Aslan, Z. Yilbasi, The production of biodiesel from safflower (Carthamus tinctorius L.) oil as a potential feedstock and its usage in compression ignition engine: a comprehensive review, Renew. Sustain. Energy Rev. 119 (2020) 109574.
[2] F. Martins, C. Felgueiras, M. Smitkova, N. Caetano, Analysis of fossil fuel energy consumption and environmental impacts in european countries, Energies 12 (2019) 1–11.
[3] M.A. Mayorga, J.G. Cadavid Estrada, J.A. Bonilla Paez, C. Lopez, M. Lopez, Se of biofuels in the aeronautical industry. Case of the Colombian air force, Tecciencia 14 (2019) 33–43.
[4] D. Zhu, S.M. Mortazavi, A. Maleki, A. Aslani, H. Yousefi, Analysis of the robustness of energy supply in Japan: role of renewable energy, Energy Reports 6 (2020) 378–391.
[5] C.H.W. Ruhe, Statistical review, JAMA, J. Am. Med. Assoc. 225 (2019) 299–306.
[6] S.S. Hassan, G.A. Williams, A.K. Jaiswal, Lignocellulosic biorefineries in Europe: current state and prospects, Trends Biotechnol. 37 (2019) 231–234.
[7] S. Datta, Arup; Hossain, Aslam; Roy, an overview on biofuels and their advantages and disadvantages, Asian J. Chem. 26 (2014) 70–73.
[8] A.B. Guerrero, E. Muñoz, Life cycle assessment of second generation ethanol derived from banana agricultural waste: environmental impacts and energy balance, J. Clean. Prod. 174 (2018) 710–717.
[9] M.A. Rajaeifar, A. Akram, B. Ghobadian, S. Rafiee, R. Heijungs, M. Tabatabaei, Environmental impact assessment of olive pomace oil biodiesel production and consumption: a comparative lifecycle assessment, Energy 106 (2016) 87–102.
[10] J.H. Ebner, R.A. Labatut, J.S. Lodge, A.A. Williamson, T.A. Trabold, Anaerobic co-digestion of commercial food waste and dairy manure: characterizing biochemical parameters and synergistic effects, Waste Manag. 52 (2016) 286–294.
[11] D.Y.C. Leung, L.C. Yu, G.C.K. Lam, H.Y.H. Kwok, W.K. Cheng, Bioethanol: is it a suitable biofuel for Hong Kong for reducing its vehicular emissions and carbon footprint? Energy Procedia 142 (2017) 2892–2897.
[12] M. Mehrpooya, M. Khalili, M.M.M. Sharifzadeh, Model development and energy and exergy analysis of the biomass gasification process (Based on the various biomass sources), Renew. Sustain. Energy Rev. 91 (2018) 869–887.
[13] L. Pattanaik, F. Pattnaik, D.K. Saxena, S.N. Naik, Biofuels from Agricultural Wastes, Elsevier Inc., 2019.
[14] K.K. Jaiswal, B. Jha, R.A. Prasath, Biodiesel production from discarded fish waste for sustainable clean energy development, J. Chem. Pharm. Sci. 2014-Decem (2014) 113–114.
[15] J.J. Milledge, The challenge of algal fuel : economic processing of the entire algal biomass, Condens. Matter -Materials Eng. Newsl. (2010) 1–5.
[16] R.W. Jenkins, N.E. Stageman, C.M. Fortune, C.J. Chuck, Effect of the type of bean, processing, and geographical location on the biodiesel produced from waste coffee grounds, Energy Fuel. 28 (2014) 1166–1174.
[17] Y. Liu, Q. Tu, G. Knothe, M. Lu, Direct transesterification of spent coffee grounds for biodiesel production, Fuel 199 (2017) 157–161.
[18] M.J. Haas, K. Wagner, Simplifying biodiesel production: the direct or in situ transesterification of algal biomass, Eur. J. Lipid Sci. Technol. 113 (2011) 1219–1229.
[19] J. Park, B. Kim, J.W. Lee, In-situ transesterification of wet spent coffee grounds for sustainable biodiesel production, Bioresour. Technol. 221 (2016) 55–60.
[20] T.R. Pacioni, D. Soares, M. Di Domenico, M.F. Rosa, R.D.F.P.M. Moreira, H.J. José, Bio-syngas production from agro-industrial biomass residues by steam gasification, Waste Manag. 58 (2016) 221–229.
[21] H.A. Kibret, Y.-L. Kuo, T.-Y. Ke, Y.-H. Tseng, Gasification of Spent Coffee Grounds in a Semi-fluidized Bed Reactor Using Steam and CO 2 Gasification Medium, 2021, 000.
[22] Z.A. Antonova, V.S. Krouk, Y.E. Pilyuk, Y.V. Maksimuk, L.S. Karpushenkava, M.G. Krivova, Exergy analysis of canola-based biodiesel production in Belarus, Fuel Process. Technol. 138 (2015) 397–403.
[23] A. Amelio, T. Van De Voorde, C. Creemers, J. Degrève, S. Darvishmanesh, P. Luis, B. Van Der Bruggen, Comparison between exergy and energy analysis for biodiesel production, Energy 98 (2016) 135–145.
[24] R.A.M. Boloy, M.E. Silva, A.E. Valle, J.L. Silveira, C.E. Tuna, Thermoeconomic analysis of hydrogen incorporation in a biodiesel plant, Appl. Therm. Eng. 113 (2017) 519–528.
[25] E. Shayan, V. Zare, I. Mirzaee, On the use of different gasification agents in a biomass fueled SOFC by integrated gasifier: a comparative exergo-economic evaluation and optimization, Energy 171 (2019) 1126–1138.
[26] Y. Wu, W. Yang, W. Blasiak, Energy and exergy analysis of high temperature agent gasification of biomass, Energies 7 (2014) 2107–2122.
[27] H. Ansarinasab, M. Mehrpooya, M. Sadeghzadeh, Life-cycle assessment (LCA) and techno-economic analysis of a biomass-based biorefinery, J. Therm. Anal. Calorim. 145 (2021) 1053–1073.

[28] T. Nakyai, Y. Patcharavorachot, A. Arpornwichanop, D. Saebea, Comparative exergoeconomic analysis of indirect and direct bio-dimethyl ether syntheses based on air-steam biomass gasification with CO2 utilization, Energy 209 (2020) 118332.
[29] M. Aghbashlo, M. Tabatabaei, S. Soltanian, H. Ghanavati, A. Dadak, Comprehensive exergoeconomic analysis of a municipal solid waste digestion plant equipped with a biogas genset, Waste Manag. 87 (2019) 485–498.
[30] I. Polygeneration, P. Plant, B.S.S. Firing, M. Alghassab, O.D. Samuel, Z.A. Khan, M. Imran, M. Farooq, Exergoeconomic and Environmental Modeling of, 2020.
[31] T. Murakami, G. Xu, T. Suda, Y. Matsuzawa, H. Tani, T. Fujimori, Some process fundamentals of biomass gasification in dual fluidized bed, Fuel 86 (2007) 244–255.
[32] D.R. Vardon, B.R. Moser, W. Zheng, K. Witkin, R.L. Evangelista, T.J. Strathmann, K. Rajagopalan, B.K. Sharma, Complete utilization of spent coffee grounds to produce biodiesel, bio-oil, and biochar, ACS Sustain. Chem. Eng. 1 (2013) 1286–1294.
[33] C.H. Dang, T.D. Nguyen, Physicochemical characterization of Robusta spent coffee ground oil for biodiesel manufacturing, Waste and Biomass Valorization 10 (2019) 2703–2712.
[34] J.L. Diaz de Tuesta, A. Quintanilla, D. Moreno, V.R. Ferro, J.A. Casas, Simulation and optimization of the CWPO process by combination of aspen plus and 6-factor doehlert matrix: towards autothermal operation, Catalysts 10 (2020).
[35] F.J. Gómez-de la Cruz, J.M. Palomar-Carnicero, Q. Hernández-Escobedo, F. Cruz-Peragón, Experimental studies on mass transfer during convective drying of spent coffee grounds generated in the soluble coffee industry, J. Therm. Anal. Calorim. 145 (2021) 97–107.
[36] E.C. Carlson, Don't gamble with physical properties for simulations - aspen Technology, Inc., Chem. Eng. Prog. (1996) 35–46.
[37] J. Han, Y. Liang, J. Hu, L. Qin, J. Street, Y. Lu, F. Yu, Modeling downdraft biomass gasification process by restricting chemical reaction equilibrium with Aspen Plus, Energy Convers. Manag. 153 (2017) 641–648.
[38] L.P.R. Pala, Q. Wang, G. Kolb, V. Hessel, Steam gasification of biomass with subsequent syngas adjustment using shift reaction for syngas production: an Aspen Plus model, Renew. Energy 101 (2017) 484–492.
[39] D. Han, X. Yang, R. Li, Y. Wu, Environmental impact comparison of typical and resource-efficient biomass fast pyrolysis systems based on LCA and Aspen Plus simulation, J. Clean. Prod. 231 (2019) 254–267.
[40] M. Haile, Integrated volarization of spent coffee grounds to biofuels, Biofuel Res. J. 1 (2014) 65–69.
[41] M.M.R. De Melo, H.M.A. Barbosa, C.P. Passos, C.M. Silva, Supercritical fluid extraction of spent coffee grounds: measurement of extraction curves, oil characterization and economic analysis, J. Supercrit. Fluids 86 (2014) 150–159.
[42] O.O.D. Afolabi, M. Sohail, Y.L. Cheng, Optimisation and characterisation of hydrochar production from spent coffee grounds by hydrothermal carbonisation, Renew. Energy 147 (2020) 1380–1391.
[43] A.B.A. de Azevedo, T.G. Kieckbush, A.K. Tashima, R.S. Mohamed, P. Mazzafera, S.A.B.V. de Melo, Extraction of green coffee oil using supercritical carbon dioxide, J. Supercrit. Fluids 44 (2008) 186–192.
[44] B. Leśniak, L. Słupik, G. Jakubina, The determination of the specific heat capacity of coal based on literature data, Chemik 67 (2013) 560–571.
[45] C. Dupont, R. Chiriac, G. Gauthier, F. Toche, Heat capacity measurements of various biomass types and pyrolysis residues, Fuel 115 (2014) 644–651.
[46] D.A. Jahn, F.O. Akinkunmi, N. Giovambattista, Effects of temperature on the properties of glycerol: a computer simulation study of five different force fields, J. Phys. Chem. B 118 (2014) 11284–11294.
[47] D.R. Morris, J. Szargut, Standard chemical exergy of some elements and compounds on the planet earth, Energy 11 (1986) 733–755.
[48] W.J. Wepfer, R. Gagglio, E.F. Obert, in: Proper Evaluation of Available Energy for HVACe, ASHRAE Trans., 1979, pp. 214–230.
[49] A. Bejan, G. Tsatsaronis, M. Moran, Thermal Design & Optimization, John Wiley & Sons, Inc., Canada, 1996.
[50] G. Song, L. Shen, J. Xiao, L. Chen, Estimation of specific enthalpy and exergy of biomass and coal ash, Energy Sources, Part A Recover, Util. Environ. Eff. 35 (2013) 809–816.
[51] S.V. Vassilev, D. Baxter, L.K. Andersen, C.G. Vassileva, An overview of the chemical composition of biomass, Fuel 89 (2010) 913–933.
[52] ASTM International, Standard Test Method for Heat of Combustion of Liquid Hydrocarbon Fuels by Bomb Calorimeter (Reapproved 2007), ASTM Stand. D240-02. i, 2009, pp. 1–9.
[53] D.L. Tinoco-Caicedo, A. Lozano-Medina, A.M. Blanco-Marigorta, Conventional and advanced exergy and exergoeconomic analysis of a spray drying system: a case study of an instant coffee factory in Ecuador, Energies 13 (2020).
[54] Interagua, Informe Anual 2018-2019, Guayaquil, 2019.
[55] H. Sheikhshoaei, M. Dowlati, M. Aghbashlo, M.A. Rosen, Exergy analysis of a pistachio roasting system, Dry. Technol. 38 (2020) 1565–1583.
[56] A. Singh, J. Sarkar, R.R. Sahoo, Experimental energy, exergy, economic and exergoeconomic analyses of batch-type solar-assisted heat pump dryer, Renew. Energy 156 (2020) 1107–1116.
[57] M. Beigi, M. Tohidi, M. Torki-Harchegani, Exergetic Analysis of Deep-Bed Drying of Rough Rice in a Convective Dryer, 2017.
[58] C. Ofori-Boateng, T.L. Keat, L. Jitkang, Feasibility study of microalgal and jatropha biodiesel production plants: exergy analysis approach, Appl. Therm. Eng. 36 (2012) 141–151.
[59] G. Khoobbakht, K. Kheiralipour, H. Rasouli, M. Rafiee, M. Hadipour, M. Karimi, Experimental exergy analysis of transesterification in biodiesel production, Energy 196 (2020).
[60] Y. Ji-chao, B. Sobhani, Integration of biomass gasification with a supercritical CO2 and Kalina cycles in a combined heating and power system: a thermodynamic and exergoeconomic analysis, Energy 222 (2021) 119980.
[61] M. Hosseini, I. Dincer, M.A. Rosen, Steam and air fed biomass gasification: comparisons based on energy and exergy, Int. J. Hydrogen Energy 37 (2012) 16446–16452.
[62] D. Tapasvi, R.S. Kempegowda, K.Q. Tran, Ø. Skreiberg, M. Grønli, A simulation study on the torrefied biomass gasification, Energy Convers. Manag. 90 (2015) 446–457.
[63] L. Jin, H. Zhang, Z. Ma, Study on capacity of coffee grounds to be extracted oil, produce biodiesel and combust, Energy Procedia 152 (2018) 1296–1301.
[64] Z. Erbay, A. Hepbasli, Assessment of cost sources and improvement potentials of a ground-source heat pump food drying system through advanced exergoeconomic analysis method, Energy 127 (2017) 502–515.
[65] H. Atalay, Comparative Assessment of Solar and Heat Pump Dryers with Regards to Exergy and Exergoeconomic Performance, 2019.
[66] R.B. Keey, Introduction to Industrial Drying Operation, Pergamon Press, New York, 1978.
[67] S. Zohrabi, S.S. Seiiedlou, M. Aghbashlo, H. Scaar, J. Mellmann, Enhancing the exergetic performance of a pilot-scale convective dryer by exhaust air recirculation, Dry. Technol. 38 (2020) 518–533.
[68] B. Fakhimghanbarzadeh, B. Farhanieh, H. Marzi, A. Javadzadegan, Evolutionary algorithm for multi-objective exergoeconomic optimization of biomass waste gasification combined heat and power system, IEEE Int. Conf. Ind. Informatics (2009) 361–366.
[69] M. Fani, B. Farhanieh, A.A. Mozafari, Exergoeconomic optimization of black liquor gasification combined cycle using evolutionary and conventional iterative method, Int. J. Chem. React. Eng. 8 (2010).
[70] A. Abuadala, I. Dincer, Exergoeconomic analysis of a hybrid steam biomass gasification-based Tri-generation system, Prog. Exergy, Energy, Environ. (2014) 51–67.
[71] Y. Kalinci, A. Hepbasli, I. Dincer, Exergoeconomic analysis and performance assessment of hydrogen and power production using different gasification systems, Fuel 102 (2012) 187–198.
[72] Z. Erbay, A. Hepbasli, Exergoeconomic evaluation of a ground-source heat pump food dryer at varying dead state temperatures, J. Clean. Prod. 142 (2017) 1425–1435.